Electron–phonon and exciton–phonon bound states

Y B LEVINSON AND É I RASHBA

L D Landau Institute of Theoretical Physics,
Academy of Sciences of the USSR, Moscow, USSR

Translator: M G PRIESTLEY

Abstract

A review is given of the theoretical and experimental work which has shown the possibility of forming bound states of an electron or an exciton with an optical phonon. The specific feature of these bound states is that an unconserved particle (a phonon) contributes to their formation; such states are stable only because their decay is forbidden by the conservation laws for energy and momentum. As distinct from the virtual phonons of a polaron 'cloud', the phonon which takes part in the formation of a bound state is almost real.

Most attention is devoted to wide-band systems, in which the width of the electron (or exciton) band is larger than the phonon frequency; this is the normal situation for semiconductors and ionic crystals. In these systems bound states are formed near the threshold for phonon emission. The formation of bound states is favoured by strong electron–phonon coupling, small phonon dispersion, and a large mass for the particle which interacts with the phonons. Hybrid states occupy an intermediate position between bound states and the usual polaron states; these arise when the energy of an optical phonon is equal to one of the electronic frequencies, and under these conditions the distinction between 'virtual' and 'real' phonons practically disappears. A discussion is also given of excitons in molecular crystals, which are treated as narrow-band systems; here the existence of bound states is not related to the presence of a threshold in the exciton spectrum. The existence of bound and hybrid states must have a marked effect on a number of physical phenomena, in particular the optical properties, as has already been demonstrated in a series of experiments.

This review was completed in June 1972.

Contents

Part I. General

1. Introduction

The multiplicity of phenomena in solid state physics is a result of the existence of a large number of different kinds of quasiparticles (electrons, phonons, magnons, etc), together with interactions between them. These interactions may enable quasiparticles to combine with one another, forming new and more complex quasiparticles (or quasiparticle complexes, as they are sometimes called). It is therefore not surprising that bound states of quasiparticles show up in a number of effects, especially in optical properties. The best known example of this is the Wannier–Mott exciton (Wannier 1937, Mott 1938), which is a bound state of an electron and a hole. Historically the first example, although it is less well known, was the Bethe spin complexes, which are bound states of magnons (Bethe 1931).

These bound states of quasiparticles have been studied intensively, both theoretically and experimentally, over the past ten years. The clearest picture has emerged for molecular and magnetic crystals, where the spectra have been successfully interpreted using the concepts of pair binding: phonon + phonon (Van Kranendonk 1959), exciton + phonon (Rashba 1966, Broude *et al* 1966), and exciton + magnon (Freeman and Hopfield 1968, Meltzer *et al* 1968, 1969). The situation is much less satisfactory for ionic and semiconductor crystals; there are a large number of papers, both experimental and theoretical, which use the concepts of exciton + exciton complexes (Moskalenko 1958, Lampert 1958), phonon + phonon complexes (Cohen and Ruvalds 1969, Ruvalds and Zawadowski 1970), exciton + phonon complexes (Liang and Yoffe 1968, Toyozawa and Hermanson 1968, Mel'nikov *et al* 1971), electron(polaron) + phonon complexes (Johnson and Larsen 1968, Mel'nikov and Rashba 1969, Levinson 1970), but an unambiguous comparison of theory with experiment has been possible only in a few cases.

The subject of the present review is the bound states formed by electrons and excitons with optical phonons. We use the term excitons to cover both Wannier–Mott excitons in crystals with wide exciton bands and Frenkel excitons (Frenkel 1931) in crystals with narrow exciton bands. The physical description of binding depends on the ratio of the bandwidth ΔE for the particle which couples to a phonon to the phonon energy ω_0 (the phonon dispersion can almost always be neglected)†.

In narrow-band systems ($\Delta E < \omega_0$) the emission and absorption of a real phonon is forbidden by energy conservation and hence phonons in these systems behave as conserved particles. If we leave out 'dressing' effects, the states of the system can be classified according to the number of 'real' phonons $N = 0, 1, \ldots$. In particular the states with $N = 1$ can be found from the two-particle problem. There is an effective interaction between a Frenkel exciton and an (intramolecular) phonon, and in the simplest case this is attractive because the vibrational frequency of an electronically excited molecule is decreased by $|\Delta|$. If this attraction is sufficiently strong, that is $|\Delta| \gtrsim \frac{1}{2}\Delta E$, then exciton–phonon bound states can exist. These

† Both here and below we use units such that Planck's constant $\hbar = 1$ and Boltzmann's constant $k = 1$.

states form a single-particle branch of the energy spectrum, which lies below the region of two-particle states which are the dissociated states of an exciton–phonon pair (figure 1). Since the single-phonon states with $N = 1$ have energies which differ considerably from those of the no-phonon states, $N = 0$, the inclusion of interactions with phonons does not lead to any qualitative change in the spectrum of the no-phonon states.

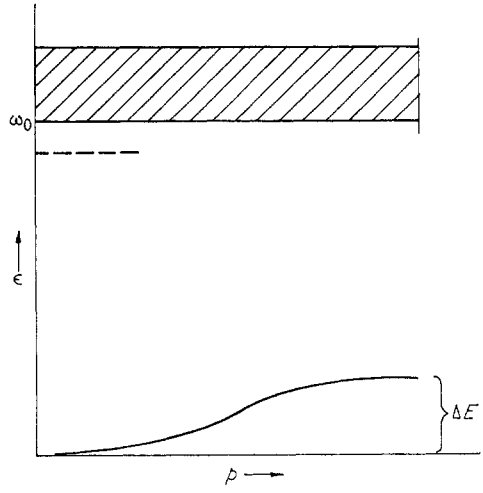

Figure 1. Energy spectrum of the states of an exciton–phonon pair in a narrow-band system. The region of dissociated states is shaded. The bound state with $p = 0$ is shown by a dashed line.

In wide-band systems ($\Delta E > \omega_0$) the situation is rather different, because then the emission of a real phonon is allowed (absorption is negligible at low temperatures $T \ll \omega_0$). The clear distinction between 'virtual' and 'real' phonons disappears, and it is no longer possible to classify the states by the number N. Hybrid states which are intermediate between no-phonon and single-phonon states can now exist, and under these conditions $0 < N < 1$. Phonon emission is possible for energies above the threshold which occurs ω_0 above the bottom of the band. It is in the neighbourhood of this threshold that interactions produce the biggest changes in the spectrum and both hybrid and bound states are formed.

Before explaining the essential features of this problem by using a simple model, we point out that the experimental results reported in the past five or six years have shown that the features of the spectrum at the threshold are clearly evident in a number of optical effects related to magnetopolarons, excitons and impurity centres (Johnson and Larsen 1966, Liang and Yoffe 1968, Onton *et al* 1967a,b).

We consider a simple model in which a particle whose spectrum has two branches $E_1(\boldsymbol{p})$ and $E_2(\boldsymbol{p})$ interacts at $T = 0$ with optical phonons of frequency ω_0 (dispersion neglected), and phonon emission transfers the particle from one branch to the other (figure 2). What is the effect of this interaction on the form of the upper branch 2? First let us suppose that the interaction with phonons is weak. It is then sufficient to consider only the single-phonon states $\phi_s(\boldsymbol{p}, \boldsymbol{q})$ ($\boldsymbol{q}$ is the phonon momentum) in addition to the no-phonon states $\phi_s(\boldsymbol{p})$ (a particle with

momentum $\boldsymbol{p}$ on branch $s = 1, 2$). The perturbed wavefunction for branch 2 is then

$$\psi_2(\boldsymbol{p}) \propto \phi_2(\boldsymbol{p}) + \int \frac{\mathrm{d}^3\boldsymbol{q}}{(2\pi)^3} \frac{\mathscr{H}_{12}(\boldsymbol{q})}{\epsilon - \omega_0 - E_1(\boldsymbol{p}-\boldsymbol{q}) + \mathrm{i}0} \phi_1(\boldsymbol{p}-\boldsymbol{q}, \boldsymbol{q}) \tag{1.1}$$

where $\mathscr{H}_{12}$ is the interaction matrix element, and the energy $\epsilon = \epsilon(\boldsymbol{p})$ is found by solving the equation

$$\epsilon - E_2(\boldsymbol{p}) = \mathscr{M}^0(\epsilon, \boldsymbol{p}) \tag{1.2}$$

where

$$\mathscr{M}^0(\epsilon, \boldsymbol{p}) = \int \frac{\mathrm{d}^3\boldsymbol{q}}{(2\pi)^3} \frac{|\mathscr{H}_{12}(\boldsymbol{q})|^2}{\epsilon - \omega_0 - E_1(\boldsymbol{p}-\boldsymbol{q}) + \mathrm{i}0}. \tag{1.3}$$

If the energy ϵ is close to the threshold ω_0, the denominator can become very small

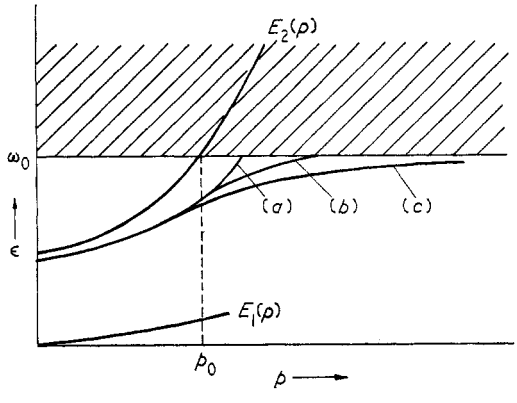

Figure 2. Change in the spectrum of a free particle due to interaction with optical phonons. Curves (*a*), (*b*), (*c*) relate to equations (1.5*a*), (1.5*b*), (1.5*c*).

(when $\boldsymbol{q} = \boldsymbol{p}$ and $E_1 = 0$). The exact energy ϵ in the denominator is thus not replaced by the unperturbed energy $E_2(\boldsymbol{p})$, that is, Wigner–Brillouin perturbation theory is used.

Above the threshold ($\epsilon > \omega_0$) there is no single particle spectrum in the usual sense; there is just a continuous spectrum of decaying states. We therefore limit the present discussion to the region below the threshold ($\epsilon < \omega_0$). In this region the contribution of the no-phonon state ϕ_2 to the state ψ_2 is

$$\begin{aligned} Z(\boldsymbol{p}) &= \left[1 + \int \frac{\mathrm{d}^3\boldsymbol{q}}{(2\pi)^3} \left| \frac{\mathscr{H}_{12}(\boldsymbol{q})}{\epsilon - \omega_0 - E_1(\boldsymbol{p}-\boldsymbol{q})} \right|^2 \right]^{-1}_{\epsilon=\epsilon(\boldsymbol{p})} \\ &= \left[1 - \frac{\partial}{\partial\epsilon} \mathscr{M}^0(\epsilon, \boldsymbol{p})\right]^{-1}_{\epsilon=\epsilon(\boldsymbol{p})}. \end{aligned} \tag{1.4}$$

In other words, the effective number of phonons contributing to the state ψ_2 is $\langle N \rangle = 1 - Z$.

Since the denominator in $\mathscr{M}^0$ can vanish for $\epsilon \geqslant \omega_0$, the value of $\mathscr{M}^0$ as a function of ϵ has a singularity as $\epsilon \to \omega_0$. The nature of this singularity is determined by the behaviour of the function inside the integral for $\boldsymbol{q}$ near to $\boldsymbol{p}$. Hence the behaviour of $\mathscr{M}^0(\epsilon)$ near the threshold is determined by that of $E_1(\boldsymbol{p})$ for $\boldsymbol{p} \simeq 0$, ie the lowest point in the spectrum, to which the particle falls after emission of a phonon, and by

the behaviour of $\mathscr{H}_{12}(\boldsymbol{q})$ for $\boldsymbol{q} \simeq \boldsymbol{p}$, ie by interaction with that phonon to which the particle transfers its momentum.

It is sometimes convenient to formulate the problem in a different way, especially when we are interested in a particular state of branch 2 (for example $\boldsymbol{p} = 0$), and this state can be dealt with by the introduction of an external parameter, for example, the magnetic field $\boldsymbol{H}$. E_2 and $\mathscr{M}^0$ will then be functions of $\boldsymbol{H}$, rather than of $\boldsymbol{p}$. Since E_2 usually increases monotonically with increasing H, just as it does with increasing p, all future discussion of the dependence of the spectrum on $\boldsymbol{p}$ is equally applicable to its dependence on $\boldsymbol{H}$ or on another external parameter.

If ϵ is not near the threshold, the right-hand side of equation (1.2) is known to be small, and by substituting $\epsilon = E_2$ we obtain the usual polaron renormalization of the spectrum, and this is small in the weak-coupling case now being considered. This is the situation in the initial portion of branch 2, and here $Z(\boldsymbol{p}) \simeq 1$, that is, we have almost no-phonon states.

When the momentum approaches p_0 the energy ϵ tends to ω_0 and the further variation of the spectrum depends on the nature of the singularity in $\mathscr{M}^0(\epsilon)$ (Pitaevskii 1959). We note that if the dependence of the spectrum on an external parameter is being studied, this approach to the threshold is indeed an approach to resonance between the phonon frequency ω_0 and the frequency $E_2 - E_1$ of a spectral transition. In such cases the threshold effects take on a resonant character.

We now consider a number of characteristic types of non-analytic behaviour which occur in particular physical problems (see table 1).

Case (*a*)

$$\mathscr{M}^0(\epsilon) = -A + B(\omega_0 - \epsilon) - C(\omega_0 - \epsilon)^{3/2} + \dots \tag{1.5a}$$

Case (*b*)

$$\mathscr{M}^0(\epsilon) = -A + B(\omega_0 - \epsilon)^{1/2} + \dots \tag{1.5b}$$

Case (*c*)

$$\mathscr{M}^0(\epsilon) = -A(\omega_0 - \epsilon)^{-1/2} + \dots \tag{1.5c}$$

Case (*d*)

$$\mathscr{M}^0(\epsilon) = -A(\omega_0 - \epsilon)^{-1} + \dots . \tag{1.5d}$$

The quantities A, B and C which appear here are real; they may be considered to be independent of p or H since this dependence does not usually affect the spectrum near the threshold. Cases (*a*) to (*c*) correspond to dispersion laws shown by the same letters in figure 2.

For a highly non-analytic case such as (*c*) the spectrum extends without limit to higher momenta, and the energy becomes practically independent of p and approximately equal to $E_1(0) + \omega_0$ (Johnson and Larsen 1966, Korovin and Pavlov 1967a, Levinson and Matulis 1970). This phenomenon is known as pinning; one speaks of the pinning of branch 2 to branch 1 + phonon. We now consider the structure of the states in the pinning region, ie for $\epsilon \to \omega_0$. It is easy to see that this also implies $Z \to 0$, that is, the unperturbed states ϕ_2 play hardly any part in the formation of these states. In the integration over $\boldsymbol{q}$ in equation (1.3) the major contribution comes from the region $E_1 \simeq 0$, and this means that in the pinning region the particle lies at the bottom of band 1 and therefore the energy and momentum of the state in the pinning region are almost completely due to the phonon. The lowering in energy of these states compared to the total energy of the

Table 1. Classification of threshold effects according to the kind of non-analyticity

Kind of non-analyticity	Physical object	Branches of the spectrum 1	2	Parameter controlling the spectrum	References
(*a*)	Exciton interacting with polarization phonons	Exciton 1s level	Levels 2s, 3s, 3d, ...	Relative position of levels 1 and 2	§ 6 of present review Toyozawa and Hermanson (1968)
(*b*)	Exciton interacting with polarization phonons	Exciton 1s level	Levels 2p, 3p, ...	Relative position of levels 1 and 2	§ 6 of present review Toyozawa and Hermanson (1968)
	Electron	Polaron branch		Momentum	Whitfield and Puff (1965)
	Exciton in a strong magnetic field	Exciton below the lowest Landau band $l = 0$	Exciton below the Landau band $l = 1$	Magnetic field	Mel'nikov *et al* (1971)
(*c*)	Electron in a strong magnetic field	Electron in the lowest Landau band $l = 0$	Electron in any Landau band with bottom below ω_0	Longitudinal component of momentum	Levinson and Matulis (1970) Levinson *et al* (1971c)
			Electron in Landau band $l = 1$	Magnetic field	Johnson and Larsen (1966) Harper (1967) Korovin and Pavlov (1967a,b)
	Electrons with $\boldsymbol{p} = 0$ (interacting with polarization phonons)	Polaron branch		None	Mel'nikov and Rashba (1969)
	Exciton in a one-dimensional crystal	Exciton branch		Momentum	Suna (1964)
(*d*)	Impurity centre	Electron ground level	Excited level	Level separation	Kogan and Suris (1966)

particle plus a phonon $E_1(0)+\omega_0$ can be interpreted as a binding energy. From this point of view states in the pinning region are bound states of a particle at the bottom of band 1 and a phonon.

States with momenta close to p_0 are intermediate between polaron states at the beginning of the branch and bound states at the end of the branch. It is easy to check that $Z(p_0)\simeq\frac{1}{2}$ for these states, that is, they contain equal amounts of both no-phonon and single-phonon states. We shall call states of this kind hybrid states. It is convenient to combine hybrid and bound states containing an appreciable contribution from a 'real' phonon into a single concept—a complex of particle+phonon.

If in equation (1.5*c*) we write $A=\alpha\omega_0^{3/2}$, then α can be regarded as a dimensionless coupling constant. It can then be shown that the hybrid states have an energy which differs from the threshold by $|\epsilon-\omega_0|\sim\alpha^{2/3}\omega_0$, whilst the bound states for which $Z\ll 1$ have energy differing from threshold by $|\epsilon-\omega_0|\ll\alpha^{2/3}\omega_0$. Thus, as the momentum increases we pass from polaron states with $\langle N\rangle\sim\alpha$ through hybrid states with $\langle N\rangle\simeq\frac{1}{2}$ to bound states with $\langle N\rangle\simeq 1$.

For a weaker non-analyticity such as case (*b*) (equation (1.5*b*)), the spectrum has a limiting point and the approach to this is a tangent to the straight line $\epsilon=\omega_0$, that is, pinning still occurs but it is more weakly developed. It is evident that $Z\to 0$ as $\epsilon\to\omega_0$, so that near the threshold we again have bound states, and there are hybrid states between these and the beginning of the branch. If we write $B=\alpha\omega_0^{1/2}$ in equation (1.5*b*), the hybrid states are separated from the threshold by $|\epsilon-\omega_0|\sim\alpha^2\omega_0$, whilst the bound states occur at $|\epsilon-\omega_0|\ll\alpha^2\omega_0$. The threshold is always smeared in practice, and unless this smearing is very small cases (*b*) and (*c*) in equations (1.5) will be qualitatively similar, since the far portion of branch (*c*) lies in the region of smearing and is not developed.

The situation described by equation (1.5*a*) corresponds to very weak non-analyticity (case (*a*)). The spectrum has a limiting point which it approaches with finite slope. It is evident that $Z\simeq 1$ everywhere, even close to the threshold, that is, neither hybrid nor bound states exist below the threshold in this case.

The possibility of introducing quasiparticles in the continuous spectrum near the threshold is also related to the degree of non-analyticity. This is possible in cases (*a*) and (*b*), when the spectrum has a limiting point (since the inverse of the quasiparticle lifetime $\Gamma(\epsilon)=\mathrm{Im}\,\mathscr{M}^0(\epsilon)\to 0$ for $\epsilon\to\omega_0$). For case (*c*) $\Gamma(\epsilon)\to\infty$ for $\epsilon\to\omega_0$, and therefore there are no quasiparticles close to the threshold. We further note that the bottom of branch 1 is lowered by the interaction with phonons; this gives a renormalization of the threshold position but does not affect the above qualitative description of the spectrum.

Case (*d*), which corresponds to impurity centres, has a number of distinguishing features. E_1 and E_2 are independent of p, and because the spectrum is discrete there is no continuum for $\epsilon>\omega_0$ and undamped states exist both above and below the threshold (figure 3). In this case there is also pinning when the relative positions of the levels E_2 and E_1 are changed (Kogan and Suris 1966).

It is clear from the above discussion that in wide-band systems, as distinct from narrow-band systems, even weak coupling (for sufficiently strong non-analyticity) leads to a qualitative restructuring of the spectrum near the threshold.

We shall now try to understand physically how the ideas developed above are modified as the coupling with phonons becomes stronger. First, the polaron renormalization of the spectrum at the beginning of the branch will no longer be

small. This means that the displacement of the threshold will be appreciable, and that the polaron states can no longer be described as states with almost no phonons. The bound states near the threshold will not now be single-phonon states, but will contain approximately one phonon more than the polaron states at the bottom of band 1. Moreover, since the perturbation theory used above is no longer applicable, it is possible that additional branches of the spectrum may appear in the region $\epsilon < \omega_0$. If these were close to the threshold they could be interpreted as bound states. For the case of an electron strongly coupled to phonons such states do in fact exist (Mel'nikov and Rashba 1969).

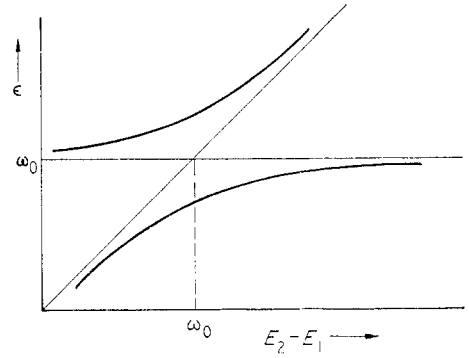

Figure 3. Change in the spectrum of an impurity centre due to interaction with optical phonons.

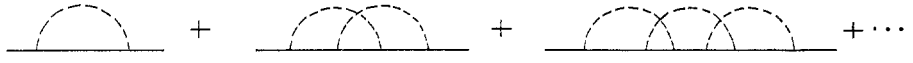

Figure 4. Diagrams for the mass operator which are important near the decay threshold.

Even for weak coupling the details of the spectra already described are far from complete. The point is that they are based on perturbation theory applied to the mass operator: the expression for $\mathscr{M}^0$ in equation (1.3) corresponds to the simplest diagram in figure 4. However, even for weak coupling it is only valid to stop at this first term if $\mathscr{M}^0(\epsilon)$ is finite at the threshold (Pitaevskii 1959). Otherwise the whole series shown in this figure should be summed. This gives a mass operator $\mathscr{M}(\epsilon)$ whose behaviour near threshold may differ qualitatively from that of $\mathscr{M}^0(\epsilon)$. The above description of the spectrum is therefore complete only for cases (*a*) and (*b*). Case (*c*) is more complicated and the nature of the spectrum depends on the behaviour of $\mathscr{M}(\epsilon)$. For a magnetopolaron below the threshold there is an infinite number of additional branches, which for all momenta describe bound states of an electron and a phonon (Levinson 1970). On the other hand, for a polaron at $H = 0$, which has the same behaviour of $\mathscr{M}^0(\epsilon)$ at $p = 0$, there are no bound states (Mel'nikov and Rashba 1969).

Part II. Polarons

2. The polaron spectrum—threshold behaviour and bound states

The polaron problem is that of the spectrum of a system consisting of an electron interacting with longitudinal optical phonons. The interaction hamiltonian is usually chosen to be of the form

$$\mathscr{H}_{\mathrm{eL}} = \sum_{\boldsymbol{q}} c_{\boldsymbol{q}} \exp(\mathrm{i}\boldsymbol{q}.\boldsymbol{r})\, b_{\boldsymbol{q}} + (\text{hermitian conjugate}) \tag{2.1}$$

where $\boldsymbol{r}$ is the electron coordinate, $\boldsymbol{q}$ is the phonon momentum, $b_{\boldsymbol{q}}$ is the phonon annihilation operator and $c_{\boldsymbol{q}}$ is the interaction matrix element. The final results of calculations usually contain the quantity

$$\mathscr{B}(q) = \frac{V}{(2\pi)^3}|c_q|^2 \tag{2.2}$$

which is independent of the normalizing volume V. In the isotropic case the magnitude of $\mathscr{B}$ is a function only of the modulus of $\boldsymbol{q}$ and it is convenient to write it as

$$\left.\begin{aligned} \mathscr{B}(q) &= \frac{\alpha}{(2\pi)^3}\frac{4\pi\omega_0^2}{p_0^3}\Phi(q) \\ p_0 &= (2m\omega_0)^{1/2} \end{aligned}\right\} \tag{2.3}$$

where ω_0 is the phonon frequency (their dispersion is neglected), α is a dimensionless coupling constant, m is the electron effective mass and the form factor

$$\left.\begin{aligned} \Phi(q) &= 1 \qquad \text{for a deformation interaction with optical phonons—DO} \\ \Phi(q) &= \frac{p_0^2}{q^2} \qquad \text{for a polarization interaction with optical phonons—PO.} \end{aligned}\right\} \tag{2.4}$$

For the PO interaction the value of α determined in this way is the same as that derived by Fröhlich:

$$\left.\begin{aligned} \alpha &= \frac{e^2}{v_0}\frac{1}{\bar{\kappa}} \\ \frac{1}{\bar{\kappa}} &= \frac{1}{\kappa_0} - \frac{1}{\kappa_\infty} \\ \tfrac{1}{2}mv_0^2 &= \omega_0^2 \end{aligned}\right\} \tag{2.5}$$

where κ_∞ and κ_0 are the high frequency and DC dielectric constants of the crystal. It is usual to distinguish between weak coupling ($\alpha \ll 1$), intermediate coupling ($\alpha \sim 1$), and strong coupling ($\alpha \gg 1$).

2.1. *Spectrum with a limiting point—weak coupling*

For weak coupling it is natural to use perturbation theory applied to the mass operator $\mathscr{M}$ to study the spectrum, and to the lowest order in the interaction we have

$$\mathscr{M}^0(\varepsilon p) = \int \mathrm{d}^3\boldsymbol{q}\,\frac{\mathscr{B}(q)}{\epsilon - \omega_0 - (\boldsymbol{p}-\boldsymbol{q})^2/2m + \mathrm{i}0}. \tag{2.6}$$

For the DO interaction the integral in equation (2.6) diverges at large q so must be cut off at some $q = q_{\max}$. However, if $p \ll q_{\max}$ the singular part of $\mathscr{M}^0$ is independent of $q_{\max}$. A direct calculation leads to equation (1.5*b*) with

$$\left.\begin{aligned} A &= \alpha\omega_0\frac{2}{\pi}\frac{q_{\max}}{p_0} \\ B &= \alpha\omega_0^{1/2}. \end{aligned}\right\} \tag{2.7}$$

For a PO interaction the integration gives

$$\mathscr{M}^0(\epsilon p) = -\alpha\omega_0 \frac{p_0}{p} \arctan\left(\frac{p^2}{2m(\omega_0-\epsilon)}\right)^{1/2}. \tag{2.8}$$

For $\epsilon \to \omega_0$ and $p \simeq p_0$ this also reduces to equation (1.5*b*) with

$$\left.\begin{aligned} A &= \alpha\omega_0 \frac{\pi}{2} \\ B &= \alpha\omega_0{}^{1/2}. \end{aligned}\right\} \tag{2.9}$$

Thus both forms of interaction give a spectrum near the limiting point which shows weak pinning with tangential contact (figure 2, curve (*b*)). This deduction is still valid when all diagrams for $\mathscr{M}$ which contain no intersecting phonon lines are summed (Whitfield and Puff 1965).

For $p = 0$ equation (2.8) reduces to equation (1.5*c*) with $A = \alpha\omega_0{}^{3/2}$. This leads us to expect that for small p and a PO interaction it is not sufficient to consider only the simplest diagram for $\mathscr{M}$. However, summation of the series of diagrams in figure 4 showed that for $p = 0$ there are no additional branches of the spectrum near the threshold $\epsilon = \omega_0$ (Mel'nikov and Rashba 1969), at least in this approximation. This means that for weak coupling there are no electron–phonon bound states with small total momentum.

These special features in the spectrum near the threshold may be reflected in optical effects. Their effect on interband absorption was considered by Dunn (1968) for a DO interaction of holes, and by Heck and Woodruff (1971) for a PO interaction of electrons and holes. We will not discuss these papers in any more detail, since they neglect an important effect, namely the Coulomb interaction between the electron and the hole.

2.2. *Bound states—strong coupling*

For strong coupling a polaron consists of an electron, which is in a discrete level (with $E_0 \simeq -0{\cdot}33\alpha^2\omega_0$) in the field of a selfconsistent lattice polarization; the effective mass of the polaron is $m^* \simeq 2{\cdot}3 \times 10^{-2}\alpha^4 m$ (Pekar 1946, Landau and Pekar 1948, Bogolyubov 1950). The binding energy of any complex containing a phonon must be less than ω_0. Since the scale of electronic energies $\alpha^2\omega_0 \gg \omega_0$, it is more convenient to look for bound states in the phonon spectrum of the crystal containing the polaron. The problem is simplified by Pekar's observation (1951) that for $\alpha \gg 1$ lattice vibrations can be described classically and the state of the electron adiabatically follows the ions. Since $m^* \propto \alpha^4$ is large, polaron recoil due to phonon emission can be neglected. Bound states of a polaron and a phonon can then be described as localized vibrations of the lattice in the neighbourhood of the polaron. The equations found by such a method are, of course, derived also in the corresponding approximation of the quantum adiabatic theory (Tjablikov 1951).

Consideration of a lattice vibration with frequency ω under these conditions leads, for the polaron ground state, to the following expression for the electric potential of the lattice polarization (Mel'nikov and Rashba 1969)

$$(\omega_0{}^2 - \omega^2)\Delta\phi(\boldsymbol{r}) = -8\pi\alpha\omega_0{}^2 v_0 \int \mathrm{d}^3\boldsymbol{r}' \sum_{n>0} \frac{\psi_0(\boldsymbol{r})\psi_n(\boldsymbol{r})\psi_0^*(\boldsymbol{r}')\psi_n^*(\boldsymbol{r}')}{E_n - E_0}\phi(\boldsymbol{r}') \tag{2.10}$$

where ψ_n and E_n ($n > 0$) refer to excited states of the hamiltonian $\mathscr{H}_0$ which describes the electron in a polarization well corresponding to the polaron ground state (with electron wavefunction ψ_0). Equation (2.10) is inconvenient in that the kernel includes all ψ_n, but if we transform from equation (2.10) to the corresponding variational principle and introduce a new unknown function f defined by

$$\psi_0 \phi = (\mathscr{H}_0 - E_0)\psi_0 f \tag{2.11}$$

we then arrive at the following equation for ω:

$$\frac{\omega_0^2 - \omega^2}{16\pi\omega_0^2} = \max_f \left(\frac{\int d^3\boldsymbol{r}\psi_0^2(\nabla f)^2}{\int d^3\boldsymbol{r}\{\nabla(\Delta f + 2\nabla f \nabla \ln \psi_0)\}^2} \right). \tag{2.12}$$

Lengths on the right hand side of this equation are written in units of $(2m\alpha^2\omega_0)^{-1/2}$, and since all the parameters cancelled out, the relative binding energies $(\omega_0 - \omega)/\omega_0 = W/\omega_0$ take on universal values.

It is interesting that in equation (2.12) all the information on the electronic spectrum of the polaron reduces to a single function ψ_0, which can be found to high accuracy. Since $\psi_0(r)$ is spherically symmetric, whilst the right hand side of equation (2.12) is positive definite, functions f, for which (2.12) takes extremal values, exist for all angular momenta; there are therefore an infinite number of eigenvalues $\omega_r < \omega_0$. An estimate for the lowest levels gives $W_r = \omega_0 - \omega_r \simeq (0{\cdot}10 \div 0{\cdot}15)\omega_0$. Since all these states lie below the threshold and W_r is considerably less than ω_0 (although here it is true that this inequality is numerical rather than algebraic), it is natural to interpret them as bound states of a polaron and a phonon. If we further take into account the dependence of the energy of these states on the total momentum of the system p, we conclude that new branches of the spectrum are formed below the threshold, at least near $p = 0$. Since $|E_0| \gg \omega_0$, the spectrum must contain multiple frequencies $n\omega_r$, but these states will be damped.

It is as yet not known how far these bound states extend into the region of intermediate coupling. It is only known (Matulis 1972) that if $\alpha \leqslant \alpha_c$, where α_c is some critical value from the intermediate coupling region ($\alpha_c \sim 1$), no bound states exist.

3. Magnetophonon resonance in the polaron spectrum

In 1966–67 it was observed that the magneto-optic absorption showed a number of new features when the cyclotron frequency ω_c of the current carriers became equal to the frequency ω_{LO} of longitudinal optical phonons, and the resonance field H_0 was thus given by the expression $eH_0/mc = \omega_{LO}$. This effect was found in InSb, where the resonance field is comparatively low ($H_0 = 34$ kG) because of the small electron effective mass ($m \simeq 0{\cdot}014m_0$). We note that the effects of this resonance on the DC conductivity were predicted by Gurevich and Firsov (1961) and observed by Puri and Geballe (1963) and Firsov *et al* (1964). A review of this subject is given by Harper *et al* (1973).

Johnson and Larsen (1966) studied interband transitions of an electron to the Landau level $l = 1$ in the conduction band and observed a splitting of the absorption line (figure 5) in fields near H_0. They gave a qualitative explanation of this splitting based on the 'polaron effect', ie the interaction of an electron with LO phonons. However, this explanation completely neglects the 'exciton effect', ie the Coulomb

interaction between the electron and the hole. We shall therefore consider in this section only the features of the intraband absorption, where the polaron effect appears in a 'pure form'. These features were found independently by two groups: Dickey *et al* (1967) and Summers *et al* (1967). They observed cyclotron resonance in InSb for fields close to H_0 corresponding to infrared radiation with $\lambda \simeq 50$ μm.

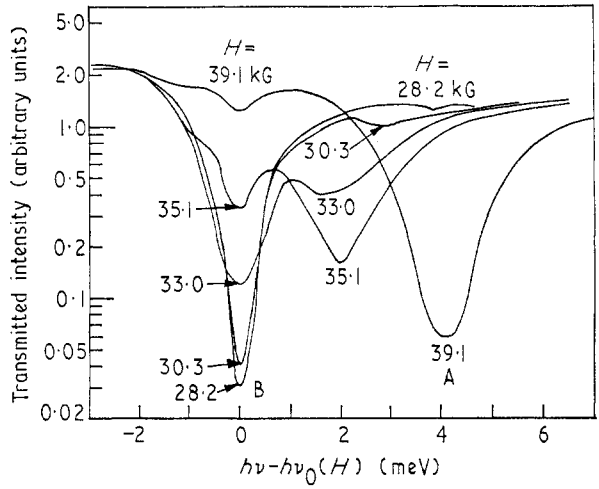

Figure 5. Split interband transition in InSb. The quantity $h\nu_0(H)$ has been chosen so that the B components line up. The resonance field $H_0 = 34$ kG. From Johnson and Larsen (1966).

The experiments were carried out on pure samples at low temperature, so that only the lowest Landau level $l = 0$ was populated, and the absorption was due to transitions to the $l = 1$ level, which has already been mentioned in connection with interband absorption. As the magnetic field was increased, it was found that the cyclotron resonance line broadened rapidly near H_0 and was displaced discontinuously to shorter wavelengths (for more details see § 3.2).

3.1. *Energy spectrum of the electron–phonon system: theory*

The features of the intraband absorption described above can be understood by considering the energy spectrum of the electron–phonon system; in this it is necessary to consider only LO phonons and their dispersion can be neglected ($\omega_{LO} = \omega_0$). At sufficiently low temperature and carrier density we may assume that all the electrons are near the bottom of the lowest Landau band $l = 0$, near $k = 0$, and that absorption of LO phonons by electrons is negligible compared to their emission. In order to show clearly the physics of this effect we neglect other scattering processes (by impurities and acoustic phonons) and assume that the system contains only one electron.

An electromagnetic wave does not interact with LO phonons, but because of the electron–phonon interaction the electron–phonon system responds as a whole. If we neglect the photon momentum, then the longitudinal (along $\boldsymbol{H}$) momentum of the electron + phonon system is zero both before and after photon absorption. Therefore, when considering absorption, we should examine the spectrum with

zero total longitudinal momentum $p = 0$. Let us first suppose that the electron–phonon interaction is not present. The states of the system with $p = 0$, which contain no phonons ($N = 0$), form a discrete spectrum $\epsilon = E_l(0)$ (figure 6), where $E_l(k) = l\omega_c + k^2/2m$ is the dispersion relation for the lth Landau band. The single-phonon states of the system ($N = 1$) are completely determined by the phonon momentum q and the number l of the electron Landau band, since it follows from $p = k + q_\parallel = 0$ that $k = -q_\parallel$. The energy of this state is $\epsilon = \omega_0 + E_l(-q_\parallel)$; because of the continuous variation of $q_\parallel$ these energies form a continuum above the threshold $\epsilon = \omega_0$. Each such state corresponds to a definite state of the electron in the Landau band, and hence the density of single-phonon states with $p = 0$ above the threshold has the same singularity as the density of no-phonon states at the bottom of the Landau band. This is shown in figure 6 by the crowding together of the lines at the threshold.

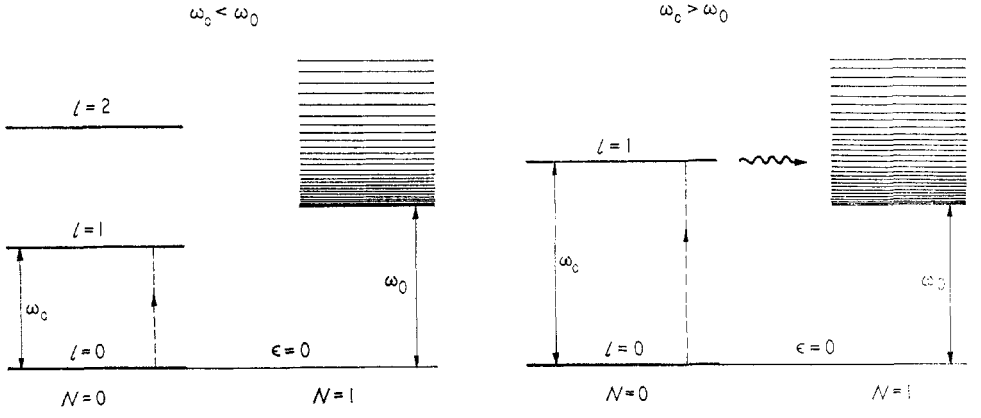

Figure 6. The spectrum of the electron–phonon system.

We now switch on the electron–phonon interaction. The level $l = 0$, $N = 0$ is repelled by all higher levels and shifts to a lower energy. The threshold of the continuous spectrum with $N = 1$ is also shifted in just the same way, but since this shift shows no rapid changes at $\omega_c = \omega_0$ we need not consider it further. The situation with the level $l = 1$, $N = 0$ is rather different. This level is displaced downwards for $\omega_c < \omega_0$ and the shift increases rapidly for $\omega_c \to \omega_0$, that is, when this level approaches the edge of the continuous spectrum, where there is a singularity in the density of states, from below. When $\omega_c > \omega_0$ this singularity lies below the level $l = 1$, so the level is shifted upwards. Moreover, for $\omega_c > \omega_0$ the $l = 1$ level lies within the continuous spectrum and becomes quasistationary. Its decay rate is proportional to the density of states at an energy $E_1(0)$ in the continuous spectrum, and therefore the level width Γ increases rapidly as $\omega_c \to \omega_0$.

At low temperature cyclotron absorption is due to transitions from the level $l = 0$ to the level $l = 1$ and, as is shown below, its behaviour is determined by the changes in the $l = 1$ level at $\omega_c = \omega_0$.

A quantitative theory using the ideas outlined above was given by Harper (1967). In terms of the model described in the introduction, branches 1 and 2 correspond to the Landau bands $l = 0$ and $l = 1$, and H is the parameter on which the spectrum depends. The dipole moment of the transition is calculated using equation (1.1), and the electronic contribution to the dielectric constant for the polarization

appropriate for cyclotron resonance is found to be of the form

$$\left.\begin{aligned} \kappa(\omega) &= 1 - \frac{\omega_p{}^2}{\omega(\omega - \omega_c - \mathscr{M}^0(\omega))} \\ \omega_p{}^2 &= \frac{4\pi n e^2}{m} \end{aligned}\right\} \tag{3.1}$$

where n is the electron density. Here $\mathscr{M}^0$ has the same type of structure as that in equation (1.3) and is given by

$$\mathscr{M}^0(\epsilon) = \int \mathrm{d}^3 q \mathscr{B}(q) \frac{(\lambda q_\perp)^2 \exp\{-(\lambda q_\perp)^2/2\}}{2(\epsilon - \omega_0 - E_0(-q_\parallel)) + \mathrm{i}0}. \tag{3.2}$$

The numerator contains the electron–phonon interaction matrix element between Landau functions $l = 0$ and $l = 1$; $q_\perp$ and $q_\parallel$ are the components of q transverse and parallel to H, and λ is the magnetic length. If we put

$$\mathscr{M}^0(\epsilon) = \Delta E(\epsilon) - \mathrm{i}\Gamma(\epsilon) \tag{3.3}$$

it is easily seen that $\Delta E(\epsilon)$ is the shift of the $l = 1$ level with energy $E_1(0) = \epsilon$, calculated in second-order perturbation theory, whilst $\Gamma(\epsilon)$ is the width of this level.

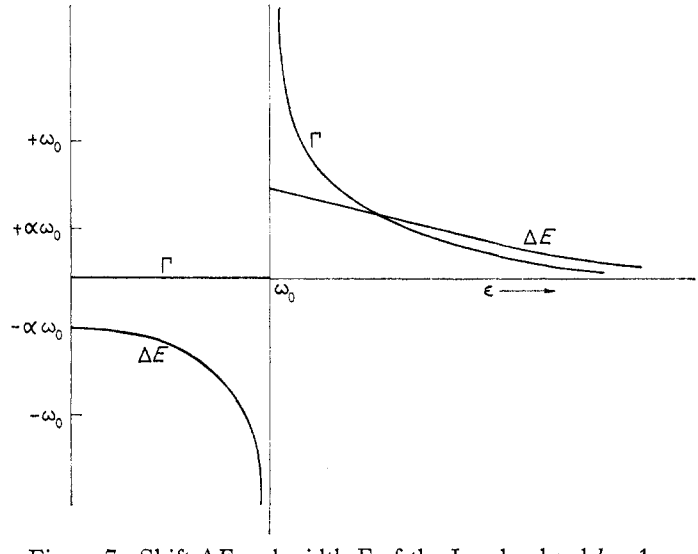

Figure 7. Shift ΔE and width Γ of the Landau level $l = 1$.

The dependence on ϵ of these quantities is shown in figure 7, which confirms the above remarks about the sign of the shift and the size of the broadening of the $l = 1$ level. It is important to note that at the threshold both the shift and the broadening tend to infinity

$$\left.\begin{aligned} \Gamma(\epsilon) &= \tfrac{1}{2}\alpha\omega_0{}^{3/2}(\epsilon - \omega_0)^{-1/2} \qquad 0 < \epsilon - \omega_0 \ll \omega_0 \\ \Delta(E) &= -\tfrac{1}{2}\alpha\omega_0{}^{3/2}|\epsilon - \omega_0|^{-1/2} \qquad 0 < \omega_0 - \epsilon \ll \omega_0 \end{aligned}\right\} \tag{3.4}$$

because of the singularity in density of states above the threshold.

Equation (3.1) has a simple interpretation. We may say that the effect of phonon interactions can be summarized by a shift ΔE and a broadening Γ of the

final state when considering the transition frequency $\omega_c = E_1(0) - E_0(0)$. All the observed features of the absorption are due to the fact that ΔE and Γ are strongly frequency dependent near the threshold.

When discussing the absorption in terms of equation (3.1) it should be remembered that this theory, which covers only single-phonon states, is valid only for $|\omega - \omega_0| \gg \alpha^2 \omega_0$ (see §4). It is important that in this region $\Gamma, |\Delta E| \ll \omega_0$, although these quantities can be much greater than their 'usual' values which are of the order of $\alpha\omega_0$, as is clear from equation (3.4). With these reservations, the frequency dependence of the absorption can be found from $\mathrm{Im}\,\kappa(\omega)$; this is shown in figure 8.

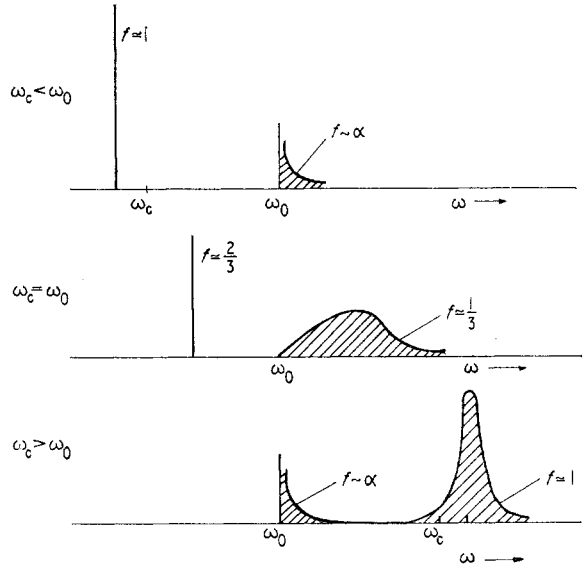

Figure 8. Variation of the free-carrier magnetoabsorption on passage through the magneto-phonon resonance.

For $\omega_c < \omega_0$ a cyclotron resonance peak shifted to *lower* frequencies by the order of $\alpha\omega_0$ has to be observed, with a width Γ', which is determined by the other unconsidered scattering mechanisms (by acoustic phonons, impurities, or by absorption of optical phonons), and oscillator strength $f \simeq 1$. There is also a weak absorption peak above the threshold which has oscillator strength $f \sim \alpha$. Two peaks, both with $f \sim 1$, should be observed at the resonance field $\omega_c = \omega_0$; one narrow peak below the threshold with width Γ', and one wide but asymmetric peak above the threshold and with a width of the order of $\alpha^{2/3}\omega_0$. Both peaks are shifted from ω_0 by the order of $\alpha^{2/3}\omega_0$. For $\omega_c > \omega_0$ a cyclotron resonance peak shifted to *higher* frequencies has to be found, with width and shift of order $\alpha\omega_0$ and oscillator strength $f \sim 1$, together with a weak absorption peak with $f \sim \alpha$ above the threshold.

The sign of the shift in the cyclotron resonance peak and its width can be understood in terms of the qualitative discussion of the spectrum given at the beginning of this section. In order to make clear the physical reasons for the appearance of a weak absorption at the threshold and also for the occurrence of two peaks close together at the resonant field, we replace the continuous spectrum of single-phonon states with a density of states singularity at the threshold by a single level at the threshold. The system will then be reminiscent of an impurity

centre and the resultant spectrum will be as in figure 3. At resonance the electron–phonon interaction splits two degenerate levels, forming two hybrid states, one below the threshold and the other above, and both of these are formed by 'mixing' the no-phonon states $l = 1$ with the single-phonon states $l = 0$ in approximately equal proportions. Because each of these states contains a large contribution from the $l = 1$ state, it is possible to have a transition with comparable oscillator strength $f \simeq 1$ to either of them from the initial state $l = 0$. This means that the cyclotron absorption peak must become a doublet at the resonant field. The interaction between these levels will become less important as the distance from resonance increases. One of them will approach $\epsilon = \omega_c$ and will contain principally the no-phonon state $l = 1$, whilst the other will approach $\epsilon = \omega_0$ and will consist mainly of the single-phonon state $l = 0$. The mixing will now be in the ratio $1 : \alpha$, and hence the oscillator strength in the line whose frequency tends to ω_0 will decrease; far from resonance this will be $f \sim \alpha$, whilst the line tending to frequency ω_c will have $f \simeq 1$.

Further development of the theory has been concerned with the effect of temperature on the distribution of electrons in the $l = 0$ Landau band. Its effect on cyclotron resonance has been discussed by Korovin (1970) (Boltzmann and Fermi distributions), Nakayama (1969) and Klyukanov and Pokatilov (1971) (Boltzmann distribution). From a qualitative point of view temperature effects are unimportant away from resonance ($\omega_c \neq \omega_0$) but have a considerable effect for $\omega_c = \omega_0$ if the thermal energy is comparable with the peak separation, ie $T \gtrsim \alpha^{2/3} \omega_0$. For InSb this means that the temperature distribution of the electrons should be taken into account for $T \gtrsim 20$ K.

We limit our discussion to nondegenerate statistics, because this is more relevant experimentally. The effect of temperature on the absorption at the resonant field is then as follows (Korovin 1970). If $T \ll \alpha^{2/3} \omega_0$, then the gap between the peaks is smeared out for $|\omega - \omega_0| \lesssim T$, and an exponentially weak absorption appears below the threshold for $|\omega - \omega_0| \gg T$, due to transitions by electrons from the tail of the distribution to the continuous spectrum. The splitting of the cyclotron resonance peak disappears for $T \gg \alpha^{2/3} \omega_0$, leaving a single peak with centre at $\omega = \omega_0$ and width of the order of T. The shoulders of this peak are sharply asymmetric; at distances $|\omega - \omega_0| \gg T$ the absorption decreases according to a power law on the high frequency side, but decreases exponentially on the low frequency side.

It was assumed above that the LO phonons had no dispersion. This is of course not strictly true, and for long waves the dispersion can be described by the expansion

$$\omega(q) = \omega_0 - \frac{1}{2\mu} q^2 \tag{3.5}$$

where μ is of the order of the geometric mean of the nuclear and electronic masses. The small parameter describing phonon dispersion is $\delta = m/\mu$. It is clear from equation (3.2) that the important values of q are $q \sim \lambda^{-1}$, and therefore the spread in phonon frequencies $\Delta\omega_0 \sim (\mu\lambda^2)^{-1} \sim \delta\omega_c \sim \delta\omega_0$. This is to be compared with the splitting $\alpha^{2/3} \omega_0$, so phonon dispersion is unimportant if $\delta \ll \alpha^{2/3}$. This was shown in a calculation of the density of states in the $l = 1$ band (Korovin and Pavlov 1968). In InSb $\alpha^{2/3} \sim 10^{-1}$ whilst $\delta \sim 10^{-3}$, and hence phonon dispersion can be neglected.

Besides the single-phonon threshold at $\epsilon = \omega_0$ considered at the beginning of this section, there are also multiphonon thresholds in the spectrum at $\epsilon = 2\omega_0$,

$3\omega_0, \ldots$. It is clear that passage of Landau levels through these thresholds will also lead to rapid variations in the spectrum of the electron–phonon system. Let us suppose, for example, that the $l = 2$ level passes through the two-phonon threshold. If we replace the singularity of each continuum by a single 'level', as was done in the previous discussion, we will then have a threefold degeneracy of the following states: $(l = 2, N = 0)$, $(l = 1, N = 1)$ and $(l = 0, N = 2)$. For $\omega_c = \omega_0$ we would therefore expect to find in the spectrum three narrowly separated 'levels' near $\epsilon = 2\omega_0$ (Korovin 1969).

The specific features of the energy spectrum of the electron + LO phonons system described in this section were a consequence only of the small dispersion of these phonons. Transverse optical (TO) phonons also have this property and hence in principle all the effects described could also occur for TO phonons at $\omega_0 = \omega_{TO}$. Additional effects could also follow from the fact that scattering by TO phonons may be accompanied by a spin flip (Pavlov and Firsov 1967). In particular this may affect the EPR spectrum when the spin splitting $\omega_s = \omega_{TO}$ (Korovin and Pavlov 1967b).

3.2. *Free-carrier absorption in InSb*

The most complete experimental results for cyclotron resonance in n-InSb in fields in the neighbourhood of H_0 were reported by Summers *et al* (1968a,b). Typical results are shown in figure 9. At low temperature (15 K, upper curve)

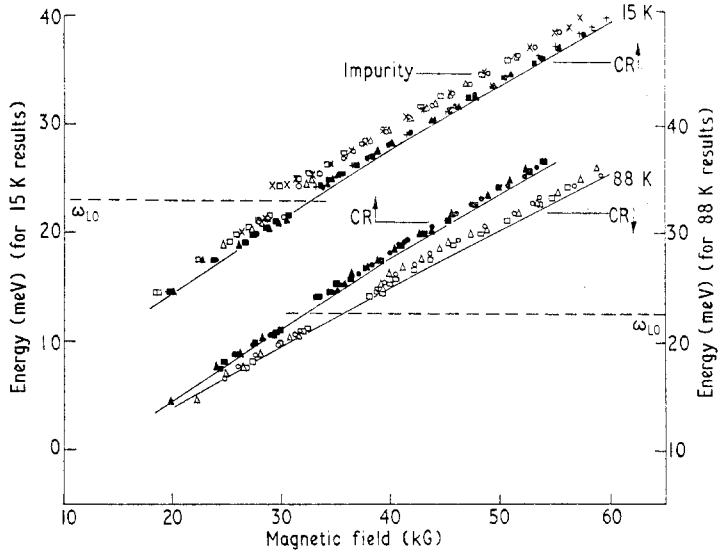

Figure 9. Variation of cyclotron resonance band position in InSb. From Summers *et al* (1968a).

impurity transitions (open points) and transitions between spin-up levels (full points) are observed. At higher temperature (88 K, lower curves, displaced downwards by 10 meV for clarity) the impurity levels are empty and transitions of free electrons with spin up (full points) and spin down (open points) are observed. The shift in the cyclotron resonance line on passing through resonance is clearly visible in both cases and its magnitude $\Delta\omega_c \simeq 0{\cdot}5$ meV. If we take $\alpha = 0{\cdot}02$ and

$\omega_{LO} = 24$ meV for n-InSb we would expect theoretically to find $\Delta\omega_c \simeq \alpha\omega_{LO} = 0{\cdot}5$ meV; this agrees very well with the observed value. The field dependence of the cyclotron resonance line width at 15 K is shown in figure 10. This increases rapidly as the resonance is approached from higher fields, which agrees completely with the behaviour of Γ in figure 7. If from the linewidth we subtract the monotonic background which is not related to the emission of optical phonons (by extrapolation in figure 10), we may compare the remaining width with the theoretical behaviour of Γ. This is done in figure 11, where the dashed line is

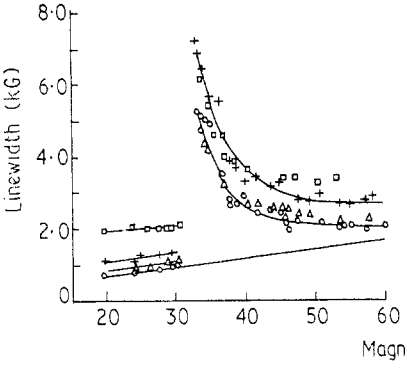

Figure 10. Variation of the cyclotron resonance linewidth on passage through magnetophonon resonance at 15 K. From Summers *et al* (1968b).

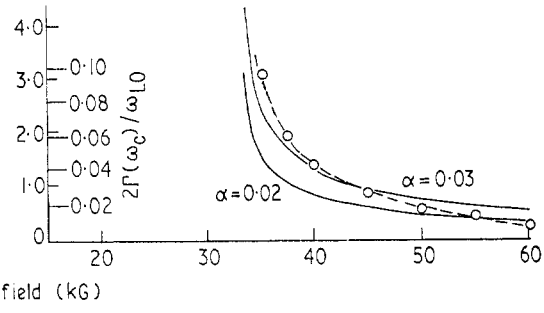

Figure 11. Comparison of theoretical and experimental cyclotron resonance linewidths at 15 K. From Summers *et al* (1968b).

drawn through the experimental points and the solid lines are the theoretical predictions for two values of α. If we note that the theory does not take account of thermal smearing ($T \simeq 1$ meV, which is comparable with $\Gamma \simeq 3$ kG $\simeq 2$ meV) the agreement is very good.

There are also experimental results on cyclotron resonance in n-InAs (Harper *et al* 1970); here $\Delta\omega_c \simeq 2$ meV which agrees well with $\alpha\omega_{LO} = 1{\cdot}5$ meV for the known values $\alpha = 0{\cdot}05$ and $\omega_{LO} = 29$ meV.

The theoretically predicted splitting of the cyclotron resonance peak at the resonant field was not observed experimentally, probably because the size of the splitting $\alpha^{2/3}\omega_{LO} \simeq 2$ meV was of the same order as the frequency range over which lattice reflection ($\omega_{LO} - \omega_{TO} \simeq 2$ meV) and lattice absorption ($|\omega - \omega'_{TO}| \simeq 1$ meV) are important (Summers *et al* 1968b).

The splitting of the peak at resonance can also be observed in combined resonance (Rashba 1964), in which a transition from the $l = 0$ level to the $l = 1$ level is accompanied by a spin flip (figure 12). Since the emission of a LO phonon takes place without spin flip, the decay threshold of the final state is $\omega_c = \omega_{LO}$, as in ordinary cyclotron resonance, although absorption occurs not at frequency $\omega = \omega_c$, but at $\omega = \omega_c + \omega_s$, where ω_s is the spin splitting of the $l = 0$ Landau level. In InSb $\omega_s \simeq 10$ meV at $H = 34$ kG, so the electronic absorption is shifted well away from the region of lattice absorption and reflection. The experimental data for InSb at 30 K (McCombe and Kaplan 1968) are shown in figure 13, which clearly shows both the peak shift (of order 0·7 meV) on passage through resonance and the peak splitting at the resonant field (of order 1·5 meV, which may be compared with the theoretical estimate of $\alpha^{2/3}\omega_{LO} \simeq 2$ meV).

It is clear that this effect must also show itself in a number of other ways besides combined resonance. Some of these are due to breakdown of the selection rule $\Delta l = \pm 1$ and the resultant possibility of observing transitions from the $l = 0$ level to the $l = 2$ level, for which the onset of decay occurs at half the field $\omega_c = \frac{1}{2}\omega_{LO}$.

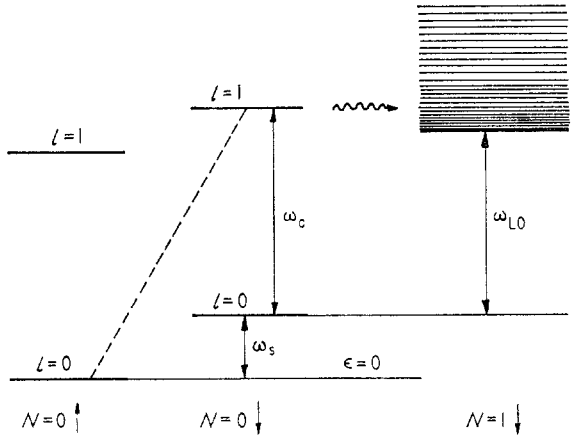

Figure 12. Level diagram and transitions in combined resonance.

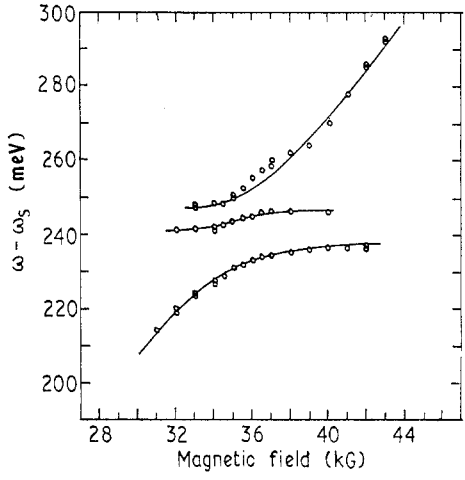

Figure 13. Position of absorption peaks in combined resonance (the spin splitting energy is excluded). From McCombe and Kaplan (1968).

Johnson and Dickey (1970) did not observe this effect but, as the authors point out, this may be due to a lack of experimental sensitivity. In this connection we note the remark made by S D Smith in the discussion following the paper of Larsen and Johnson (1966), that anomalies were observed in the Faraday and Voigt effects at both $\omega_c = \omega_{LO}$ and at $\omega_c = \frac{1}{2}\omega_{LO}$.

Another consequence of this effect is due to the existence in the spectrum of multiphonon thresholds at $\epsilon = 2\omega_{LO}, 3\omega_{LO}, \ldots$, when a new channel becomes available for the decay of the final level with the emission of the appropriate number of phonons. Anomalies in the intensity of combined resonance, found at $H \simeq 70$ kG in InSb (McCombe *et al* 1968), are probably due to the passage of the $l = 1$ level

through the threshold $2\omega_{LO}$ at $\omega_c = 2\omega_{LO}$. In principle, one would also expect to find anomalies in the cyclotron–phonon resonance (Bass and Levinson 1965, Bakanas and Levinson 1969) when the transition between two Landau levels is accompanied by the emission of an LO phonon. However, although a resonance of this type has definitely been observed (McCombe *et al* 1967, Enck *et al* 1969), the corresponding anomaly at $\omega_c = \omega_{LO}$ has not yet been found (Summers *et al* 1968b).

3.3. *Impurity transitions in InSb*

Absorption anomalies at resonant fields are observed not only for free electrons but also for bound electrons localized on impurity centres. The effect of a magnetic field on an impurity centre is determined by the ratio of the magnetic energy ω_c to the Coulomb energy $R = me^4/2\kappa_0^2 \ldots$, ie on the parameter $\gamma = \omega_c/R$. For

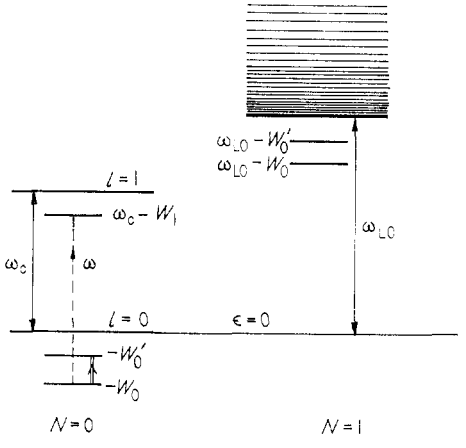

Figure 14. Level scheme and transitions for impurity absorption in a magnetic field.

electrons in InSb we have $R \simeq 1$ meV, so $\gamma \simeq 20$ at the resonant field. This means that the Coulomb field is a small perturbation, and hardly mixes the states in different Landau bands. Since the Coulomb perturbation does not remove the axial symmetry about $\boldsymbol{H}$ it does not mix states with different angular momentum components along $\boldsymbol{H}$. It follows that the impurity field affects only the motion along $\boldsymbol{H}$; the result is that each Landau band has beneath it its own system of localized levels, which are shifted in practically the same way as the corresponding band (Elliott and Loudon 1960) by the application of a magnetic field. It is useful to note that for $\gamma \gg 1$ and the polarization used in cyclotron resonance a single transition between the lowest localized levels in bands $l = 0$ and $l = 1$ is dominant (Hasegawa and Howard 1961).

A typical level scheme is shown in figure 14. The left hand side corresponds to no-phonon states. Two localized levels with binding energies W_0 and W_0' are shown below the bottom of the $l = 0$ band, and a single localized level with binding energy W_1 is shown below the $l = 1$ band. The dominant transition is shown by a dashed line. The right hand side of the figure corresponds to single-phonon states to which the localized no-phonon states are connected by the electron–phonon interaction. Only states related to the $l = 0$ band are shown; the discrete spectrum is associated with a localized electron, and the continuous with a free electron.

In InSb $W_0 \simeq 3$ meV (Kaplan 1966) for fields near to resonance. There are no free carriers at helium temperature and only impurity cyclotron resonance is observed (Kaplan and Wallis 1968) at a frequency $\omega = \omega_c + (W_0 - W_1)$, which gives $W_0 - W_1 \simeq 1$ meV.

Let us now consider the changes in the absorption as H increases and the final state with energy $\omega_c - W_1$ moves upwards. For $\omega_c = \omega_0 - (W_0 - W_1)$ this level becomes degenerate with the lowest level of the single-phonon system at $\omega_0 - W_0$. This degeneracy is lifted by the electron–phonon interaction so the absorption peak at $\omega = \omega_0$ must be split. At a somewhat higher field, when $\omega_c = \omega_0 - (W_0' - W_1)$, the final state has the same energy as the next state of the single-phonon system, with energy $\omega_0 - W_0'$; hence a splitting of the peak should be observed at a frequency $\omega = \omega_0 + (W_0 - W_0')$. Finally, for $\omega_c = \omega_0 + W_1$ the final state enters the continuous spectrum, which must give rise to a split peak at a frequency $\omega = \omega_0 + W_0$ together with a rapid broadening of its short-wavelength component.

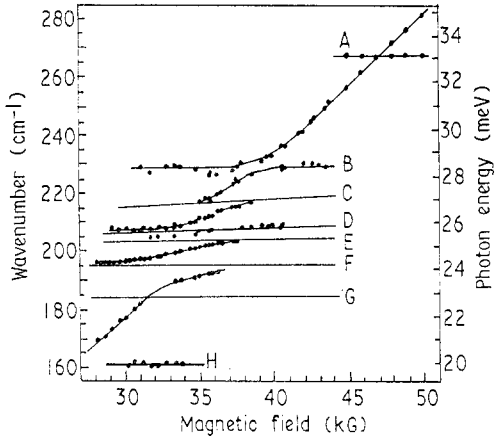

Figure 15. Impurity absorption in InSb in a strong magnetic field: A, LO + 2Δ; B, LO + Δ; C, LO + (001); D, LO + (0$\bar{2}$0); E, LO + (0$\bar{1}$0); F, LO; G, TO; H, LO − Δ. From Kaplan and Wallis (1968).

The experimentally observed splittings and corresponding pinnings agree well with this picture. The most detailed description is given by photoconductivity measurements in InSb, whose spectral variation parallels that of the absorption coefficient (Kaplan and Wallis 1968). It is clear from figure 15 that the first pinning, as expected, occurs at the frequency of the LO phonon, and this is followed by three pinnings at frequencies of the LO phonon + the energy of a transition in the impurity centre. It is important for the interpretation that these energies were determined independently by far infrared measurements (Kaplan 1966) (heavy line in figure 14). The absorption peaks in figure 15 denoted by LO ± Δ and LO + 2Δ have not been clearly identified. An attempt was made by Ruvalds *et al* (1971) to explain the pinning at LO + Δ by postulating the existence of a bound state consisting of two phonons: LO and TA(L) (a transverse acoustic phonon at the Brillouin zone boundary).

It should be remembered that the above description of the various splittings assumed that the size of the splitting was small compared to both the binding energies and their differences. This is not always satisfied in InSb, and consequently there is an overlap in the field ranges where split peaks are observed, and as a result

more than two peaks are observed at the same time. The experimental results of Kaplan and Wallis (1968) have been analysed by Wallis *et al* (1970).

Two superposed pinnings have also been observed in combined resonance of localized electrons (Dickey and Larsen 1968, McCombe and Kaplan 1968). In the former paper the presence of two pinnings was explained by the participation of TO phonons as well as LO phonons. However, careful measurements (McCombe *et al* 1969, McCombe and Wagner 1971) eliminated this interpretation and showed that TO phonons do not affect the absorption.

Meanwhile pinning arising due to coupling of holes to both LO and TO phonons was found recently in spectra of acceptor centres in InSb (Kaplan *et al* 1972).

The broadening in the impurity cyclotron resonance peak as the level enters the continuous spectrum is similar to that for free-carrier cyclotron resonance (Summers *et al* 1968a,b); this shows that the broadening is related to the dissociation of the localized state. In recent experiments of impurity cyclotron–phonon resonance and cyclotron resonance harmonics in InSb, Ngai and Johnson (1972) observed pinning at various two-phonon energies.

3.4. *Resonant polaron effects in CdTe*

For a number of reasons CdTe is a very attractive material for the study of the magneto-optic effects of polaron phenomena. There are now available very pure samples ($n = 2 \times 10^{14}$ cm^{-3} at $T = 77$ K) with high mobilities ($\mu = 6 \times 10^4$ cm^2 V^{-1} s^{-1}, which corresponds to a relaxation time $\tau = 3 \times 10^{-12}$ s) (Mears *et al* 1968). Polaron effects should be prominent, as $\alpha = 0{\cdot}4$. For this moderate value of the coupling constant it is still reasonable to interpret effects from the point of view of the weak coupling theory, or perhaps of some of its improvements, by intermediate-coupling methods (Larsen 1964). Finally, because the effective mass ($m = 0{\cdot}096m_0$) is not too large, the resonant field is still attainable experimentally ($H_0 \simeq 180$ kG). A simple spherical band makes quantitative calculations possible.

Experiments on infrared and far infrared absorption in fields H up to 100 kG were reported by Waldman *et al* (1969) and Harper *et al* (1970). The Landau level $l = 2$ enters the continuous spectrum at $H \simeq 90$ kG and polaron effects should be observable. Although these considerations have been applied to the interpretation of experiments on the $l = 1 \rightarrow l = 2$ transition, the interpretation is not yet unambiguous.

A more convincing demonstration of the presence of a resonant interaction with optical phonons is given by the impurity absorption spectrum for transitions between Zeeman levels (Cohn *et al* 1970, 1972). For CdTe, unlike InSb, $\gamma < 1$ even in the highest available fields, so that the dominant transitions are the same as for $H = 0$. The transitions $1s \rightarrow 2p_M$, $M = \pm 1$ were observed, and the position of the $1s \rightarrow 2p_{+1}$ line showed a deviation which it is natural to explain by pinning of the $2p_{+1}$ level to the level $1s + $ LO phonon at a field $H \simeq 100$ kG.

3.5. *Raman scattering*

The electron–phonon interaction has a strong effect on Raman scattering, since a free electron with a parabolic dispersion relation gives no inelastic scattering of light when it is placed in a magnetic field. This can be understood from the correspondence principle by noting that such an electron is a harmonic oscillator and therefore does not mix frequencies. This follows formally from the selection rules

for l and the equal spacing of the electron Landau spectrum. The selection rules allow Raman scattering with transitions $\Delta l = \pm 2$, ie with a frequency shift $\bar{\omega} = \pm 2\omega_c$, but because of energy conservation and the equal spacing of the spectrum the matrix element for this transition is zero. Interaction with phonons does not change the selection rules (see §4), but it does disturb the equal spacing of the spectrum; this allows scattering with $\bar{\omega} \simeq \pm 2\omega_c$. At low temperature and carrier densities, when only the level $l = 0$ is populated, only Stokes scattering associated with a transition to the $l = 2$ level will be observed. It is clear that anomalies in the Raman scattering must be expected when this level passes through the threshold of the single-phonon or two-phonon spectra, ie for $\omega_c = \frac{1}{2}\omega_0$ or $\omega_c = \omega_0$.

The first case was considered theoretically by Harper (1969), who showed that the Raman scattering line for ω_c near $\frac{1}{2}\omega_0$ behaves in just the same way as the cyclotron resonance line for ω_c near ω_0 (it is shifted and broadened as H increases). The oscillator strength of this line $f \sim \alpha^2$. At resonance $\omega_c = \frac{1}{2}\omega_0$ the Raman scattering line becomes a doublet with $f \sim \alpha^{4/3}$ and a splitting of order $\alpha^{2/3}\omega_0$.

The second case was studied by Ngai (1971) who showed that the Raman scattering line splits into a triplet at resonance (see the end of §3.1).

There have as yet been no experimental measurements of Raman scattering effects of the kind described in §3.2. However, we should note in this connection the experiments of Vella-Coleiro (1969) who measured the intensity of anti-Stokes Raman scattering with frequency shift $\bar{\omega} = \omega_{LO}$ in CdS for magnetic fields of 100–250 kG. It was found that this intensity increased in a resonant manner when the LO phonon energy was equal to the separation between two Landau levels, including the spin splitting, ie $\omega_{LO} = \Delta l\omega_c + \Delta s\omega_s (\Delta l = 3\text{–}8, \Delta s = 0, \pm 1)$.

4. The magnetopolaron spectrum near the decay threshold: bound states

The problem of calculating the magnetopolaron spectrum in the neighbourhood of the threshold for emission of an LO phonon arose in connection with the experiments on magnetophonon resonance in absorption (see §3). The most natural approach to the problem was suggested by Korovin and Pavlov (1967), who calculated the Green function G of an electron in the $l = 1$ Landau level, taking into account only the simplest diagram $\mathcal{M}_1$ (figure 16) for the mass operator $\mathcal{M}$.

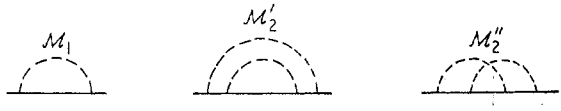

Figure 16. Diagrams for the self-energy operator. The dashed lines correspond to phonons and the full lines to electrons.

This corresponds to a model including only no-phonon and single-phonon states, as in §§1 and 3.1. In the resonant situation $\omega_c = \omega_0$, structure with a characteristic scale $\alpha^{2/3}\omega_0$ appears in the spectrum near the threshold $\epsilon = \omega_0$, and this is responsible for the absorption anomalies. It turns out, however, that despite the weak coupling ($\alpha \ll 1$), perturbation theory for the mass operator (an expansion of $\mathcal{M}$ in powers of α) is not valid near the threshold $\epsilon = \omega_0$, and moreover this invalidity is not related to the resonance $\omega_c = \omega_0$. A calculation of the subsequent terms $\mathcal{M}_2'$ and $\mathcal{M}_2''$ in the above mentioned expansion (figure 16) shows that the lowest order term dominates only for $|\epsilon - \omega_0| \gg \alpha\omega_0$. This estimate justifies the calculation

of the resonant structure of the spectrum on a scale $\alpha^{2/3}\omega_0$; however, it is natural to ask whether there exists some finer structure in the spectrum, unrelated to the resonance, in the region near the threshold where perturbation theory is inapplicable.

Diagrams with no intersecting phonon lines (type $\mathscr{M}_2'$) become important for $|\epsilon-\omega_0|\sim\alpha\omega_0$. These may easily be summed to all orders in α (Korovin and Pavlov 1968, Levinson *et al* 1971b); this gives a value of $\mathscr{M}$ which differs from $\mathscr{M}_1$ only by a minor renormalization of the threshold by a quantity of order $\alpha\omega_0$. However, in the region $|\epsilon-\omega_0|\lesssim\alpha^2\omega_0$ diagrams with phonon intersections (type $\mathscr{M}_2''$) become important. A summation of these diagrams was carried out by Levinson (1970), and this leads to an integral equation for the electron–phonon vertex Γ. A study of this equation for Γ showed that below the threshold in the energy range $|\epsilon-\omega_0|\lesssim\alpha^2\omega_0$ there are indeed additional branches of the magnetopolaron spectrum which form an infinite sequence with the threshold as its limit. The states corresponding to these branches are bound states of an electron and a phonon for all values of the longitudinal momentum p.

4.1. *The energy-level scheme and the effect of bound states on the absorption*

We shall discuss here the results of theoretical calculations of the magnetopolaron spectrum by Levinson (1970), Levinson *et al* (1971c) and Kaplan and Levinson (1972a). The theory itself is described in §4.2. The theory is based on the assumptions enumerated in §3.1, together with the assumption that the interaction is weak $\alpha\ll 1$.

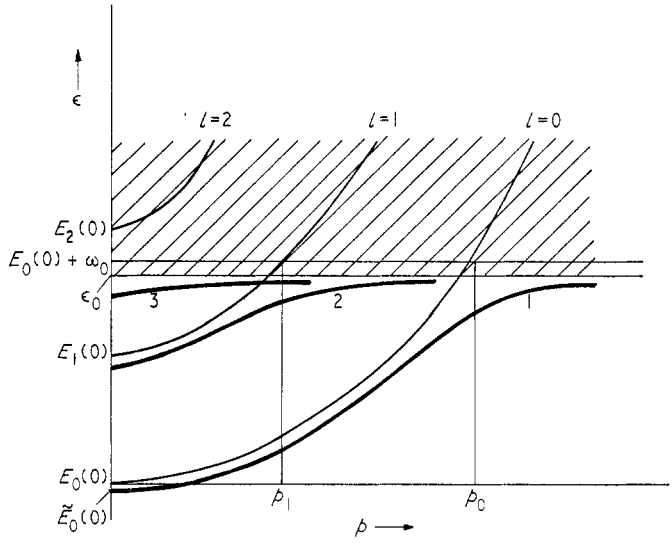

Figure 17. Various branches in the magnetopolaron spectrum. The shaded region corresponds to the continuous spectrum.

The structure of the spectrum is illustrated in figure 17. The thin lines represent the unperturbed electron spectrum $E_l(p)$ in the absence of the interaction, and the heavy lines show the spectrum of the system with interaction. If the bottom of the unperturbed band l lies below the threshold ω_0 ($l=0,1$ in the figure), there is a threshold momentum p_l corresponding to this band. For $p<p_l$ there is only a slight

renormalization of the unperturbed spectrum, which for small p reduces to a shift in the bottom of the band and a change in the effective mass. Both these effects are proportional to α (Larsen 1964). It is obvious that the lowering of the bottom of the $l = 0$ band leads to a renormalization of the threshold; the true threshold ϵ_0 lies below the unperturbed ω_0. When p tends to p_l and ϵ tends to ϵ_0 a major reconstruction of the unperturbed branch takes place. The spectrum does not reach the threshold for $p \simeq p_l$, but remains below it by an amount proportional to $\alpha^{2/3}$. For $p > p_l$ the spectrum asymptotically approaches the threshold, remaining below it by an amount proportional to α^2. This picture corresponds to the unlimited pinning described in § 1.

Besides the branches which are genetically related to the branches of the unperturbed spectrum (1 and 2 in figure 17), the true spectrum contains additional branches whose existence is entirely due to the interaction (3 in figure 17). There are an infinite number of such branches, all lying at a distance proportional to α^2 away from the threshold and forming a sequence whose limit is at the threshold (this is not shown in figure 17).

The states in the two types of branches described above differ appreciably in the average number of phonons $\langle N \rangle$ which take part in their formation. For branches of the first type $\langle N \rangle$ increases as p increases, from $\langle N \rangle \sim \alpha$ to $\langle N \rangle \simeq 1$; but for branches of the second kind $\langle N \rangle \simeq 1$ for all p. Hence the states in these branches can all be described as bound states of an electron and a phonon for all p. If we write the dispersion relation for these branches in the form

$$\epsilon(p) = \tilde{E}_0(0) + \omega_0 - W_l(p) \tag{4.1}$$

where $\tilde{E}_0(0)$ is the displaced bottom of the $l = 0$ band, then W is the binding energy. This interpretation is supported by the following argument. Since the energy $\epsilon(p)$ of an elementary excitation is practically independent of its momentum p, it is clear that the electron contribution to the total momentum and total energy of the excitation is small, otherwise the dependence of ϵ on p would be as strong as in the unperturbed spectrum. Hence, the electron is at the bottom of the $l = 0$ band, and the energy and momentum are almost entirely carried by the phonon; the electron determines only the charge and spin of the elementary excitation.

We have a peculiar situation for the resonance at $\omega_c = \omega_0$ for the branch with $l = 1$, since there is a branch of the spectrum which is genetically related to the unperturbed spectrum for $\omega_c < \omega_0$, but there is no such branch for $\omega_c > \omega_0$. We now consider in more detail the lowest state with $p = 0$. For $\omega_c < \omega_0$ this is a polaron state with $\langle N \rangle \sim \alpha$, but for $\omega_c > \omega_0$ it is a bound state with $\langle N \rangle \simeq 1$. At resonance, for $\omega_c = \omega_0$, it is a hybrid state with $\langle N \rangle \simeq \frac{1}{2}$, lying about $\alpha^{2/3}\omega_0$ below the threshold. It follows that a transition from polaron states to bound states via hybrid states can be made both by varying p for fixed H and by varying H for fixed p.

In order to clarify the role of the magnetic field in the formation of bound states we now consider the emission of a phonon by an electron in the lowest Landau band (figure 18). The transition probability for this process is

$$w = 2\pi |\langle \mathscr{H}_{eL} \rangle|^2 \rho(\epsilon - \omega_0). \tag{4.2}$$

This contains the interaction matrix element, whose square is small and proportional to α, and the level density in the final state with energy $\epsilon - \omega_0$. If ϵ lies near the threshold ω_0, the final state is almost at the bottom of the band where the level density has a singularity. Hence, despite the weakness of the interaction, the

transition probability w may no longer be small, and this means that the interaction is effectively no longer weak. This is just the reason why bound states may arise. Usually the number of phonons in the 'cloud' $\langle N\rangle \sim \alpha \sim w/\omega_0 \ll 1$. It follows from this that to produce a bound state, where $\langle N\rangle \simeq 1$, we must satisfy the condition $w \sim \omega_0$. The energy range above the threshold in which this condition is satisfied

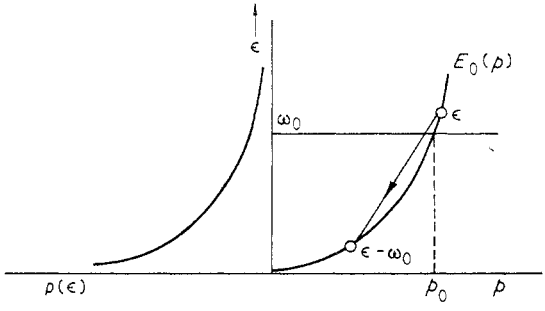

Figure 18. Electron transition with emission of an optical phonon and density of states in the Landau band.

can be estimated by substituting in equation (4.2) the well known expression for the density of states

$$\rho(\epsilon) = \frac{V}{(2\pi)^3}\frac{2\pi}{\lambda^2}\left(\frac{2m}{\epsilon}\right)^{1/2} \tag{4.3}$$

and by writing $|\langle \mathscr{H}_{eL}\rangle|^2 \sim |c_q|^2$. Then, by taking $\omega_c \sim \omega_0$ and $\Phi \sim 1$, we find that the range is $\epsilon - \omega_0 \sim \alpha^2\omega_0$. It is reasonable to suppose that the energy range of bound states below the threshold is of the same order of magnitude, ie that the binding energy $W \sim \alpha^2\omega_0$.

The existence of electron–phonon bound states with $p = 0$ strongly affects the spectral dependence of optical effects such as absorption or Raman scattering, in which the electronic transition is accompanied by the creation of an optical phonon. In this type of process the continuous spectrum above the threshold must be accompanied by a discrete spectrum below the threshold (Kaplan and Levinson 1972b), in complete analogy to the way in which this occurs in the well known situation of exciton absorption. The expected form of the electronic absorption in the neighbourhood of the LO phonon frequency is shown in figure 19. The dashed curve shows the absorption calculated from perturbation theory, without taking bound states into account.

The branches of both the true spectrum and the unperturbed spectrum can both be labelled by Landau quantum numbers, despite the fact that the electron–phonon interaction mixes states with different l. This apparently paradoxical assertion can be justified as follows. The true spectrum can be regarded as that of some effective hamiltonian $\mathscr{H}_{eff}$ instead of the unperturbed $\mathscr{H} = (1/2m)(\boldsymbol{p} - e\boldsymbol{A}/c)^2$. If the electron–phonon system is axially symmetric in a magnetic field, $\mathscr{H}_{eff}$ must be a function of $(\boldsymbol{p} - e\boldsymbol{A}/c)_\perp{}^2$ and $p_\parallel{}^2$ (the subscripts $\perp$ and $\parallel$ denote components with respect to $\boldsymbol{H}$); but then the usual Landau wavefunctions will be eigenfunctions of $\mathscr{H}_{eff}$. It is thus clear that the selection rules for transitions between the states of the true spectrum will be just the same as those between the unperturbed states. We note that the bound state branches exist not only for $l \geqslant 0$, as in the unperturbed

spectrum, but also for $l<0$. The retention of the term 'Landau quantum number' for negative l is justified by the fact that transitions with $l<0$ are governed by the same selection rules as for $l\geqslant 0$ (Kaplan and Levinson 1972b). Thus, if as in §3.1 we suppose that there are electrons only at the bottom of the $l=0$ band, then bound states with $l=\pm 1$ will contribute to intraband absorption of left or right hand circularly polarized light. States with $l=0, \pm 2$ will take part in Raman scattering. The binding energies $W_l(0)$ for $l=0, \pm 1, \pm 2$ have the same dependence

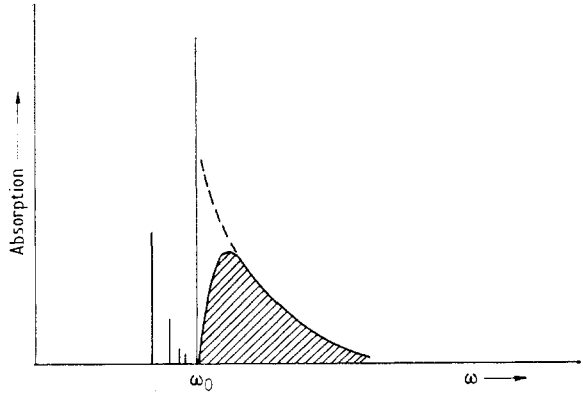

Figure 19. Effect of bound states on electronic absorption in a magnetic field.

on H and are of the same order of magnitude. Kaplan and Levinson (1972b) showed that for the important case of a polarization electron–phonon interaction

$$\left.\begin{aligned} W_l(0) &\sim \alpha^2\omega_0\left(\frac{\omega_c}{\omega_0}\right)^4 \qquad \omega_c \ll \omega_0 \\ &\sim \alpha^2\omega_0 \qquad\qquad \omega_c \gg \omega_0. \end{aligned}\right\} \tag{4.4}$$

It is easy to reach the high-field region for InSb, but the corresponding value of W is of the order of 10^{-2} meV which is not observable experimentally. One should therefore use materials with a greater coupling constant α and the lowest possible effective mass m. The best combinations of α and m are found in II–VI compounds made up of heavy elements (ionic–metallic binding). In CdTe (see §3.4) fields in which $\omega_c \sim \omega_0$ are experimentally attainable, and here we have $W\sim 3$ meV. Collision broadening is much less than this in pure samples; $1/\tau \sim 0{\cdot}2$ meV. We may therefore expect bound states to be clearly evident in the optical properties, even if an unfavourable numerical factor reduces the magnitude of W by an order of magnitude.

4.2. *Theory (weak coupling)*

The spectrum of charged excitations of the electron–phonon system is determined by the poles of the single-particle (electron) Green function G, or by the poles of the two-particle (electron–phonon) Green function K; moreover, because the number of phonons is not conserved, the spectra of G and K are the same (Kaplan and Levinson 1972a).

Near the threshold $\epsilon=\omega_0$ the function G may be found by using a method developed by Levinson *et al* (1971c), and based on the ideas of Pitaevskii (1959)

on the study of the spectrum near a decay threshold. Technically, the problem is simplified by the fact that the exact Green function is diagonal in the Landau representation (Holstein 1964, Dworin 1965, Levinson *et al* 1971a), and also because a gauge-invariant diagram technique may be used which does not contain the electron quantum numbers p_x or M, the choice of which depends on the calibration of the vector potential (Levinson *et al* 1971a). This approach was used to derive the spectrum of G for $l \geqslant 0$ and the DO interaction (Levinson 1970, Levinson *et al* 1971c).

An equivalent but technically more convenient approach is based on an examination of the two-particle function K and of the corresponding amplitude $\mathscr{T}$ for the scattering of a phonon by an electron. In this method the spectrum of bound states is determined by the poles of $\mathscr{T}$, and the wavefunctions of these states can be found from the residues of K. Separation of the troublesome sections over one electron and

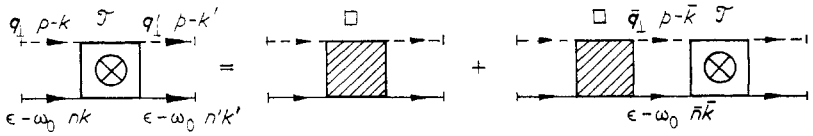

Figure 20. Equation for the scattering amplitude of a phonon by an electron.

one phonon line in $\mathscr{T}$ leads to the equation in figure 20, where □ has no troublesome sections. In this figure n is the oscillatory Landau quantum number, k is the longitudinal (parallel to $\boldsymbol{H}$) electron momentum, p is the total longitudinal momentum of electron and phonon, ϵ is the total energy parameter and $\boldsymbol{q}_\perp$ is the transverse phonon momentum.

Since both the Green function G of the internal line with energy $\epsilon - \omega_0 \simeq 0$ and □ can be expanded in powers of α, then to lowest order we may replace G by the free particle G^0 and take the diagrams with two vertices for □ (figure 21). In the

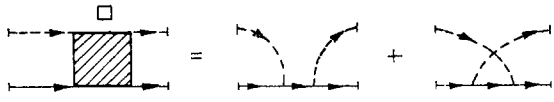

Figure 21. Kernel of the equation for the scattering amplitude.

integration in the troublesome section it is necessary to take into account the contribution only from states near the threshold, for which a real decay is possible, ie $\bar{n} = 0$ and $\bar{k} = 0$. If we put $n = n' = 0$ and $k = k' = 0$, we get an equation for $\mathscr{T}$ which is an integral equation in just $\boldsymbol{q}_\perp$. In this we may put $\epsilon = \omega_0$ in □ and in the other regular quantities. The equation then takes the following form

$$\mathscr{T}(\epsilon p;\, \boldsymbol{q}_\perp \boldsymbol{q}'_\perp) = \square(p;\, \boldsymbol{q}_\perp \boldsymbol{q}'_\perp)$$

$$+ \tilde{\mathscr{M}}(\epsilon) \int \frac{\mathrm{d}\bar{\boldsymbol{q}}_\perp}{2\pi/a^2} \square(p;\, \boldsymbol{q}_\perp \bar{\boldsymbol{q}}_\perp) \Phi(p;\, \bar{\boldsymbol{q}}_\perp)$$

$$\times \exp\left(-\frac{\mathrm{i}a^2}{2}[\boldsymbol{q} - \bar{\boldsymbol{q}}, \bar{\boldsymbol{q}} - \boldsymbol{q}']\right) \mathscr{T}(\epsilon p;\, \bar{\boldsymbol{q}}_\perp \boldsymbol{q}'_\perp) \qquad (4.5)$$

where the square brackets denote the component along $\boldsymbol{H}$ of the vector product,

$$\left.\begin{aligned} \tilde{\mathscr{M}}(\epsilon) &= -\mathrm{i}\tilde{\alpha}\omega_0 \frac{p_0}{\{2m(\epsilon-\omega_0)+\mathrm{i}0\}^{1/2}} \\ \operatorname{Im}\tilde{\mathscr{M}}(\epsilon) &< 0 \\ \tilde{\alpha} &= \frac{\alpha}{2}\frac{\omega_c}{\omega_0} \\ a^2 &= c/eH \end{aligned}\right\} \tag{4.6}$$

$$\left.\begin{aligned} \Phi(p;\, q_\perp) &= 1 \qquad \text{DO} \\ &= \frac{{p_0}^2}{{q_\perp}^2+p^2} \qquad \text{PO.} \end{aligned}\right\} \tag{4.7}$$

In order to eliminate the phase factor and symmetrize the kernel we replace $\mathscr{T}$ and $\square$ by the primed quantities according to the prescription

$$\mathscr{T}'(\boldsymbol{q}_\perp, \boldsymbol{q}'_\perp) = [\Phi(p;\, q_\perp)\,\Phi(p;\, q'_\perp)]^{1/2} \exp\left(-\frac{\mathrm{i}a^2}{2}[\boldsymbol{q}_\perp, \boldsymbol{q}'_\perp]\right)\mathscr{T}(\boldsymbol{q}_\perp \boldsymbol{q}'_\perp) \tag{4.8}$$

and similarly for $\square'$. It then turns out that $\square'$, and also $\mathscr{T}'$, are functions only of the difference in the azimuthal angles ϕ and ϕ' of the momenta $\boldsymbol{q}_\perp$ and $\boldsymbol{q}'_\perp$. We expand them in a Fourier series of the form

$$\left.\begin{aligned} \mathscr{T}'(\boldsymbol{q}_\perp, \boldsymbol{q}'_\perp) &= \sum_{l=-\infty}^{+\infty} \exp\{\mathrm{i}l(\phi-\phi')\}\mathscr{T}_l(t,t') \\ t &= a^2 {q_\perp}^2/2 \end{aligned}\right\} \tag{4.9}$$

and obtain separate integral equations in t with kernels $\square$ for each $\mathscr{T}_l$. Let us now introduce the dimensionless quantities

$$\left.\begin{aligned} \lambda &= -\frac{1}{\omega_0}\tilde{\mathscr{M}} \\ L &= -\omega_0 \square \\ R &= -\omega_0 \mathscr{T}. \end{aligned}\right\} \tag{4.10}$$

The equation for $\mathscr{T}_l$ then transforms to the standard form of a Fredholm equation for the resolvent

$$R(t,t') = L(t,t') + \lambda \int_0^\infty \mathrm{d}\bar{t}\, L(t,\bar{t})\, R(\bar{t},t') \tag{4.11}$$

where the parameter λ is a function of ϵ and the kernel L is a function of lp.

It is now clear that $\mathscr{T}$ has a singularity in ϵ when $\lambda(\epsilon)$ is equal to one of the eigenvalues λ^r of the kernel L. This eigenvalue, as is the kernel, is a function of lp. The singularity corresponds to a bound state if it is below the threshold, ie for $\epsilon < \omega_0$ when $\lambda(\epsilon) > 0$. We therefore finally obtain the result that the spectrum is determined by the positive eigenvalues of the kernel, and from equations (4.6) and (4.10) we have the dispersion relation

$$\epsilon_l^r(p) = \omega_0\left(1 - \frac{\tilde{\alpha}^2}{(\lambda_l^r(p))^2}\right). \tag{4.12}$$

For $l \geqslant 0$ this spectrum is the same as that of G. For $l < 0$ we obtain new branches, which have not been found previously, since the branches with $l < 0$ in G have a smaller residue than the branches with $l \geqslant 0$.

The use of the above approach to the study of the spectrum is determined by the form of the kernel L, which for the most interesting case $p = 0$ we shall write as

$$\left.\begin{aligned} L_l(t,t') &= (\Phi(t)\,\Phi(t'))^{1/2} \exp\left(-\frac{t+t'}{2}\right) \\ &\quad \times \sum_{n=0}^{\infty} \frac{1}{n!}(tt')^{n/2}\left(\mathrm{J}_{l+n}(2(tt')^{1/2})\frac{\sigma}{n+\sigma} + \delta_{ln}\frac{\sigma}{n-\sigma}\right) \\ \Phi(t) &= 1 \qquad \text{DO} \\ &= \sigma/t \qquad \text{PO} \\ \sigma &= \omega_0/\omega_c \end{aligned}\right\} \tag{4.13}$$

where J_l is a Bessel function.

We first consider high fields, $\sigma \ll 1$, when only the term with $n = 0$ is important in the summation. An exact solution for equation (4.11) can be found for a DO interaction and $l \neq 0$ (Kaplan and Levinson 1972a), by using the invariance of Laguerre polynomials under a Bessel transformation. The eigenfunctions and eigenvalues are

$$\left.\begin{aligned} \chi_l^r(t) &\propto t^{|l|/2} \exp\left(-\frac{t\sqrt{5}}{2}\right) L_r^{|l|}(t\sqrt{5}) \qquad r = 0, 1, 2, \ldots \\ \lambda_l^r &= (-1)^{l+r}\,\rho^{-(2r+|l|+1)} \\ \rho &= \tfrac{1}{2}(\sqrt{5}-1). \end{aligned}\right\} \tag{4.14}$$

Hence, for any nonzero l there exists an infinite sequence of positive λ_l^r, which increase without limit, and according to equation (4.12) this leads to the existence of an infinite sequence of states with the threshold as limit. For $l = 0$ the kernel consists of two terms, corresponding to the two in the bracket; one containing J_0 and whose solution is obtained from equation (4.14) for $l = 0$, and the second with (-1) which corresponds to a factorizable kernel. An equation for λ can therefore be obtained in the form

$$\left.\begin{aligned} \bar{\Gamma}(\lambda) &= -1/\lambda \\ \bar{\Gamma}(\lambda) &= \frac{3\rho - 1}{\rho^2} \sum_{r=0}^{\infty} \frac{(-\lambda_0^r)^{-1}}{\lambda - \lambda_0^r}. \end{aligned}\right\} \tag{4.15}$$

A graphical solution for $\lambda > 0$ is shown in figure 22, and from this it is clear that the behaviour of the eigenvalues is the same for $l = 0$ as for $l \neq 0$, that is, this case also has a spectrum of bound states which tends to a limit at the threshold.

We have not been able to find an exact solution for the physically more important case of a PO interaction. However, by comparing the PO kernel with that for the DO interaction and by using certain general theorems of the theory of integral equations, it can be shown (Kaplan and Levinson 1972a) that the spectrum for a PO interaction remains qualitatively the same.

For weak fields, $\sigma \gg 1$, the kernel in equation (4.13) can be rewritten in a series of the form $\sum_s (1/\sigma^s)(tt')^{s/2}$ (Levinson *et al* 1971c) and can be approximated by degenerate kernels. The kernel in this case also has an infinite number of positive

eigenvalues, which increase without limit, so that bound states also exist in weak fields.

It should be noted that the equation derived by Pitaevskii (1959) for the vertex Γ was algebraic rather than integral. The integral nature of the equations for Γ and $\mathscr{T}$ in the present case is due to the fact that the phonon energy is independent of $\bar{q}_\perp$; hence all states with differing values of $\bar{q}_\perp$ are near the threshold and an integration over these states is preserved in the troublesome section.

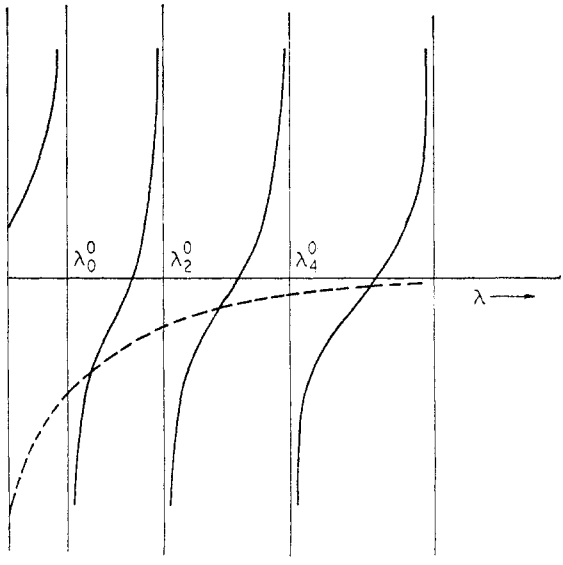

Figure 22. Graphical solution of equation (4.15).

The bound states considered above arise as a result of the usual electron–phonon interaction which is linear in the phonon amplitudes. In some cases it is possible to have an interaction which is quadratic in these amplitudes, and this interaction can also produce a bound state of an electron and a phonon in the presence of a magnetic field (Levinson and Rashba 1972). These bound states have a number of special features, in particular they cannot be found from the poles of the function G, but only from the poles of K. This means that the electron is not bound to the phonon which it emits itself, but to a phonon which is already present in the crystal. The probability of finding such bound states therefore increases in the presence of a nonequilibrium phonon distribution (see §7.3.). Binding can take place either with LO or with TO phonons.

Part III. Impurity centres

5. Resonant electron–phonon coupling in impurity centres

As was shown above in §3 for the example of magnetopolarons, the electron–phonon interaction gives the largest effects when ω_0 is in resonance with one of the electronic frequencies. These resonance effects are expressed most clearly in impurity centres, since the electronic subsystem then has a discrete spectrum, and because of the infinite mass of a centre phonon, emission is not accompanied by any recoil.

In the resonant situation two discrete levels arise; one above ω_0 and the other below, as was shown in figure 3. These are both hybrid states and are formed by the superposition of zero-phonon and single-phonon states in the ratio of approximately 1:1. They can therefore be considered as a special form of localized vibrations and have been called dielectric vibrations. Of course, the origin of these vibrations is quite different from that of the usual localized vibrations, which are due to differences in mass or force constants.

The existence of this new type of localized vibration was first pointed out by Kogan and Suris (1966), who explained its basic features, using the example of a two-level system. The first experimental observation of these vibrations was made by Onton *et al* (1967a,b) for donors in Si, and then in other crystals. If the ionization potential R of the impurity in the crystal is comparable to phonon frequencies, it is then quite likely that ω_0 is close to one of the electronic frequencies; the distance from resonance can be varied by a magnetic field or by pressure. This is the situation which we shall examine below. The case $R \ll \omega_0$, when the resonance is created by a high magnetic field, such that $\omega_c \simeq \omega_0$, has already been considered in § 3.3.

5.1. *Theory*

We take as a model system an impurity centre with a nondegenerate ground state and a single degenerate excited level. The eigenfunctions of the excited level will be labelled by the index λ while O refers to the ground state. The excitation energy of the centre is denoted by W.

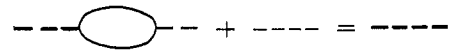

Figure 23. Graphical equation for the phonon Green function.

If we take only a simple loop in the phonon polarization operator, we can solve the graphical equation for the phonon Green function, shown in figure 23. Near to resonance ($|W-\omega_0| \ll \omega_0$) this solution has the form

$$D(\epsilon, \boldsymbol{q}\boldsymbol{q}') = D^0(\epsilon \boldsymbol{q})\,\delta_{\boldsymbol{q}\boldsymbol{q}'} + D^0(\epsilon \boldsymbol{q}) \frac{\Sigma_\lambda \langle 0|v_{-\boldsymbol{q}}|\lambda\rangle\langle\lambda|v_{\boldsymbol{q}'}|0\rangle}{\epsilon - W - \mathscr{M}(\epsilon) + \mathrm{i}0} D^0(\epsilon \boldsymbol{q}') \tag{5.1}$$

where

$$\left.\begin{aligned} D^0(\epsilon \boldsymbol{q}) &= \frac{|c_{\boldsymbol{q}}|^2}{\epsilon - \omega(\boldsymbol{q}) + \mathrm{i}0} \\ v_{\boldsymbol{q}} &= \exp(\mathrm{i}\boldsymbol{q}.\boldsymbol{r}) \\ \mathscr{M}(\epsilon) &= \int \mathrm{d}^3\boldsymbol{q}\, \mathscr{B}(q) \frac{|\langle\lambda|v_{\boldsymbol{q}}|0\rangle|^2}{\epsilon - \omega(\boldsymbol{q}) + \mathrm{i}0}. \end{aligned}\right\} \tag{5.2}$$

The function D is nondiagonal, since the impurity centre violates the translational symmetry. The quantity $\mathscr{M}(\epsilon)$ is interpreted as the mass operator for an electron. Since the electron has a discrete spectrum and the only source of dispersion in the system is $\omega(q)$, the phonon dispersion, this has been taken into account in equation (5.2).

The energies of excited states are found from the condition

$$\epsilon - W = \mathscr{M}(\epsilon) \tag{5.3}$$

which is the usual equation of degenerate perturbation theory; it was discussed in this context by Kogan and Suris (1966) and by Rodriguez and Schultz (1969). Isolated roots of this equation correspond to local vibrations. If phonon dispersion is neglected, $\mathscr{M}(\epsilon)$ takes the form in equation (1.5*d*), and equation (5.3) then always has two isolated roots which vary with electronic frequency as shown in figure 3. The separation of the branches is of order $\alpha^{1/2}\omega_0$ at resonance, but away from resonance the distances from the asymptotes decrease as $\alpha\omega_0^2/(W-\omega_0)$. By analogy with § 3 it can easily be seen that the states near the resonance are hybrid; near the asymptote $\epsilon = \omega_0$ they are bound states of a phonon at the impurity centre, but near the asymptote $\epsilon = W = E_2 - E_1$ they are purely electronic. The localized modes discussed here can therefore be described in other terms as complexes of an impurity centre plus a phonon.

It can be seen from equations (5.1) and (5.2) that the quantities

$$\Psi_\lambda(\boldsymbol{q}) \propto \frac{c_{\boldsymbol{q}}^* \langle 0 | v_{-\boldsymbol{q}} | \lambda \rangle}{\epsilon - \omega(\boldsymbol{q})} \tag{5.4}$$

are essentially the wavefunctions of localized modes. For a PO interaction at $\omega(\boldsymbol{q}) = \omega_0$ (Dean *et al* 1970) then

$$\left.\begin{aligned} \Psi_{2s}(\boldsymbol{q}) &\propto \frac{q}{\{(3/2a)^2 + q^2\}^3} \\ \Psi_{2p,z}(\boldsymbol{q}) &\propto \frac{\cos\theta}{\{(3/2a)^2 + q^2\}^3} \end{aligned}\right\} \tag{5.5}$$

where a is the Bohr radius in the crystal. The nonanalytic behaviour for small $\boldsymbol{q}$ should be noted, that is, the limit for $q \to 0$ depends on the direction of $\boldsymbol{q}$; this is a consequence of the singularity of the polarization interaction.

The intensity of light absorption by localized modes is determined by the contribution of no-phonon states to the excited state wavefunction. It is therefore proportional to Z (cf equation (1.4)) and decreases as the localized mode is pinned to ω_0.

On the other hand, Raman scattering of light is determined mainly by the direct interaction of electromagnetic waves with phonons. Hence the scattering probability $\boldsymbol{k} \to \boldsymbol{k}'$ with the excitation of a local mode λ is

$$w_{\boldsymbol{k}\to\boldsymbol{k}'} \propto |\Psi_\lambda(\boldsymbol{k}' - \boldsymbol{k})|^2. \tag{5.6}$$

Since $ka \ll 1$, a comparison of equations (5.5) and (5.6) gives the important result (Dean *et al* 1970) that scattering by p-modes is considerably stronger than that by s-modes.

It is clear from equation (5.5) that $\Psi_\lambda(\boldsymbol{q})$ has a characteristic radius a^{-1}, and therefore $|\Psi_\lambda(\boldsymbol{q} \simeq 0)|^2 \sim a^3$. Since we always have $a^3/v \gg 1$ (v is the volume of the unit cell) for centres with $R \sim \omega_0$, it follows from equation (5.6) that impurity Raman scattering is anomalously large; for a single impurity centre it is a factor of a^3/v stronger than the intrinsic scattering calculated for a single unit cell. This effect has the same origin as the giant cross section for impurity absorption near an exciton band (Rashba 1957, Rashba and Gurgenishvili 1962); it is due to the coherence of vibrations over a volume $\sim a^3$.

A nonresonant situation was also recently analysed, and it was shown (Rashba 1972a) that localized modes with all values of angular momentum arise in the absence of phonon dispersion. There are an infinite number of modes for each value of the angular momentum. Their frequencies lie in a region near ω_0 whose width is of order $0{\cdot}1\omega_0\kappa_0/\bar{\kappa}$ and each mode corresponds to a bound state of a phonon at the localized centre. For fixed $\kappa_0/\bar{\kappa}$ and $R \gg \omega_0$ the phonon binding energy is independent of R, and therefore bound states will also occur for deep centres.

5.2. *Experimental results for absorption and Raman scattering*

In the absorption spectrum of Bi donor centres in Si the band corresponding to the transition $1s(A_1) \rightarrow 2p_0$ (the level classification is that of Kohn (1957)) is anomalously broad, and its frequency of 59·5 meV is close to that of TO phonons along $\langle 100 \rangle$ (58·7 meV). This may mean that because of the finite width of the phonon branch, equation (5.3) no longer has isolated roots, that is, the system has only a continuous spectrum. This hypothesis was put forward by Onton *et al* (1967a,b) and also confirmed experimentally; the band splits into two under uniaxial deformation, and its high frequency component narrows rapidly. The large width of the 63 meV Ga acceptor band in Si (Hrostowski and Kaiser 1958) is also presumably due to resonance with the Raman frequency of 64·8 meV (Onton *et al* 1967b). We emphasize that these results are for a purely homopolar crystal with a relatively weak electron–phonon interaction. The disappearance under pressure of the band $1s(A_1) \rightarrow 1s(T_1)$ in the spectrum of Te donors in AlSb was interpreted in an analogous manner (Ahlburn and Ramdas 1968).

In their study of local modes Dean *et al* (1970) used Raman scattering very successfully (see also Manchon and Dean 1970). Measurements were made on S, Te, Si and Sn donor centres in GaP (Raman frequency $\omega_0 = 50{\cdot}2$ meV), and the corresponding frequencies for $1s \rightarrow 2s$ and $2s \rightarrow 2p$ transitions lie in the range 58–94 meV. For each of these centres a single impurity band was observed at the long-wavelength edge of the intrinsic Raman scattering band, and this impurity band was displaced by 0·8–1·6 meV with respect to the intrinsic band (figure 24). According to the ideas of § 5.1 these were ascribed to p-states.

s-type local modes in GaP were found in the vibronic spectrum accompanying the luminescence of excitons associated with neutral donors. Their frequencies are displaced by 1·2 meV (S) and 1·9 meV (Te) with respect to the Raman frequencies. Similarly, local modes were found in the luminesence spectrum of CdS, displaced by 3·3, 2·7 and 1·4 meV with respect to the Raman frequency $\omega_0 = 38$ meV (Reynolds *et al* 1971). These belong to a neutral acceptor with $W = 168$ meV. Although these modes lie in an energy range containing a high density of states in the phonon spectrum, their width is fairly small.

There is no doubt that the local modes found in GaP and CdS are dielectric; this was shown convincingly in the papers we have quoted. However, it is clear from the results given above that for some of the impurities in GaP, and particularly for CdS, that the energies of electronic transitions in impurity centres considerably exceed ω_0, that is, there is no resonance. The estimates of the frequency shifts, made by Dean *et al* (1970) and by Reynolds *et al* (1971) using a two-level model, are in satisfactory agreement with experiment but a complete analysis must be based on a more rigorous theory (Rashba 1972a). It would be especially interesting to sort out the sequence of levels with the same angular momentum.

The opposite case $R < \omega_0$ was recently investigated with donor centres in CdS and CdSe (Henry and Hopfield 1972). In their spectra features were found which may be connected with some quasilocalized modes.

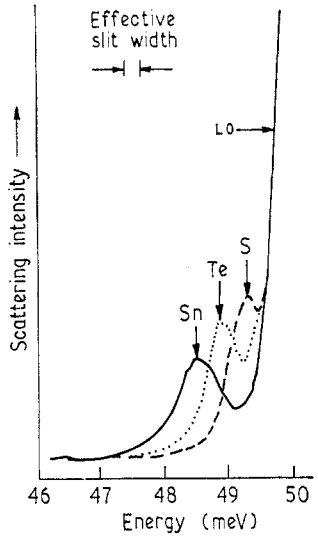

Figure 24. Impurity bands in the Raman scattering of GaP at 20 K. From Dean *et al* (1970).

If localized vibrations of the usual type are present in the spectrum of the crystal, pinning is expected to occur as the electronic frequencies approach those of the localized vibrations. This situation was studied in AgBr by Brandt *et al* (1970), and a theory was provided by Ivanov (1966) and by Davies and Zeiger (1970).

Part IV. Excitons

6. Exciton–phonon complexes

The study of exciton–phonon interactions was given a new impetus by the experiments of Liang and Yoffe (1968), who found a characteristic structure on the high frequency side of the fundamental exciton band in ZnO, separated from this band by an energy close to or equal to a multiple of ω_0—the frequency of polarization phonons with $q = 0$. Analogous structures were soon found in the spectra of a number of other crystals.

This structure was explained in terms of final-state interactions, ie an interaction between an exciton and a phonon produced in the optical transition. However, no detailed interpretation of the experimental results has yet been made. We therefore begin by describing the experimental results and formulating the questions which arise naturally in their analysis; we then examine the theories which have been put forward, and finally we compare, in so far as this is possible, theory and experiment.

6.1. *Experimental results*

The long-wavelength edge of the intrinsic absorption spectrum of ZnO is shown in figure 25 (Liang and Yoffe 1968). The exciton bands A ($n = 1$) and

B ($n = 1$) correspond to direct allowed transitions from the two successive valence bands at the point Γ (ie $\boldsymbol{k} = 0$). These are followed by two close pairs of satellites (L_{1a}, L_{1b} and L_{2a}, L_{2b}) and a further weak satellite L_3. Successive satellites (L_1, L_2, L_3) are separated by approximately equal intervals $\Delta\omega \simeq 73$ meV, which is close to $\omega_0 = 71$ meV. It is therefore natural to suggest that these satellites correspond to the creation of from one to three phonons together with the exciton.

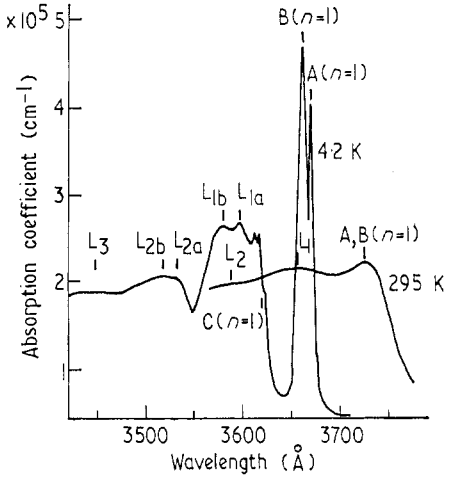

Figure 25. Absorption spectrum of hexagonal ZnO at 4·2 K and 295 K. From Liang and Yoffe (1968).

It is usually assumed that the exciton and the optical phonon, produced by the absorption of a photon, fly apart immediately and afterwards move independently. It is natural to call this two-particle absorption. If this two-particle absorption occurs in a region of the spectrum where there are no purely electronic transitions, it can easily be calculated by applying second-order time dependent perturbation theory to the electron–phonon transitions. This absorption is in the form of 'steps' which begin at a distance ω_0 from the intrinsic exciton band; its maximum is displaced from this threshold by the order of R. 'Steps' of this kind are usually taken to be a characteristic sign of exciton–phonon transitions.

An unusual feature of the satellites L_{1a} and L_{1b} is that they show clearly developed maxima, and not thresholds, located at a distance $\Delta\omega \simeq \omega_0$ from the exciton bands. The sharp distinction between this picture and that described above led Liang and Yoffe to put forward the idea of 'exciton–phonon complexes'. They did not construct any detailed model of these complexes, but it was assumed that the energy of the complex was not simply the sum of the energies of the exciton and the phonon.

Another important point that should be noted here is that the binding energy of A and B excitons, which are 67 and 63 meV, are less than ω_0. Hence both satellites, L_{1a} and L_{1b}, lie in the exciton ionization continuum, that is, where, in the absence of exciton–phonon coupling, one would expect continuous absorption corresponding to pair formation. This situation is shown schematically in figure 26(*a*). Consequently, a correct description of the absorption (even if it is assumed that no new types of state appear) must include the change in the no-phonon absorption,

calculated according to the same second-order perturbation theory. At the time of the experiments of Liang and Yoffe (1968) such a calculation had not yet been carried out.

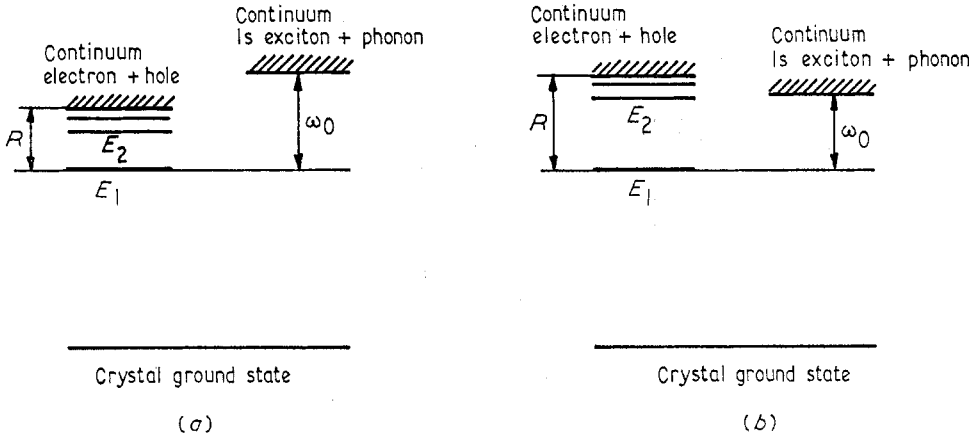

Figure 26. Energy level diagrams for (*a*) $R<\omega_0$ and (*b*) $R>\omega_0$.

Table 2. Exciton spectra data indicating satellite structure

R is the exciton binding energy, ω_0 is the Raman frequency, and $\Delta\omega$ is the separation between the phonon satellite and the exciton band. The references are to the papers in which $\Delta\omega$ was determined.

Substance	R (meV)	ω_0 (meV)	$\Delta\omega$ (meV)	Reference
ZnO	65	71	73	a
BeO	170	136	130	b
MgO	85	89	60	b, c
CdS	30	38	30	d
CdSe	15	26	19	d
CdTe	9·5	21	19	d
TlBr	6	14	$\simeq\omega_0$	e
	10	15	$(0{\cdot}6\div0{\cdot}7)\,\omega_0$	f
TlCl	10	22	$\simeq\omega_0$	e
	12	22	$(0{\cdot}6\div0{\cdot}7)\,\omega_0$	f
AgBr	19	17	15	g
			13	h
AgCl	—	24	18	h

a, Liang and Yoffe (1968).
b, Walker *et al* (1968).
c, Whited and Walker (1969).
d, Dillinger *et al* (1968).
e, Bachrach and Brown (1968).
f, Kurita and Kobayashi (1969, 1970, 1971).
g, Brandt and Brown (1969) for band excitons.
h, Kanzaki *et al* (1967, 1968) for impurity excitons.

Analogous structure was soon discovered in the exciton spectra of a number of other crystals; these data are summarized in table 2. It is clear from this that for most cases $\Delta\omega<R$, that is, the satellite maximum lies in the exciton ionization continuum, as for ZnO. This group includes the cadmium chalcogenides, in which electron–phonon coupling can be considered to be weak ($\alpha\leqslant1$), and TlBr and TlCl, which are typical crystals with intermediate coupling ($\alpha\sim3$).

BeO, MgO, AgBr, and possibly AgCl, are somewhat anomalous. The spectrum of BeO is shown in figure 27. In BeO and MgO we find $\Delta\omega\simeq0{\cdot}75R$, so that the satellite seems to have a natural interpretation as a 2s exciton band (figure 26(*b*)).

However, the intensity of the satellite in MgO is $\simeq 0{\cdot}6$ of that in the exciton band (Whited and Walker 1969), which is in sharp contradiction to the n^{-3} law (Elliott 1957). It was therefore suggested that exciton–phonon coupling plays an important role in this material. But if we represent the effect of the electron–phonon interaction in the same terms as those applied to impurity centres in § 5, we would then expect to find the biggest effect in BeO, where $\Delta\omega \simeq \omega_0$; however, this does not agree with the results of Whited and Walker (1969). It is therefore not possible at the present time to draw any firm conclusions from the results for MgO and BeO.

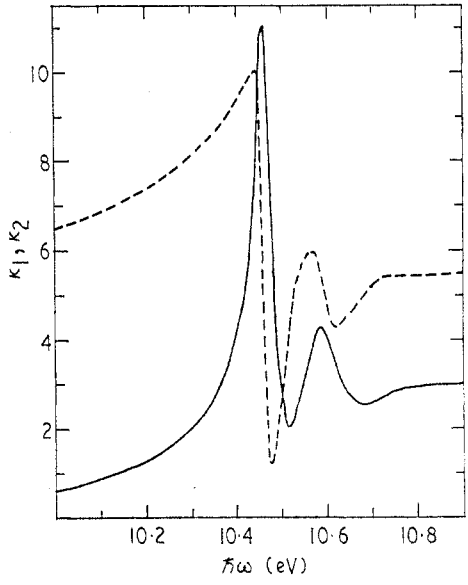

Figure 27. Real, κ_1 (– – – –), and imaginary, κ_2 (———), parts of the dielectric constant for BeO at 77 K. The exciton peak corresponds to a direct allowed transition at Γ. From Walker *et al* (1968).

The experiments on AgBr are interesting, but need to be developed further. Here the bands which are ascribed to a complex are observed for both band excitons (Brandt and Brown 1969) and for impurity excitons (Kanzaki *et al* 1967, 1968). Similar features are also found in the spectra of ionic crystals when the exciton radius is relatively large ($n = 1$ excitons in LiI and $n = 2$ in RbI and KI (Baldini *et al* 1969, Baldini and Bosacchi 1969, 1970)).

The experiments listed above have stimulated the development of both a theory of exciton–phonon complexes, which are a direct analogy of the impurity centre plus phonon complexes, and of a theory of absorption in the exciton continuum.

6.2. *Theory of the energy spectrum and of absorption (weak and intermediate coupling)*

The hamiltonian of a Mott exciton interacting with polarization phonons has the standard form

$$\mathscr{H} = \sum_{\lambda} E_\lambda a_\lambda^+ a_\lambda + \omega_0 \sum_{\boldsymbol{q}} \mathscr{C}_{\boldsymbol{q}}^+ \mathscr{C}_{\boldsymbol{q}} + \frac{1}{2M}(\boldsymbol{P} - \sum_{\boldsymbol{q}} \boldsymbol{q} \mathscr{C}_{\boldsymbol{q}}^+ \mathscr{C}_{\boldsymbol{q}})^2 + \sum_{\lambda\lambda'\boldsymbol{q}} (c_{\boldsymbol{q}} \langle \lambda | \rho_{\boldsymbol{q}} | \lambda' \rangle a_\lambda^+ a_{\lambda'} \mathscr{C}_{\boldsymbol{q}} + \mathrm{HC}). \tag{6.1}$$

Here a_λ is the exciton annihilation operator in the state λ,

$$\left.\begin{aligned} \rho_{\boldsymbol{q}}(\boldsymbol{r}) &= \exp(\mathrm{i}\beta_\mathrm{h}\,\boldsymbol{q}.\boldsymbol{r}) - \exp(-\mathrm{i}\beta_\mathrm{e}\,\boldsymbol{q}.\boldsymbol{r}), \\ \beta_{\mathrm{e,h}} &= \frac{m_{\mathrm{e,h}}}{M}, \\ M &= m_\mathrm{e} + m_\mathrm{h}, \end{aligned}\right\} \tag{6.2}$$

m_e and m_h are the masses of electrons and holes, and $\boldsymbol{P}$ is the total exciton momentum. The coordinates of the exciton centre of mass have been eliminated in the derivation of equation (6.1) (Lee *et al* 1953).

It is clear from equation (6.1) that there are two differences between the hamiltonian of an exciton and that of an impurity centre: (i) the exciton has a finite mass (the third term in equation (6.1)), hence there is a recoil on emission of phonons, and (ii) $\rho_{\boldsymbol{q}}(\boldsymbol{r})$ replaces $\exp(\mathrm{i}\boldsymbol{q}.\boldsymbol{r})$. The first of these is the more important. We limit our discussion to the states $P = 0$ which are the most important in absorption.

6.2.1. *Weak coupling.* For weak coupling it is sufficient to consider just no-phonon and single-phonon states. The second and third terms in equation (6.1) then reduce to

$$\sum_{\boldsymbol{q}} \omega^*(\boldsymbol{q})\, \mathscr{C}_{\boldsymbol{q}}^+ \mathscr{C}_{\boldsymbol{q}} \tag{6.3}$$

where $\omega^*(\boldsymbol{q}) = \omega_0 + q^2/2M$. Here the exciton recoil could be taken into account by introducing an effective phonon dispersion.

In our approximation for the exciton mass operator (the first diagram in figure 4) we get

$$\mathscr{M}_{\lambda\lambda'}(\epsilon) = \int \mathrm{d}^3q\, \mathscr{B}(\boldsymbol{q}) \sum_\nu \frac{\langle\lambda|\rho_{\boldsymbol{q}}|\nu\rangle\langle\nu|\rho_{\boldsymbol{q}}^+|\lambda'\rangle}{\epsilon - E_\nu - \omega^*(\boldsymbol{q}) + \mathrm{i}0}. \tag{6.4}$$

We take first the situation shown in figure 26(*b*) and consider the correction to the position of the excited exciton level with energy $E_1 + W$, with which are associated the Coulomb eigenfunctions ψ_λ. If λ and λ' belong to the same term, then $\mathscr{M}_{\lambda\lambda'} = \mathscr{M}\delta_{\lambda\lambda'}$. At resonance, when $W \simeq \omega_0$, singularities in $\mathscr{M}$ arise from the term $\nu = 1$ (1s state). Unlike the case of the impurity centre (cf (5.2)), the dispersion in $\omega^*(q)$ is considerable and is already apparent for momenta $q \sim \pi/a$. The dependence of $\langle\lambda|\rho_{\boldsymbol{q}}|1\rangle$ on $\boldsymbol{q}$ for small $\boldsymbol{q}$ is therefore important, and this is determined by the symmetry of the resonance level (we assume that state 1 is an s-state).

For s- or d-levels $\langle\lambda|\rho_{\boldsymbol{q}}|1\rangle \sim (aq)^2$ and $\mathscr{M}(\epsilon)$ is determined by equation (1.5(*a*)) with

$$\left.\begin{aligned} A &\sim \alpha_\mu \frac{M}{\mu}\omega_0 \\ B &\sim \alpha_\mu \left(\frac{M}{\mu}\right)^2 \\ C &\sim \alpha_\mu \left(\frac{M}{\mu}\right)^{5/2} \omega_0^{-1/2} \end{aligned}\right\} \tag{6.5}$$

where μ is the reduced mass, and α_μ is the Fröhlich coupling constant, calculated

for mass μ (cf equation (2.5)). Hence complexes do not occur here for sufficiently weak coupling (cf § 1), pinning is absent, and the intensity of absorption hardly changes as the level approaches the threshold. There is weak damping proportional to $\{\epsilon-(E_1+\omega_0)\}^{3/2}$ beyond the threshold and the state can be considered to be autoionizing.

It is important to note that the coefficients in equations (6.5) contain progressively increasing positive powers† of M/μ together with the small quantity α_μ. If $M/\mu \gg 1$, then it is possible to have $B \sim 1$ even in the region of weak binding for both particles ($\alpha_\mu \ll 1$, $\alpha_M = \alpha_\mu (M/\mu)^{1/2} \ll 1$). The contribution of no-phonon states Z is then appreciably less than unity (cf equation (1.4)), that is, the resonant coupling is large and a complex is formed. In the case considered $B \gg A/\omega_0$, and consequently the relative correction to the intensity is greater than the correction to the level, since, according to equations (1.4) and (1.5), the first of these is of the order of B whilst the second is of the order of A/ω_0. The occurrence of complexes for $M/\mu \gg 1$ is to be expected, since the properties of the exciton must then tend to those of an impurity centre.

For p-states $\langle \lambda | \rho_q | 1 \rangle \sim aq$ and $\mathscr{M}(\epsilon)$ is given by equation (1.5(b)) with

$$\left.\begin{aligned} A &\sim \alpha_\mu \frac{M}{\mu}\omega_0 \\ B &\sim \alpha_\mu \left(\frac{M}{\mu}\right)^{3/2} \omega_0^{1/2}. \end{aligned}\right\} \tag{6.6}$$

Therefore exciton–phonon complexes arise for weak coupling and pinning occurs, as follows from § 1. We emphasize one condition necessary for the derivation of this result: the coordinate matrix element between states 1 and λ must be nonzero.

In the limit $M/\mu \to \infty$ the properties of an exciton become identical with those of an impurity centre and in this case, as was noted in § 5, a system of phonon states bound to the centre arises even in the absence of resonance. We must therefore expect analogous bound states of a phonon and an exciton when the ratio M/μ is sufficiently large. The appropriate condition is $\mu/M \lesssim 0{\cdot}1(\kappa_0/\bar{\kappa})(\omega_0/R)$ (Rashba 1972a), which is not excessively severe.

We now turn to the situation described by figure 26(a); this was investigated by Sak (1970a,b). It has already been pointed out that for $\omega_0 > R$ it is important to include the change in absorption in the electron–hole continuum, due to exciton–phonon coupling. The conductivity $\sigma(\omega) \propto \operatorname{Im} F(\omega)$, where F is the exciton Green function. Using second-order perturbation theory we have

$$\sigma(\omega) \propto \operatorname{Im} \sum_{\lambda\lambda'} \psi_\lambda(0)\psi^*_{\lambda'}(0) \Big\{ F^0_\lambda(\omega)\,\delta_{\lambda\lambda'} + F^0_\lambda(\omega) \int \mathrm{d}^3\boldsymbol{q}\, \mathscr{B}(\boldsymbol{q}) \langle \lambda | \rho_{\boldsymbol{q}} | 1 \rangle F^0_1(\omega - \omega^*(q)) \langle 1 | \rho^+_{\boldsymbol{q}} | \lambda' \rangle F^0_{\lambda'}(\omega) \Big\}. \tag{6.7}$$

In the second term the residues of F^0_1 describe absorption with the formation of a 1s exciton and a phonon, whilst the residues of F^0_λ and $F^0_{\lambda'}$ describe the change in absorption in the electron–hole continuum. Because of the complexity of the Coulomb functions ψ_λ explicit expressions for $\sigma(\omega)$ were not obtained. However,

† It is possible that just this tendency of the binding energy of complexes to increase with increasing M is the reason why $\Delta\omega$ for impurity excitons in AgBr is less than for band excitons (cf table 2).

a numerical calculation (Sak 1970a), using the parameters for CdTe, gave satisfactory agreement with the experimental results of Dillinger *et al* (1968); a maximum appears in the ionization continuum, near the threshold (figure 28).

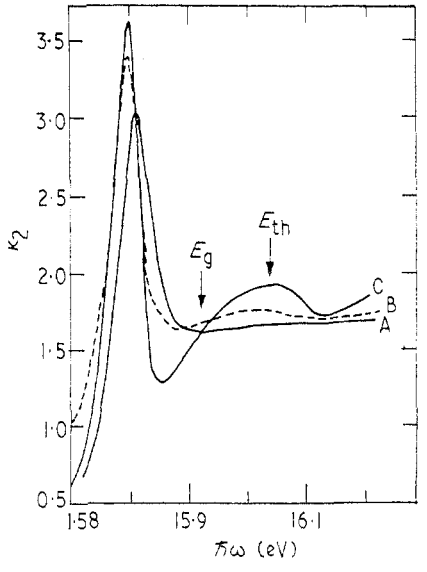

Figure 28. Imaginary part of the dielectric constant for CdTe: curve A, without exciton–phonon interaction; curve B, experiment, at 77 K; curve C, theory. The calculations (Sak 1970a) are made for $m_e = 0{\cdot}11m_0$, $m_h = 0{\cdot}5m_0$, $\kappa_0 = 10$, $\kappa_\infty = 6$, $\omega_0 = 21$ meV and $R = 10$ meV. To facilitate comparison of theory and experiment, a phenomenological width was introduced into the calculation in order to give the right shape for the 1s band.

It is clear from the above considerations that the maximum in the absorption derived by Sak (1970a,b) is purely an interference effect†. On the other hand, in as much as the results of Sak's paper were derived by applying perturbation theory to the Green function, they cannot in principle exhibit the presence of any type of bound states. If, therefore, the results for other crystals with weak coupling can be satisfactorily accounted for by using equation (6.7), then the question of the existence of 'complexes' in ZnO and similar materials does not arise. One cannot, of course, automatically extend this conclusion to crystals with intermediate coupling.

6.2.2. *Intermediate coupling.* Toyozawa and Hermanson (1968) and Hermanson (1970) investigated exciton–phonon complexes in the intermediate coupling region, using the variational procedure of Lee *et al* (1953). These papers have played an important role in stimulating further experiments.

First the hamiltonian in equation (6.1) is canonically transformed, using the operator $\exp(iU)$, where

$$U = \sum_{\mathbf{q}} (d_{\mathbf{q}} \mathscr{C}_{\mathbf{q}} - d \mathscr{C}^{*+}_{\mathbf{q}\,\mathbf{q}}) \tag{6.8}$$

and the parameters $d_{\mathbf{q}}$ are chosen to minimize the energy of the 1s state of the exciton. The wavefunction of the lowest excited exciton state is then written in the

† In this sense it is reminiscent of the Fano effect (Fano 1961).

form

$$\chi = \sum_q s_q \mathscr{C}_q^+ a_{1s}^+ |0\rangle + t a_{2s}^+ |0\rangle \tag{6.9}$$

where the s_q are determined by a variational method. The single-phonon approximation of equation (6.9) shows the basic limitation of this theory, since it corresponds to the retention of only the first term in the sequence of threshold diagrams in figure 4. This approach should then be useful mainly for the description of resonance effects.

The dependence of the energy of this level on R is shown in figure 29(a) for two values of the parameters. The curves touch the phonon continuum at a finite

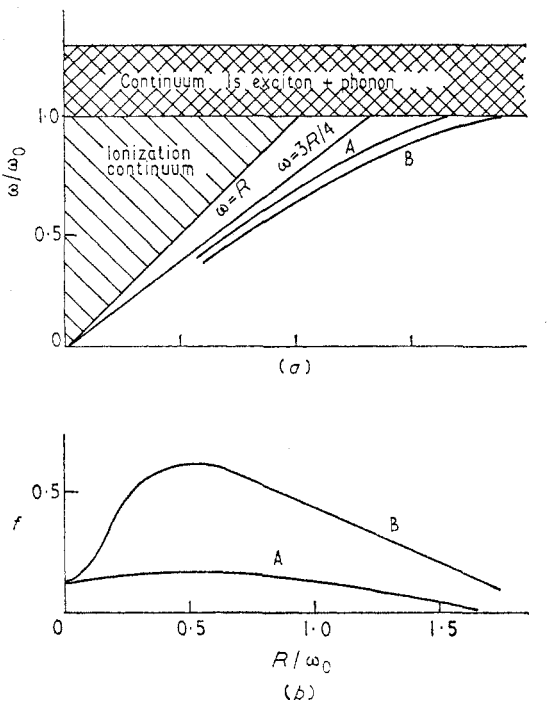

Figure 29. (a) Energy of the first excited exciton state, and (b) intensity of optical transitions to this state. Curve A is for $\kappa'/\bar{\kappa} = 1$, $M/\mu = 8$, and curve B for $\kappa'/\bar{\kappa} = 2$, $M/\mu = 8$. Here $\kappa' = (\mu/m_0)\,a$, where a is the effective Bohr radius. From Hermanson (1970).

angle, in agreement with § 1. The threshold values of R at which the single-particle branch disappears are $\sim(1{\cdot}5\text{–}2)\,\omega_0$.

The ratio of the optical transition probability into the state χ to the transition probability to the 1s ground state of the exciton is

$$f = \frac{f_\chi}{f_{1s}} = \sum_q \left| s_q d_q + t \frac{\psi_{2s}(0)}{\psi_{1s}(0)} \right|^2. \tag{6.10}$$

The dependence of f on R is shown in figure 29(b). A comparison of figures 29(a) and 29(b) shows that for given values of the parameters the intensity of absorption is very small when the level enters the continuum. The dependence of f on R is non-monotonic and it is in this that the difference from the weak coupling case shows most clearly.

The weak-coupling theory includes only the second term in equation (6.10), but for the parameters given in figure 29 the first term is the larger. The magnitude of this term is a measure of the contribution of single-phonon states to χ, so that we may conclude that this is considerable. Therefore, despite the fact that t remains finite even at the threshold, it is admissible to consider the resultant state as a bound state of an exciton and a phonon.

We now return to the situation shown in figure 26(*a*). Toyozawa (1971) put forward a variant of the theory and used this, in the spirit of Liang and Yoffe (1968), to reach the conclusion that in this case there is a branch of quasi-bound states of an exciton and a phonon with $\epsilon < \omega_0$, which lies in the electron–hole continuum. However, these states are very broad, and in a typical example considered by Toyozawa their width $2\Gamma \simeq 0{\cdot}8\omega_0$ for a binding energy $\omega_b \simeq 0{\cdot}15\omega_0$. Because $2\Gamma \gg \omega_b$ the validity of these results is not certain.

7. Magnetophonon resonance in the exciton spectrum

Effects in the absorption spectrum due to resonance between the cyclotron frequency and ω_0 were first discovered experimentally by Johnson and Larsen (1966), in the intrinsic absorption spectrum of InSb. The physical picture of this is, in principle, considerably more complicated than for cyclotron resonance (cf § 3). Interband absorption of a photon simultaneously creates an electron and a hole, which then interact both between themselves and with phonons. It is impossible to ignore the Coulomb interaction between electron and hole, since all the distinct structure in the absorption edge is due to exciton bands, whose contribution to the absorption is increased by the application of high magnetic fields (Elliott and Loudon 1960). On the other hand, the phonon interactions are responsible for the resonance effect under discussion. Hence the investigation of the spectrum of exciton–phonon bound states is equivalent to solving the problem of three interacting particles, and naturally this is possible only in limiting cases. The lower part of the spectrum in this resonance situation was investigated by Mel'nikov *et al* (1971) and by Rashba and Edel'shtein (1971); the nonresonant case was discussed by Levinson (1972).

7.1. *General features of the spectrum*

$R = \mu e^4/2\kappa_\infty^2$ characterizes the Coulomb interaction energy in an exciton. A magnetic field H is considered to be strong if the cyclotron frequencies of both carriers $\omega_e, \omega_h \gg R$. An analogous situation for impurity centres was considered in § 3.3.

Under these conditions the motion of an electron and a hole is quasi-one-dimensional; the transverse motion is practically completely determined by the magnetic field, and only the slow longitudinal motion is controlled by the Coulomb attraction (Elliott and Loudon 1960, Hasegawa and Howard 1961, Gor'kov and Dzyaloshinskii 1967). The wavefunction of their relative motion is highly extended along $\boldsymbol{H}$; its transverse dimensions are of order λ, but its longitudinal dimensions are of order a/L, where $L = \ln(a/2\lambda)^2$. In sufficiently high fields $L \gg 1$ and we shall assume this to hold.

Since the exciton is a neutral particle, its momentum $\boldsymbol{P}$ remains an integral of the motion in the presence of a magnetic field (Knox 1963, Gor'kov and

Dzyaloshinskii 1967). Because we shall be considering absorption spectra, we limit our discussion to states with $\boldsymbol{P} = 0$.

Each pair of Landau bands (one electron and one hole, with quantum numbers l_1 and l_2) gives rise to a series of exciton levels E_n, with $n = 0, 1, \ldots, \infty$. For the ground state $E_0 \simeq -RL^2$ and for excited states $E_n \simeq -R/n^2$ $(n \geqslant 1)$. An increasing fraction of the total absorption is concentrated in the $n = 0$ band as H increases, and its intensity increases as HL.

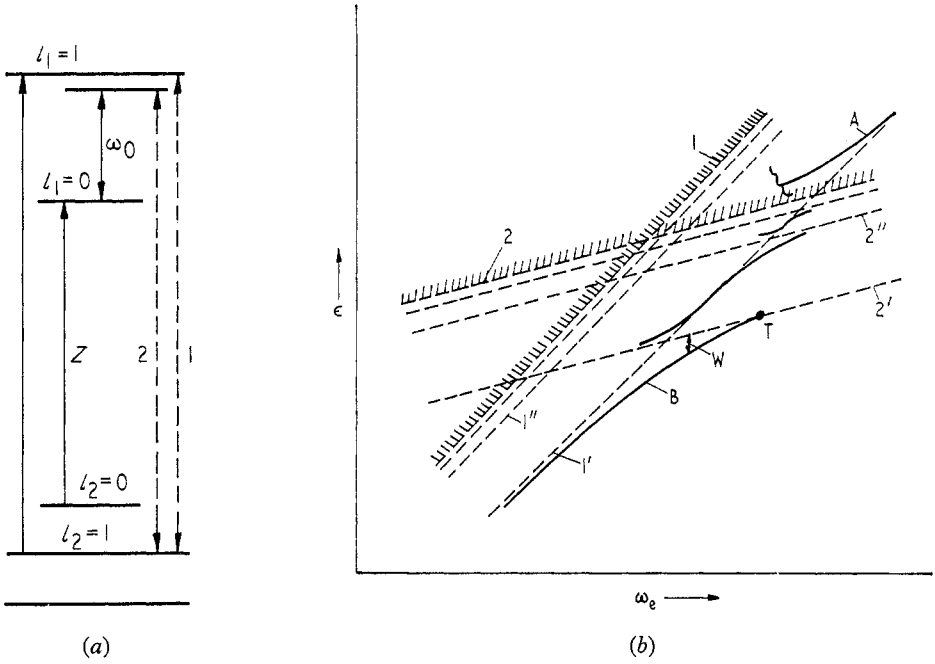

Figure 30. (*a*) Electron and hole Landau level scheme. (*b*) Schematic energy spectrum of the system when the Coulomb interaction and electron–phonon coupling are included.

Let us suppose that the resonance condition $\omega_e \simeq \omega_0$ is satisfied for the electron† but not for the hole. Coupling with phonons is considered to be weak $(\alpha \ll 1)$ and we shall consider only resonance effects. Consequently the interaction of the hole with phonons may be neglected. As yet we place no limitation on the ratio of the Coulomb energy R to the resonant interaction energy $\alpha^{2/3}\omega_0$ of an electron with phonons (§ 3). However we shall assume everywhere, with the exception only of the end of § 7.2, that $R \gg \alpha^2 \omega_0$ (cf § 4).

A schematic diagram of the electron levels (for $\boldsymbol{P} = 0$), not including the Coulomb interaction, is shown in figure 30(*a*). Allowed electron transitions are shown by full vertical arrows. The dashed arrow 1 shows the energy of a purely electronic excitation of the system when the electron and the hole are in bands $l_1 = l_2 = 1$, and the dashed arrow 2 shows the energy of an electron–vibrational excitation (with the electron in the band $l_1 = 0$); these energies are equal for $\omega_e = \omega_0$. Figure 30(*b*) shows by dashed lines the variation with H of all the levels of the electron plus hole system which arise from levels 1 and 2 (in figure 30(*a*)) as a

† This condition, combined with the condition $\omega_e \gg R$, means that we are now considering crystals with $\omega_0 \gg R$, unlike § 6.

consequence of the Coulomb interaction. The lowest levels of the corresponding exciton series are shown by the dashed lines 1′ and 2′. The transition to the 1′ level is expected to be dominant in the absorption spectrum, but weak transitions to higher levels of this series (1″, etc) must also be present, together with transitions to the spectral continuum (beyond the dashed line 1).

By analogy with §§ 3 and 5 we may expect that weak coupling with phonons will lead to pinning near the intersection of lines belonging to systems 1 and 2. The first pinning for the fundamental band 1′ must occur at its intersection with 2′, but we may also expect pinning near subsequent intersections (with 2″, etc). The levels constructed in this way are shown by thick lines in figure 30(*b*). State B, which can be considered as an exciton–phonon complex, is stable with respect to emission of an optical phonon, and this is the single-particle branch of the spectrum. Higher states can decay with the formation of two-particle states—a free phonon and a free exciton (in the state $l_1 = 0$, $l_2 = 1$, $n = 0$); these are relatively stable only for small α. When this condition is satisfied, level 1′ must reappear after passage through resonance—curve A in figure 30(*b*). However, it is not obvious how the corresponding absorption behaves as resonance is approached, and therefore the curve A is broken off in this region. The description given in figure 30(*b*) should be supplemented by the pinning of 1″ and other excited levels.

We thus see that a number of general features can be predicted by analogy with §§ 3, 5 and 6. However, we need to construct a detailed theory before we can establish specific features of the spectrum and explain over what range of values of H the state B exists, how the intensity of transitions to this state varies with H, how band A changes near to resonance, etc. The results of an investigation of the low frequency part of the spectrum—on curve B and near the point T—are given below.

7.2. *Theory for weak coupling*

The irreducible electron–hole vertices Γ_0 and Γ_1 which must be included in our approximation are shown in figure 31. The upper line corresponds to the electron, the lower to the hole, the dashed line to a phonon, and the wavy line to the Coulomb interaction. The numbers label the Landau bands; the values of l_1 and l_2 in the

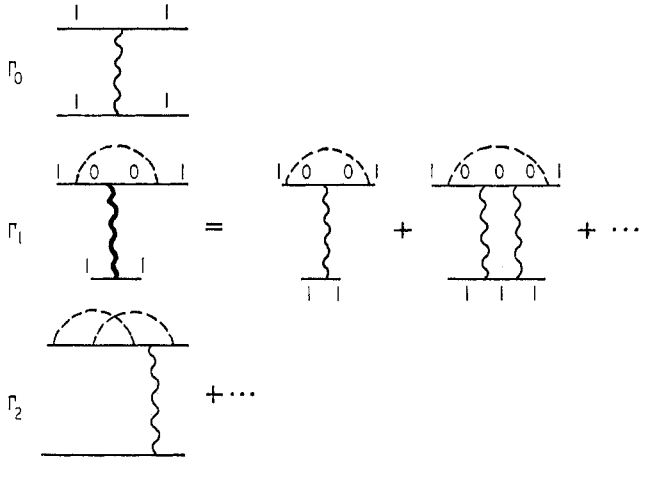

Figure 31. Vertices for an exciton interacting with phonons.

external lines are clear from figure 30(*a*). We put $l_1 = 0$ in the internal lines, because this gives rise to resonance denominators. Vertices of type Γ_2 are small for $\alpha^2\omega_0/R \ll 1$ (cf § 4).

If we take only the first diagram in figure 4 to describe the electron–phonon interaction, then for the Green function $F(\epsilon \boldsymbol{P}|z, z')$, which describes internal longitudinal motion in the exciton, we find that

$$(\epsilon - \omega_e - \omega_0 - \mathscr{H}_{\boldsymbol{P}}^{11}(z))\, F(z, z') - \int \mathscr{M}(\epsilon \boldsymbol{P}|z, z'')\, F(z'', z')\, dz'' = \delta(z - z') \quad (7.1)$$

where the mass operator

$$\mathscr{M}(\epsilon \boldsymbol{P}|z, z') = \int d^3\boldsymbol{q}\, |\gamma(\boldsymbol{q})|^2 \langle z|(\epsilon - \mathscr{H}_{\boldsymbol{P}-\boldsymbol{q}}^{01})^{-1}|z'\rangle \exp\{-i\beta_h q_z(z - z')\} \quad (7.2)$$

and the electron–phonon vertex $\gamma(\boldsymbol{q})$ is

$$|\gamma(\boldsymbol{q})|^2 = \mathscr{B}(\boldsymbol{q})\, \tfrac{1}{2}(\lambda q_\perp)^2 \exp\{-\tfrac{1}{2}(\lambda q_\perp)^2\}. \quad (7.3)$$

Here

$$\mathscr{H}_{\boldsymbol{P}}^{l_1 l_2} = \frac{p_z^2}{2\mu} + \frac{P_z^2}{2M} + U_{\boldsymbol{P}}^{l_1 l_2}(z). \quad (7.4)$$

where $U_{\boldsymbol{P}}^{l_1 l_2}(z)$ is the Coulomb energy, averaged by the function of the transverse motion of an electron–hole pair with momentum P and Landau quantum numbers l_1, l_2. For $|z| \gg \lambda$ all $U_{\boldsymbol{P}}^{l_1 l_2} \simeq -e^2/|z|$ but for $|z| \lesssim \lambda$ they are of order $-e^2/\lambda$. For each value of ω_e the value of ϵ in equation (7.1) is reckoned from curve 2 in figure 30(*b*).

The energy spectrum is determined by the poles of F, whilst the intensity of absorption is given by

$$\sigma(\omega) \propto \operatorname{Im} F(\omega, \boldsymbol{P} = 0|z = 0, z' = 0). \quad (7.5)$$

Substitution of F at the point $z = z' = 0$ is analogous to the appearance of the well known factor $|\psi(0)|^2$ in the usual formula for exciton absorption (Elliott 1957).

In order to clarify whether curve B has a limiting point, we need to find the behaviour of $\mathscr{M}(\epsilon \boldsymbol{P} = 0)$ near the threshold, when W (figure 30(*b*)) is small. By using equations (2.4), (7.2) and (7.3) we get an equation of the form of equation (1.5(*b*)) for $\mathscr{M}$, but with $\omega_0 - \epsilon$ replaced by W. It follows that $\mathscr{M}$ is bounded and that curve B has a limiting point T, at which it is tangential to the curve 2′. Near this point $Z(\epsilon) \propto W^{-1/2} \to \infty$ (equation (1.4)), so that near T the branch B is a bound state of an exciton and a phonon. Hence the spectrum of a magnetic exciton shows a marked difference from that of a magnetopolaron (§ 3) because of the presence of a limiting point. This arises because the transverse mass $M_\perp \simeq \mu(a/\lambda)^2/L$ of an exciton is still finite, although it is large.

We now consider two limiting cases for which it has proved possible to obtain explicit results.

7.2.1. *Strong Coulomb interaction*, $L^2 R \gg (\alpha/2)^{2/3}\omega_0$ (Mel'nikov *et al* 1971, Rashba and Edel'shtein 1971). We limit our investigation to the lower part of the spectrum, and then in a bilinear expansion of the resolvent in equation (7.2) we need retain only the first term, which corresponds to the exciton ground state ($n = 0$).

The variation of B, the single-particle branch of the spectrum, is shown in figure 32. The effect of the electron–phonon interaction can be characterized by the displacement of the level at resonance and by the distance from resonance of the limiting point. These are:

$$\left.\begin{aligned} W_0 &\simeq \omega_e^T - \omega_e^0 \simeq 3{\cdot}6\alpha^* LR \\ \alpha^* &= \frac{\alpha}{2L^{3/2}}\left(\frac{a}{\lambda}\right)^3\left(\frac{m_h{}^3}{m_e M^2}\right)^{1/2} \end{aligned}\right\} \tag{7.6}$$

and both are linear functions of α. The parameter $\alpha^* \gg \alpha$ acts as an effective coupling constant, and the theory is valid for $\alpha^* \ll L$. At the limiting point the curve B touches the line 2′. There is a region of width of order $\alpha^{*2}RL$ near the limiting

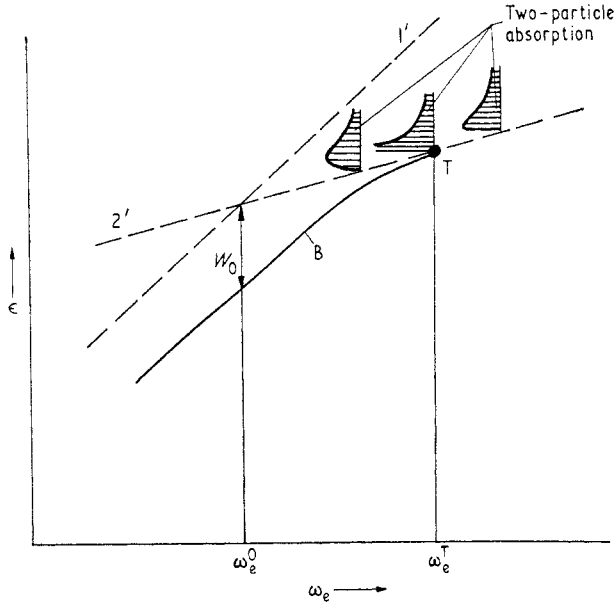

Figure 32. Behaviour of the single-particle level and the spectral distribution of two-particle absorption for a strong Coulomb interaction. Lines 1′ and 2′ are those shown in figure 30(*b*).

point, in which a quadratic expansion is valid for the curve B and its slope is considerably reduced; in this region Z is large (see equation (1.4)) and exciton–phonon complexes are formed. Thus, complexes are formed only in a narrow region near ω_e^T for $\alpha^* \ll 1$, but if $\alpha^* \sim 1$ they exist right up to ω_e^0.

The absorption spectrum consists of two bands, and the intensity of band B decreases as T is approached. Besides this there is a two-particle band corresponding to the formation of exciton plus phonon pairs. This lies above the line 2′, and the distribution of absorption in this band for different values of ω_e is shown in figure 32.

Since curve B is tangential to 2′ at the point T, pinning must occur. However, for $\alpha^* \ll 1$ it must be weakened by the rapid variation in slope of curve B near T. It is possible that the pronounced picture of pinning observed experimentally is to

some extent due to the simultaneous presence of one- and two-particle absorption for $\omega_e < \omega_e^T$ and by the existence of two-particle absorption near 2′ for $\omega_e > \omega_e^T$.

7.2.2. *Weak Coulomb interaction,* $L^2 R \ll (\alpha/2)^{2/3}\omega_0$ (Rashba and Edel'shtein 1971). In this case we can solve equation (7.1) by expanding $\mathscr{M}$ in powers of U, keeping only the linear term. This corresponds to the retention of the first diagram in the vertex Γ_1 (figure 31); the next is smaller by a factor $\sim R/\alpha^{2/3}\omega_0$. The resultant nonlocal potential $\mathscr{U}(\epsilon, z, z')$ is large only for $|z|, |z'| \lesssim |2\mu\epsilon|^{-1/2}$ (we assume that $M \sim \mu$). If the exciton radius in the single-particle branch is much larger than $|2\mu\epsilon|^{-1/2}$, the potential $\mathscr{U}$ may be replaced by a local potential. In a logarithmic approximation the effect of the Coulomb interaction can then be completely described by the effective potential

$$\tilde{U}(\epsilon, z) = \left(1 - \frac{d\mathscr{M}(\epsilon)}{d\epsilon}\right) U(z) \tag{7.7}$$

where $U(z) \simeq U^{11}_{P=0}(z) \simeq U^{01}_{P=0}(z)$, and $\mathscr{M}(\epsilon) = -\frac{1}{2}\alpha\omega_0 |\omega_0/\epsilon|^{1/2}$ is the electron mass operator (cf (3.3) and (3.4)). The first term in $\tilde{U}$ corresponds to Γ_0, and the second

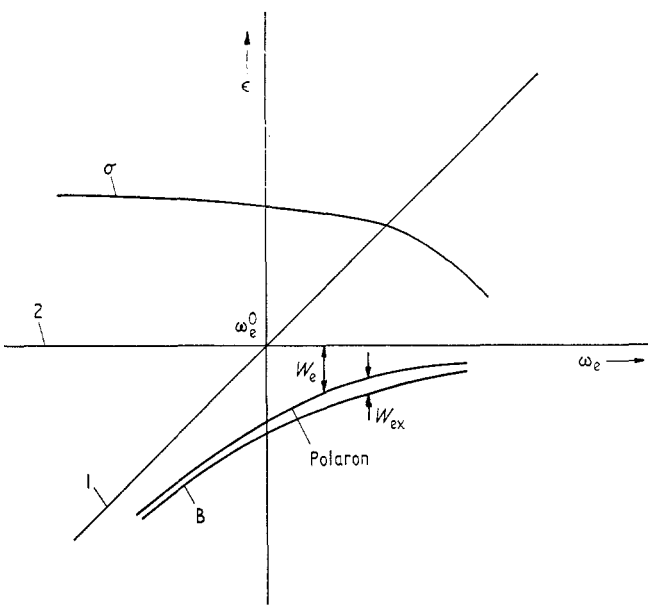

Figure 33. Schematic dependence on ω_e of the energy of a single-particle excitation (curve B) and of the intensity of absorption in the single-particle band. The dependence of the polaron energy on ω_e is also shown. The separation between curve B and the polaron curve gives the exciton binding energy W_{ex}. W_e is the binding energy of the electron–phonon complex. Lines 1 and 2 are those in shown figure 30(*b*).

to Γ_1. The quantity $(-d\mathscr{M}/d\epsilon)$ is equal to $\frac{1}{2}$ for $\omega_e = \omega_e^0$ (figure 33); it increases rapidly to the right of this point and decreases to the left. Hence at some point to the right of ω_e^0 the effective potential is considerably larger than the initial Coulomb interaction and is determined by the vertex Γ_1.

We can find W_{ex} and the exciton radius a_{ex} by using equation (7.7). Since $W_e \gg W_{ex}$ in the present case, we can put $\epsilon \simeq -W_e$ and consider W_{ex} and a_{ex} as

functions of W_e:

$$\left.\begin{aligned} a_{ex}(W_e) &\simeq \frac{a}{L_1(1+\mathrm{d}\mathscr{M}/\mathrm{d}W_e)} \\ W_{ex}(W_e) &\simeq RL_1^2\left(1+\frac{\mathrm{d}\mathscr{M}}{\mathrm{d}W_e}\right) \\ L_1(W_e) &= \ln\left(\frac{a_{ex}(W_e)}{2\lambda}\right)^2. \end{aligned}\right\} \tag{7.8}$$

It is clear from equations (7.8) that a_{ex} decreases to the right of ω_e^0, but W_{ex} increases. It follows from equation (7.5) that

$$\sigma_{W_e}(\omega) \propto \frac{a_{ex}^{-1}(W_e)}{1+\mathrm{d}\mathscr{M}/\mathrm{d}W_e}\,\delta(\omega-\omega_B(W_e)). \tag{7.9}$$

The denominator of this expression gives the contribution of the no-phonon state to the wavefunction of the electron–phonon complex, whilst the numerator comes from the factor $|\psi(0)|^2$. Comparison with equation (7.8) shows that the factor $1+\mathrm{d}\mathscr{M}/\mathrm{d}W_e$ cancels out, and therefore σ_{W_e} is independent of the magnetic field (to a factor $L_1(W_e)$).

This point deserves careful attention. It might have been expected that the Coulomb interaction would be of little importance for $L^2R \ll \alpha^{2/3}\omega_0$, but in fact this applies only to the position of the level B; it is indeed near the edge of the electron–hole continuum. At the same time the intensity of absorption at the edge of the 'electron–phonon complex plus hole' continuum in the absence of the Coulomb interaction decreases rapidly to the right of ω_e^0 as $(1+\mathrm{d}\mathscr{M}/\mathrm{d}W_e)^{-1}$ (Korovin and Pavlov 1967a). On the other hand, the intensity in the band due to the exciton–phonon complex is almost constant; this provides considerable support for the description in terms of pinning.

Since a_{ex} decreases with increasing ω_e, it is at some point comparable with $(2\mu W_e)^{-1/2}$. For larger ω_e the intensity of the band corresponding to a bound state of an exciton and a phonon decreases rapidly, $\sigma_{W_e} \propto W_e^2$, and also $W_{ex} \propto W_e^{1/2}$.

It has always been assumed above that $T = 0$. Real phonons are present in the crystal for $T \neq 0$, and they may also be created under nonequilibrium conditions (Vella-Coleiro 1969, Litton *et al* 1970). Therefore exciton absorption near phonons must occur with the formation of complexes. It was shown by Rashba and Edel'shtein (1971) that the intensity of this process is very large; a calculation for one phonon gave an answer of about five orders of magnitude larger than for exciton absorption in an ideal lattice, calculated for one unit cell. This effect has not yet been discovered experimentally.

The problem of three interacting particles—electron, hole and optical phonon—was recently investigated for a nonresonant situation (Levinson 1972). If, as distinct from the above discussion, we now put $R \ll \alpha^2\omega_0$, it can be shown that 'quasi-bound' states exist below the threshold for the creation of these three particles. The energy of these states lies in the continuum of electron–hole pairs, and therefore they can decay with the annihilation of the phonon; the corresponding width is, however, less than the binding energy, which justifies the investigation of such states.

7.3. *Experimental results*

The experimental results for interband absorption in InSb are shown in figure 5 and clearly demonstrate the splitting of the absorption peak near $\omega_e = \omega_0$. Exciton absorption is dominant at high magnetic fields (Elliott and Loudon 1960), and therefore the results of Johnson and Larsen (1966) must be interpreted in terms of a model which includes the Coulomb attraction (this was ignored in the original paper, where the role of the resonant electron–phonon interaction was explained).

It was shown later that the spectral structure was considerably more complex than that shown in figure 5. Part of this structure is shown in figure 34. The

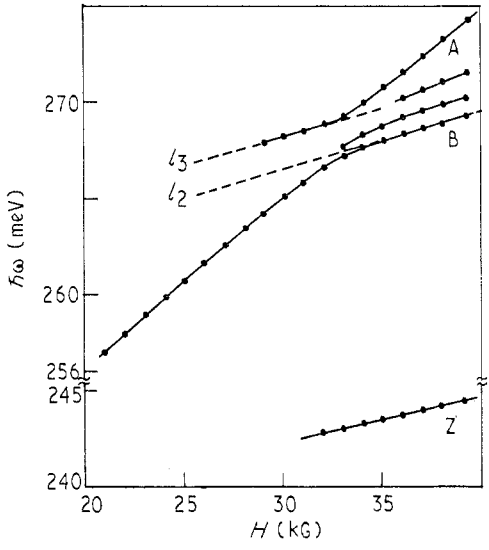

Figure 34. Magnetic field dependence of the position of various minima in transmission for InSb. The straight lines l_2 and l_3 are asymptotes near which pinning is observed. From Larsen and Johnson (1966).

energy levels between which transitions occur and the notation for the bands are similar to those in figure 30(*a*). It can be seen that the line Z has no special features over the range of values of H where A and B show pinning; this directly proves that the reconstruction of the spectrum takes place in the neighbourhood of term intersections. The general features of the spectrum are similar to those shown in figure 30(*b*), but there is as yet no more detailed interpretation. It is natural to ascribe the separation of the asymptotes l_2 and l_3 (~ 2 meV) to the effect of the Coulomb interaction. It is possible that pinning is so clearly developed as a result of the large mass ratio $m_h/m_e \gg 1$.

An estimate of the parameters applicable to InSb for $\omega_e \simeq \omega_0$ gives $(a/2\lambda)^2 \simeq 4{\cdot}6$, $L \simeq 1{\cdot}5$, $(\alpha/2)^{2/3}\omega_0 \simeq 0{\cdot}8$ meV, and $L^2R \simeq 0{\cdot}6$ meV. The logarithmic approximation is not therefore very accurate and the electron–phonon coupling is of the same order as the Coulomb interaction. Nevertheless the fact that the separation of l_2 and l_3 is appreciably larger than L^2R may be due to an increased Coulomb interaction to the right of resonance (§ 7.2). There is no absorption in figure 34 which might be interpreted as two-particle absorption (cf figure 32); its observation would be very important for the whole concept of bound states. Unfortunately,

there are no very important data on the intensity changes along curve B, and hence more detailed experiments are needed.

It is interesting to compare the features of pinning in InSb ($\alpha \simeq 0{\cdot}02$) with pinning in TlBr and TlCl ($\alpha \simeq 2{\cdot}5$), as measured by Kurita and Kobayashi (1971). Their results are shown in figure 35. Bands 1–3 corresponds to successive terms of

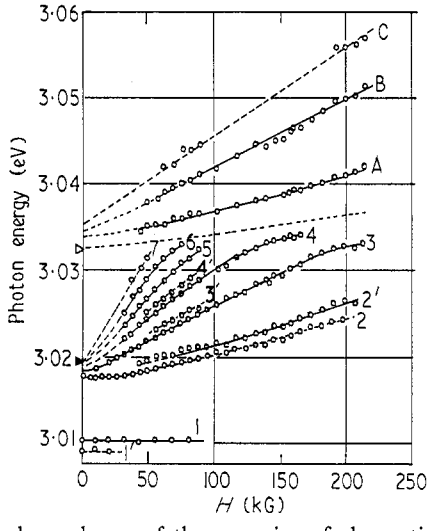

Figure 35. Magnetic field dependence of the energies of absorption peaks in TlBr at 4·2 K. The full triangle marks the limit of the exciton series for $H = 0$. The open triangle corresponds to an energy $E_{2s} + \omega_0$, for which a kink in the absorption is observed; the broken line leading from this triangle shows the field dependence of this kink.

the lowest exciton series, and bands 4–7 are due to excitons in subsequent magnetic sub-bands. Here $\omega_0 \gg R \gtrsim \omega_c$, that is, magnetic fields of the order of 100 kG do not correspond to the high-field limit; although for excited states of the exciton ω_c is larger than the Coulomb binding energy. For this combination of parameters and for $\alpha \simeq 2{\cdot}5$, the best we can hope for at the present time is a purely qualitative interpretation of the observed features.

It is seen from figure 35 that pinning is clearly developed; the intensity of the bands falls to zero in the pinning region. As distinct from InSb, a continuation of bands 4–7 similar to A in figure 34 was not observed, and it is natural to explain this in terms of the short lifetime of the corresponding metastable states due to the large value of α.

In the observations of pinning in TlBr there is one important feature which Kurita and Kobayashi (1971) noted but did not explain; pinning occurs in the neighbourhood of $E_{\text{pin}} \simeq E_{2s} + \omega_0$ and not near the energy $E_{1s} + \omega_0$ which corresponds to the first decay threshold. This feature is naturally explained on the basis of the results of § 6.2.1†. It was shown there that it was only if the transition $1 \to 2$ was dipole allowed that the term E_2 could show strong pinning near $E_1 + \omega_0$, with a decrease of the intensity to zero. Since states 3–7 are s-type (only these states are observable in the optical absorption), their pinning must be associated with p-states. This gives $E_{\text{pin}} \approx E_{np} + \omega_0$ $(n \geqslant 2)$ which agrees with experiment (within experimental error).

† Although these results were derived for weak coupling, it may be expected that they are still qualitatively correct for intermediate coupling.

8. Vibronic spectra of molecular crystals

The exciton absorption spectra of molecular crystals of aromatic type (benzene, naphthalene, anthracene, etc) begin with a group of strongly polarized bands (Prikhot'ko 1948) which form a Davydov multiplet (Davydov 1951). These are followed by a large number of bands which can be ascribed to various intramolecular electronic–vibrational (vibronic) transitions. In a number of cases these have been successfully interpreted by supposing that an intramolecular vibronic excitation moves as a whole through the lattice (Davydov 1951). The opposite situation of weak vibronic coupling has also been considered, using perturbation theory (McRay 1961, 1963).

A much fuller description of vibronic spectra has recently been obtained by the use of a dynamic theory (Rashba 1966, 1968) in which an exciton and a phonon are considered as stable interacting quasiparticles. This dynamical theory was successfully applied to the analysis of experimental results, and spectra corresponding to bound and dissociated states of this pair were identified (Broude *et al* 1966, 1967, Sheka 1971).

This approach also was applied to electron–phonon complexes in crystals with narrow bands (Rashba 1966) and was successfully used to describe kinetic effects (Munn and Siebrand 1970a).

8.1. *Dynamical theory of vibronic spectra*

The hamiltonian of a Frenkel exciton interacting with intramolecular vibrations can be written in the form:

$$\mathscr{H} = \sum_{m \neq n} \mathfrak{M}^0_{mn} \psi^+_m \psi_n + \omega_0 \sum_n \phi^+_n \phi_n + \mathscr{H}_{\mathrm{eL}} \tag{8.1}$$

where the first term is the exciton hamiltonian, the second is the phonon hamiltonian (phonon dispersion is neglected) and $\mathscr{H}_{\mathrm{eL}}$ is the full hamiltonian for the intramolecular electron–phonon interaction:

$$\mathscr{H}_{\mathrm{eL}} = \sum_n \psi^+_n \psi_n \{\xi(\phi^+_n + \phi_n) + \tfrac{1}{2}\Delta(\phi^+_n + \phi_n)^2\}. \tag{8.2}$$

The first term in equation (8.2) represents the shift in equilibrium positions of the oscillators due to electronic excitation of the molecule; this is nonzero only for fully symmetric vibrations (the Jahn–Teller effect is assumed to be absent). The second term described the change in vibrational frequencies due to electronic excitation of the molecule.

Our basic assumption is as follows—that the frequency ω_0 is much larger than the exciton band width. Hence, despite the fact that $\mathscr{H}_{\mathrm{eL}}$ contains terms which change the total number of phonons, the dominant contribution to the wavefunction comes from states conserving the number of phonons; the contribution of other states is of order ω_0^{-1}.

We may eliminate from $\mathscr{H}$ terms which are nondiagonal in the number of phonons, by using ω_0^{-1} as a small parameter. Contributions of this type to the second term in $\mathscr{H}_{\mathrm{eL}}$ are small for $|\Delta| \ll \omega_0$ and they can immediately be neglected. However, the linear term in $\mathscr{H}_{\mathrm{eL}}$ is in general large; this and the phonon energy dominate in $\mathscr{H}$, and consequently perturbation theory cannot be used immediately. It is therefore convenient to eliminate those terms, in which the number of phonons is not conserved, in two steps. First we eliminate them from the main terms in $\mathscr{H}$

by an exact canonical transformation, and then by a second transformation we eliminate them from the small terms by perturbation theory.

The first canonical transformation

$$\mathscr{H} \to \mathrm{e}^{S}\,\mathscr{H}\,\mathrm{e}^{-S} \tag{8.3}$$

where

$$S = \gamma \sum_n (\phi_n^+ - \phi_n)$$

and

$$\gamma = \xi/\omega_0$$

reduces the hamiltonian to the form

$$\mathscr{H} = -\frac{\xi^2}{\omega_0}\sum_n \psi_n^+\psi_n + \omega_0 \sum_n \phi_n^+\phi_n + \Delta \sum_n \psi_n^+\psi_n\phi_n^+\phi_n + \sum_{m\neq n} \mathfrak{M}_{mn}^0\,\mathrm{e}^{S}\psi_m^+\psi_n\,\mathrm{e}^{-S}. \tag{8.4}$$

In this hamiltonian the first three terms strictly conserve the number of phonons. Contributions which do not conserve the total number of phonons appear only in the last term, but now they are multiplied by the small coefficients $|\mathfrak{M}_{mn}^0| \ll \omega_0$. It is therefore simple to make a second canonical transformation which eliminates terms nondiagonal in the number of phonons to order $\mathfrak{M}^0$; this introduces corrections of order $|\mathfrak{M}_{mn}^0|^2/\omega_0$ into the diagonal terms, which may be neglected. Hence it is sufficient to take only the diagonal part of the last term. We consider only single-phonon states and drop the first two terms in equation (8.4), which give an additive contribution to the energy. We then find

$$\mathscr{H} = \sum_{m\neq n} \mathfrak{M}_{mn}\psi_m^+\psi_n + \Delta \sum_n \psi_n^+\psi_n\phi_n^+\phi_n + \gamma^2 \sum_{m\neq n} \mathfrak{M}_{mn}\psi_m^+\psi_n\{(\phi_m^+\phi_n + \phi_n^+\phi_m) - (\phi_n^+\phi_n + \phi_m^+\phi_m)\} \tag{8.5}$$

where $\mathfrak{M}_{mn} = \mathfrak{M}_{mn}^0 \exp(-\gamma^2)$. Since this hamiltonian conserves the number of phonons, we have reduced a field problem to a dynamical one. The hamiltonian in equation (8.5), which was first obtained by Rashba (1966, 1968), forms the basis of the dynamical theory of vibronic states, valid for large ω_0. We now examine it in more detail.

The first term is the renormalized exciton energy, and the second is the exciton–phonon interaction energy due to a change in vibrational frequency (Nieman and Robinson 1963); the interaction is always attractive, since $\Delta < 0$. For the moment we consider only vibrations which are not fully symmetric, for which the third term is zero. The structure of the resultant spectrum is determined by the ratio of the exciton band width $\mathfrak{M}$ to Δ, and this ratio can vary over a wide range. If $|\Delta|$ is small, only the two-particle spectrum is present, but when $|\Delta|$ becomes comparable with $\frac{1}{2}\mathfrak{M}$ a discrete level appears (see figure 1) which corresponds to a single-particle state and which is called a vibron. The radius of the resultant state is large when its binding energy is small—the exciton moves over a wide region around the site on which the dispersionless phonon is located. As $|\Delta|$ increases, so does the binding energy, whilst the radius of the state decreases and finally, when $\mathfrak{M} \ll |\Delta|$, the exiton wavefunction is almost completely concentrated on the same site as the phonon; this asymptotic case is practically reached for $\mathfrak{M} \simeq |\Delta|$.

The limiting case $\mathfrak{M} \ll |\Delta|$ corresponds to a model (Davydov 1951, 1964) in which an intramolecular electronic–vibrational excitation moves as a whole through the crystal. This model was developed further by Craig and Walmsley (1961).

If intramolecular electronic–vibrational transitions are allowed, the vibronic absorption in the crystal at $T = 0$ is determined by the conductivity

$$\sigma(\omega, \boldsymbol{k}) = -\frac{1}{\pi} \operatorname{Im} F(\omega, \boldsymbol{k}) \tag{8.6}$$

where $F(\omega, \boldsymbol{k})$ is the Fourier transform of the two-particle time dependent Green function

$$F(\boldsymbol{n} - \boldsymbol{m}, t) = -\mathrm{i}\langle T\psi_{\boldsymbol{n}}(t)\,\phi_{\boldsymbol{n}}(t)\,\psi^{+}_{\boldsymbol{m}}(0)\,\phi^{+}_{\boldsymbol{m}}(0)\rangle. \tag{8.7}$$

For vibrations which are not fully symmetric

$$\left.\begin{aligned} F(\omega, \boldsymbol{k}) &= F(\omega) \\ \frac{1}{F(\omega)} &= \frac{1}{G(\omega)} - \Delta \end{aligned}\right\} \tag{8.8}$$

where $G(\omega)$ can be expressed simply in terms of the exciton Green function $G(\omega, \boldsymbol{k}) = (\omega - \epsilon(\boldsymbol{k}) + \mathrm{i}0)^{-1}$:

$$G(\omega) = \int \frac{\mathrm{d}^3\boldsymbol{k}}{(2\pi)^3} G(\omega, \boldsymbol{k}) = \int \frac{\rho(\varepsilon)\,\mathrm{d}\varepsilon}{\omega - \varepsilon + \mathrm{i}0}. \tag{8.9}$$

Here $\epsilon(\boldsymbol{k})$ and $\rho(\epsilon)$ are the dispersion law and density of states in the exciton band. The frequencies in σ and F are shifted by ω_0 compared to those in G.

The position of the single-particle level is determined by the pole of $F(\omega)$ and according to equation (8.8) this can be found from the equation $G(\omega_1) = \Delta$. This is the same as the equation for localized exciton levels in a crystal containing an isotopic impurity, if we interpret Δ as the difference between the excitation energies of the guest molecule and the host molecules. There is thus a connection between vibronic and impurity spectra; this is discussed in detail in the papers of Rashba (1972b) and Sheka (1972). The intensity of single-particle absorption is determined by the residue of $F(\omega)$, and this is equal to

$$|a|^2 = \left[\frac{G^2(\omega)}{|\mathrm{d}G(\omega)/\mathrm{d}\omega|}\right]_{\omega=\omega_1}. \tag{8.10}$$

The magnitude of $|a|^2$ has a simple physical meaning—it is the probability of finding an exciton and a phonon on the same site. This tends to zero as ω_1 approaches the edge of the two-particle spectrum but quickly increases to 1 as ω_1 departs from it. The intensity of two-particle absorption is

$$\sigma(\omega) = \frac{\rho(\omega)}{\{1 - \Delta \int \rho(\omega')\,\mathrm{d}\omega'/(\omega - \omega')\}^2 + (\pi\Delta\rho(\omega))^2}. \tag{8.11}$$

The general features of the absorption are shown in figure 36.

It is important to note that the problem can be inverted by expressing $G(\omega)$ in terms of $F(\omega)$. This enables us to express $\rho(\omega)$ in terms of $\sigma(\omega)$ (Rabin'kina *et al* 1970):

$$\rho(\omega) = \frac{\sigma(\omega)}{\{1 + \Delta \int \sigma(\omega')\,\mathrm{d}\omega'/(\omega - \omega')\}^2 + (\pi\Delta\sigma(\omega))^2} \tag{8.12}$$

where the integration includes both the single- and the two-particle spectrum. Since $\sigma(\omega)$ is directly measured experimentally, this expression enables $\rho(\omega)$ to be determined from the vibronic absorption.

We now consider fully symmetric vibrations. For these $\xi \neq 0$ and the third term in equation (8.5) must now be included. The parameter γ^2 which appears there is the ratio of the Franck–Condon energy of the intramolecular electron–phonon interaction E_{FC} to ω_0. For the aromatic molecules, to which most of the experimental results refer, this ratio is not small; in fact we usually have $\gamma \sim 1$ and therefore this last term is important. It has an unusual form: the first component describes simultaneous transfer of an exciton and a phonon (resonance interaction) and the second an exchange of sites between electron and phonon (exchange–resonance interaction); the two last terms represent the effect of the phonon on the transfer of the exciton.

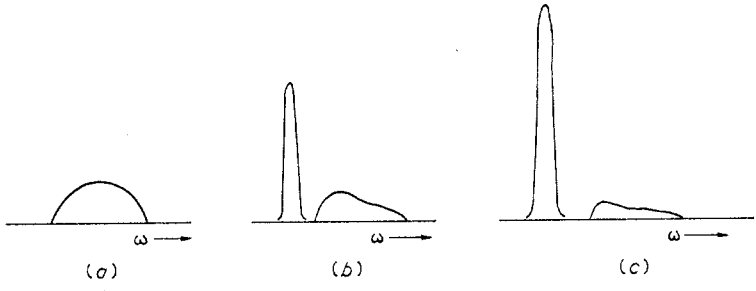

Figure 36. Dependence of the vibronic absorption spectrum on Δ for $\Delta < 0$. (*a*) $|\Delta|$ small, only the two-particle spectrum is present; (*b*) two-particle and single-particle spectra have comparable intensities; (*c*) $|\Delta|$ large, single-particle absorption is dominant. The integrated intensity of the spectrum is independent of Δ.

An exact solution of the hamiltonian in equation (8.5) can be obtained if we include interactions with only a finite number of neighbours. However, certain conclusions can be drawn in the general case. If $\gamma^2 \ll 1$, the third term is small and can be treated as a perturbation; if $|\Delta|$ is also small, then only the two-particle spectrum exists. For $\gamma^2 \gg 1$ the third term dominates, and the eigenstates describe an exciton and a phonon which exchange places in turn between a given pair of sites. It is especially interesting to note that an exact solution also exists for $\gamma^2 = 1$ (Rashba 1968); it can be shown directly that the function

$$\Psi_k = \sum_n \exp(i\boldsymbol{k}.\boldsymbol{n})\, \psi_n^- \phi_n^+ |0\rangle$$

is an eigenfunction of equation (8.5) with $\gamma = 1$. Moreover, just this particular state is 'prepared' at the absorption of a quantum, because both the exciton and the phonon occur on the same site. Since this state decays slowly for $\gamma \simeq 1$, it can be regarded as a quasi-single-particle state, even if it lies in the region of the two-particle spectrum. A narrowing of the spectrum should therefore be expected as $\gamma^2 \to 1$. In the general case both single- and two-particle absorption must be present; there may be several single-particle bands, and they may be either above or below the two-particle absorption. As distinct from the phonons which are not fully symmetric, the structure of this spectrum is determined by the details of the exciton dispersion relation $\epsilon(\boldsymbol{k})$ (and not just by the density of states $\rho(\omega)$), and also the energy of vibrons depends strongly on their momentum $\boldsymbol{k}$.

There is one unique feature of the hamiltonian in equation (8.5) which deserves attention; the exciton–phonon interaction is completely determined by the dispersion relation in the exciton band and the quantities Δ and γ^2, which are known from

the spectra of free molecules, that is, the interaction hamiltonian does not contain any new unknown parameters.

Another important point should be stressed. Linear coupling with phonons is usually much stronger than quadratic coupling, since E_{FC} is as a rule much larger than $|\Delta|$. However, in the theory of vibronic spectra the role played by quadratic coupling is strongly emphasized for $\mathfrak{M} \ll \omega_0$, since E_{FC} must be compared with ω_0, whilst $|\Delta|$ must be compared with the much smaller quantity $\mathfrak{M}$. Quadratic coupling is therefore as important as linear coupling in the present case.

The dynamic model was also applied to multiphonon states (Rashba 1966, Philpott 1967), but because of the complexity of the problem only limited results have so far been obtained. The effect of impurities has also been considered (Rashba 1966, Broude *et al* 1967, Philpott 1970a). Rashba (1970) studied light absorption at $T \neq 0$ involving thermal phonons, which leads to the formation of vibrons, and showed that this has a large cross section. The role of polariton effects was analysed by Philpott (1970b), who also discussed (Philpott 1969) certain mathematical techniques of the theory.

It is interesting to note that the historical development of the dynamic model in the theory of vibronic spectra of molecular crystals took place in the opposite direction to that taken in the theory of bound states of other types of quasiparticles. The usual starting point has been the concept of noninteracting particles and the theoretical problem was to determine the spectra of bound (single-particle) states. On the other hand, the starting point for the spectroscopy of molecular crystals was the concept of a composite particle (the vibron), and effects related to its virtual or real decay into an exciton and a phonon were considered only much later on the basis of a dynamic model.

The dynamic approach has also been applied to electrons in molecular crystals (Rashba 1966). The presence of an electron on one of the bonds (or sites) changes its stiffness and hence also changes Δ for the vibrational frequency. If the electron band is fairly narrow, we can therefore expect to find bound states of an electron and a phonon, analogous to the exciton–phonon bound states† already considered. These must have a large effective mass, determined by the phonon dispersion.

An increase in the electron mass can therefore be due either to the usual 'dressing' by virtual phonons, or to binding of the electron to real phonons.

8.2. *Vibronic spectra of aromatic crystals*

Aromatic hydrocarbons form typical molecular crystals in which intermolecular interactions are considerably weaker than those within the molecules. Their lower excited states are very well described by the model of Frenkel excitons. Most of these crystals show a clear Davydov splitting (Davydov 1951), as a result of the fact that their unit cells contain several molecules. In this group of crystals the spectra of benzene, naphthalene and anthracene have been studied in most detail. A general analysis of their first vibronic transitions was made by Sheka (1971), using the dynamical theory.

Let us begin with the spectrum of naphthalene, whose unit cell contains two molecules. There are therefore two exciton bands, but in $\boldsymbol{k}$-space these touch on

† The difference from the exciton case is basically due to the long range of the Coulomb interaction. The effect of this on the theory of localized vibrations was considered by Bryksin and Firsov (1970a,b).

one of the Brillouin zone boundaries. Hence the density of exciton states is nonzero everywhere within a certain spectral range of width $\mathfrak{M} \simeq 180\ \text{cm}^{-1}$. Phonon dispersion can be neglected.

The absorption spectrum begins with a Davydov doublet A_1–B_1 (figure 37). For the non-fully symmetric vibration with $\omega_0^{(1)} = 509\ \text{cm}^{-1}$, the frequency shift $\Delta = -86\ \text{cm}^{-1}$ is large enough to give rise to a single particle—an exciton–phonon bound state. This produces the narrow absorption band M_1. The broad-band

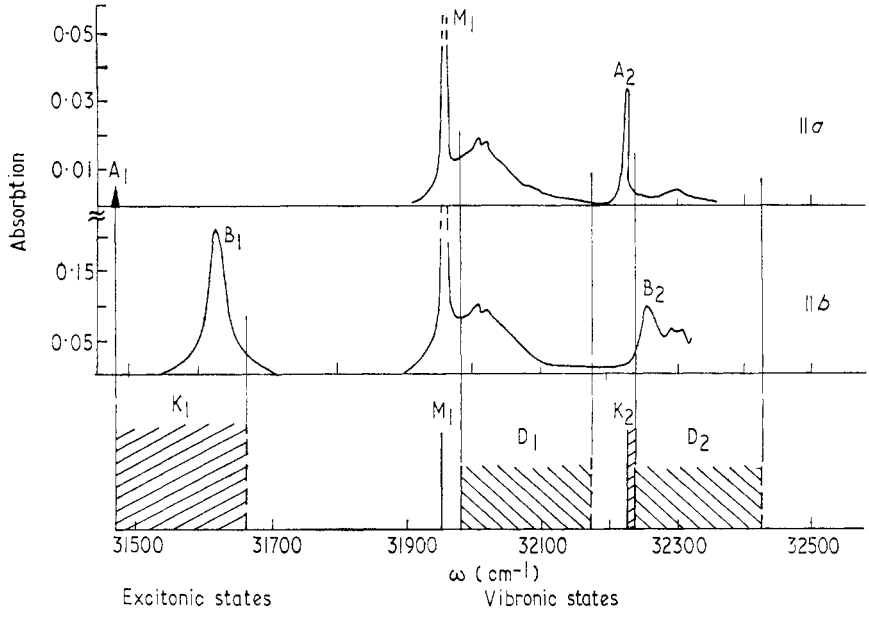

Figure 37. Exciton and vibron absorption spectra of naphthalene for light polarization parallel to *a* and *b* crystal axes. K_1 shows the region of exciton spectra; A_1–B_1 is the first Davydov doublet, D_1 and D_2 are the regions of the two-particle spectra for the non-fully symmetric vibration $\omega_0^{(1)}$ and the fully symmetric vibration $\omega_0^{(2)}$; M_1 and K_2 correspond to single-particle states. From Soskin (1962).

absorption (D_1) which follows this is mainly due to two-particle absorption†, that is, it corresponds to dissociated states of the exciton–phonon pair. The intensities of M_1 and D_1 are comparable. For the fully symmetric vibration $\omega_0^{(2)} = 760\ \text{cm}^{-1}$ the frequency shift $\Delta = -58\ \text{cm}^{-1}$, and in this case there is only one single-particle branch associated with the A_2 band. The band B_2 and the absorption in the *b*-component of the spectrum which accompanies it are due to two-particle aborpion. The criterion $\omega_0^{(1)}, \omega_0^{(2)} \gg \mathfrak{M}$ for the applicability of the dynamical theory is satisfied.

The correctness of this interpretation can be confirmed by an analysis of the spectrum of deformed naphthalene crystals (Broude and Tomashchik 1964, Prikhot'ko *et al* 1964). As is seen from figure 38, the A_1–B_1 splitting is reduced by a factor of two; the width of the exciton band (and hence of the two-particle spectrum) evidently changes in approximately the same way. The band M_1 must then move away from the edge of the two-particle spectrum, and the magnitude of $|a|^2$ must increase rapidly, according to equation (8.10); as a result the intensity of the

† Part of this band has a different origin and is due to the contribution of external vibrations.

band M_1 must increase and that of the band D_1 must decrease. In fact the D_1 band almost disappears (see figure 38), and only a small shoulder of the M_1 band remains, which is partially related to the effects of external vibrations. The band B_2 in the second transition is considerably narrowed, because it is now outside the region of the two-particle spectrum, that is, this also corresponds to bound states.

A quantitative analysis based on comparing vibronic spectra associated with non-fully symmetric phonons with the excitonic spectra of crystals containing isotopic impurities (Broude *et al* 1967, Rabin'kina *et al* 1970) fully confirms this interpretation.

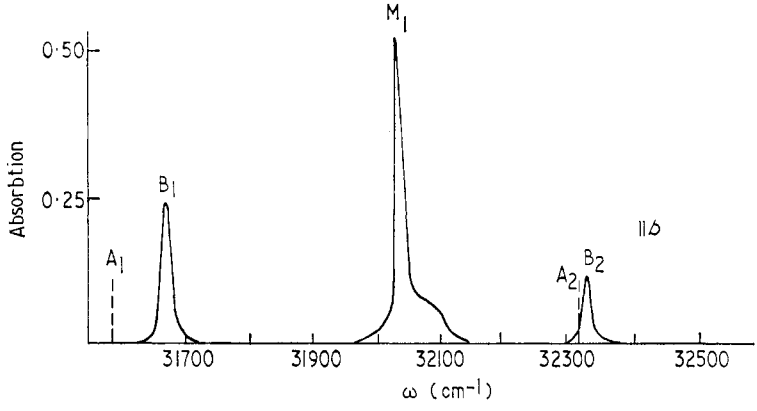

Figure 38. Electronic and vibronic spectrum of naphthalene crystals under homogenous tension for light polarized parallel to the *b* crystal axis. From Prikhot'ko *et al* (1964).

Hence, both single- and two-particle spectra occur with comparable intensities in naphthalene. The situation in benzene is quite different; there $\mathfrak{M} \simeq 60\ \text{cm}^{-1}$ and for the non-fully symmetric vibration with $\omega_0 = 606\ \text{cm}^{-1}$ the frequency shift $\Delta = -86\ \text{cm}^{-1}$, that is, it is large. Consequently single-particle absorption is dominant, and the fraction of two-particle absorption is only 2–5%.

Anthracene is an example of the third case; here $\mathfrak{M} \sim 250\text{–}500\ \text{cm}^{-1}$, whilst $|\Delta| \sim 5\ \text{cm}^{-1}$. There are therefore no single-particle states for either the non-fully symmetric vibrations or for the fully symmetric vibrations with small γ^2. There is, however, a vibration at $\omega_0 = 1400\ \text{cm}^{-1}$ with $\gamma^2 \simeq 0{\cdot}9$, for which single-particle states could in principle occur. A calculation is not possible, because the dispersion law is unknown, but analysis of the experimental data shows that all the associated absorption lies in the two-particle region. Consequently all the vibronic absorption in anthracene is two-particle absorption. This conclusion gives a natural explanation for an important experimental fact, which has been known for many years, but which for a long time was not clearly explained: the vibronic luminescence† at low temperature consists of a series of very narrow lines, but the 'mirror' absorption consists wholly of wide bands.

We thus find three types of vibronic spectra in the series benzene, naphthalene, anthracene, and all three are included in the dynamic model. Bound states are dominant in the benzene spectrum, the spectrum of naphthalene shows both bound and dissociated states, and there are no bound states in anthracene.

† This corresponds to transitions from the lower exciton level to the vibrational sublevels of the crystal ground state.

8.3. *Excitons in molecular chains*

Suna (1964) made the first investigations for a molecular chain of the spectrum near the edge of the region of two-particle excitations of an exciton, which interacts with optical phonons. The exciton–phonon interaction was chosen to be of the form in equation (8.2) with $\Delta = 0$. The analysis was carried out using perturbation theory, and including the first diagram in figure 4; there was no limitation on the ratio $\mathfrak{M}/\omega_0$. If $\mathfrak{M} > \omega_0$ the mass operator for the exciton near the threshold for phonon emission contains a singularity of the type in equation (1.5*c*), and the dispersion relation shows pinning similar to that in curve (*c*) in figure 2. A single-particle branch must therefore exist for all values of k. We emphasize that in this case the singularity is much stronger than in the three-dimensional problem (cf § 6).

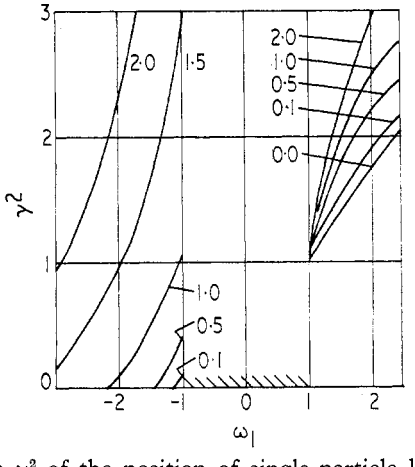

Figure 39. Dependence on γ^2 of the position of single-particle levels ω_1 for a chain. The numbers on the curves are the value of the parameter $|\Delta/4|$; it is assumed that $\Delta < 0$, $\mathfrak{M}_{01} = 1$. The region of two-particle states is shown by shading. From Davydov and Serikov (1970).

An additional branch of the spectrum, located directly above the two-particle region, was also obtained. According to the ideas of the present review one would expect this to be accompanied by bound states; these would be stable for $\omega_0 > \mathfrak{M}$. However, as has already been pointed out, the whole series in figure 4 must be summed in the immediate neighbourhood of the threshold, and the corresponding analysis shows that the results for the pinning region are still valid, but the additional branch disappears. Fedoseev (1970) summed the diagrams in figure 4 and showed that an additional branch appears below the two-particle region when the phonon dispersion $\omega(q)$ is large and certain inequalities for $\epsilon(k)$ and $\omega(q)$ are satisfied. This also appears when $\Delta \neq 0$ (Davydov and Serikov 1971).

For $\omega_0 \gg \mathfrak{M}$, and for arbitrary exciton–phonon coupling, the vibronic spectra of chains were considered on the basis of the dynamical theory by Rashba (1968) and by Davydov and Serikov (1970). The results are given in figure 39, which shows the positions of single-particle levels with $k = 0$ as a function of the interaction constant.

8.4. *Some related systems*

In accordance with the basic theme of the present review we have so far been concerned with the interaction of phonons with excitons and electrons. Since,

however, there are many common features in the spectra, due to the interaction of various quasiparticles, in systems which may be regarded as narrow-band, we shall now discuss several such systems briefly, but with no attempt at completeness.

Bound states of two phonons were first studied by Gush *et al* (1957, 1960) in the spectra of crystalline para-hydrogen (figure 40). The detailed theory was developed by Van Kranendonk (1959, 1960). The binding of two phonons is a consequence of a reduction in the rotational frequency of a molecule on excitation of an intramolecular vibration. The physical description is completely analogous to the interaction of excitons with non-fully symmetric vibrations. Since the reduction in rotational energy is $\simeq 18\ \text{cm}^{-1}$ for a rotational branch of width $\sim 20\ \text{cm}^{-1}$ and a vibrational branch of width $\sim 3\ \text{cm}^{-1}$, the conditions are favourable for binding.

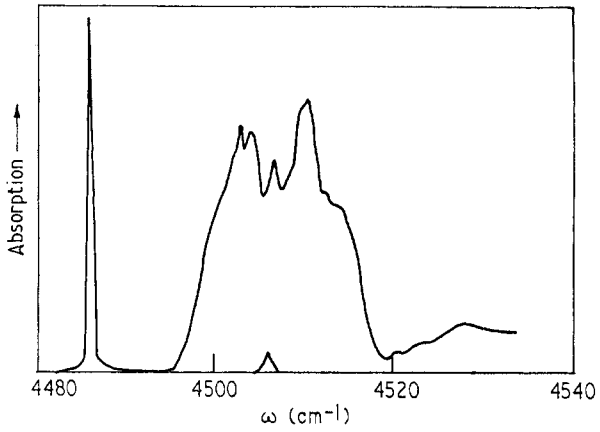

Figure 40. Absorption spectrum of para-hydrogen at 1·9 K. The narrow band corresponds to a bound state of two phonons, and the wide band to dissociated states of this pair. From Gush *et al* (1960).

Biphonons have also been found in HCl (Ron and Hornig 1963). The role of these states in Fermi resonance and the effect of impurities on the biphonon spectrum etc have also been investigated (Jortner and Rice 1966, Agranovich *et al* 1970a,b, 1971).

The conditions for the formation of biexcitons were discussed by Trlifaj (1963), Patzer (1969) and Kozhushner (1971).

Bound states of excitons and magnons were discovered by Meltzer *et al* (1968, 1969); a theory was developed by Freeman and Hopfield (1968). The change in shape of the two-particle spectrum as a result of the exciton–magnon interaction was investigated by Elliott *et al* (1968).

Spin complexes, ie bound states of several magnons, are a classic topic. The possibility of their existence was shown in a pioneering paper by Bethe (1931) for the one-dimensional case, and by Wortis (1963) and Hanus (1963) for the three-dimensional case. Since then the theory of spin complexes has been developed continuously and has received particular attention in recent years (see eg Orbach (1958), Boyd and Callaway (1965), Zilberglitt and Harris (1968), Torrence and Tinkham (1969a), Majumdar (1970), Ono *et al* (1971) and Oguchi (1971)). These years have also been marked by major experimental advances: the study of the effect of magnon–magnon interactions on the two-magnon spectra (Elliott *et al*

1968, Fleury 1968), the discovery of cluster resonance in a $CoCl_2.2H_2O$ crystal with a chain structure (Date and Motokawa 1966, 1968), and, finally, the discovery by Torrence and Tinkham (1968, 1969b)—also in the same crystal—of spin complexes containing up to five spins.

Part V. Summary

9. Conclusions

(1) Bound states which include phonons have a qualitative difference from ordinary bound states: they contain particles whose number is not conserved. Such states are therefore stable only if their real decay with disappearance of the phonon is forbidden by the conservation laws (of energy for a localized electron, and of energy and momentum for a free electron or an exciton). It should also be emphasized that the occurrence of these bound states has nothing in common with the well known intersection of boson spectral branches, which was first considered in relation to the theory of the interaction of electromagnetic radiation and optical phonons by Tolpygo (1950) and Huang (1951), although many features of this (eg figure 3) are very similar†. The difference between these phenomena can be made clearer by the following example, applied to the resonance situation. For the case of intersecting boson branches both resonating states are single-particle states, but on the other hand, for the systems which we have considered, one is a single-particle state whilst the other is a two-particle state. Different results therefore follow: the appearance of limiting points, additional branches, etc.

(2) The general properties of the spectra of bound states in narrow-band systems, including vibronic excitations in molecular crystals, are common to most of these systems. There is at the present time qualitative agreement between the experimentally observed vibronic spectra and their theoretical description in terms of the dynamical model. Quantitative agreement has been reached in a few cases for phonons corresponding to non-fully symmetric vibrations. A more detailed analysis of transitions which include fully symmetric phonons is probably only a matter of time. Unfortunately, there is as yet no direct proof of the existence of bound states of electrons and phonons in these crystals.

(3) In wide-band systems, on the other hand, the nature of the bound states depends strongly on the type of particle which is coupled to a LO phonon. For electron–phonon coupling the effects are strongest when the electron is localized at an impurity centre; the energy scale of the spectral structure is of order $\alpha^{1/2}\omega_{LO}$ at resonance and $\alpha\omega_{LO}$ away from resonance (it is assumed that $\alpha \ll 1$). The effects are weaker for an electron in a magnetic field, which is 'localized' only transverse to the field; here the scale is of order $\alpha^{2/3}\omega_{LO}$ at resonance and $\alpha^2\omega_{LO}$ away from it. In the absence of a magnetic field bound states exist only for strong coupling ($\alpha \gg 1$), and possibly for intermediate coupling. An exciton, being a neutral particle, is not 'localized' by a magnetic field, and therefore there are no such sharp distinctions in the behaviour of complexes comprising magnetoexciton plus LO phonon or exciton plus LO phonon. However, a strong magnetic field increases the transverse mass of a magnetoexciton, so that it behaves more like a magnetopolaron, and this favours the formation of bound states with LO phonons. An increase in the

† The intersection of boson branches with the participation of a longitudinal optical phonon is considered in the review by Palik and Furdyna (1970).

mass ratio of hole and electron in a normal exciton, which makes its properties more like those of an impurity centre, has a similar effect.

(4) For wide-band systems the comparison of theory and experiment is so far only in its initial stages, and in a number of cases not even qualitative agreement has yet been obtained.

The only situation in which there is complete qualitative, and even semi-quantitative, agreement is intraband absorption in n-InSb under conditions of magnetophonon resonance. For interband absorption under the same conditions there is no doubt that the reason for the effect is correctly understood, however the quantitative features of the spectrum have not yet been derived. Bound states have not been looked for in nonresonant conditions, although their discovery seems reasonably likely in crystals, such as CdTe, which are more polar than InSb. It may be expected that such states would produce fine structure in the peaks of cyclotron–phonon resonance.

There is no doubt that bound states of a localized electron and a LO phonon (dielectric local vibrational modes) have been observed experimentally, in both resonant and nonresonant situations. However, it is not yet quite clear how the levels of the theoretical spectrum are related to these results.

For an exciton with no magnetic field there is practically no correspondence between theory and experiment, and the origin of the spectral features in the energy region of the electron–hole continuum remains unsettled; it is not clear whether they are due to exciton–phonon complexes, or are simply the result of interference effects.

(5) The most natural way for bound states to show up is in optical absorption experiments as a result of the interaction of particles which were themselves produced by the absorption of the photon (final-state interaction). The same bound states could also be observed in principle in hot luminescence—this time as a result of an interaction in the initial state. In certain circumstances they may also show up in luminescence as a result of interaction in the final state, analogously to the way in which bound states of a centre plus a phonon are observed in the vibronic luminescence of impurity excitons.

Bound states can lead to a number of interesting changes in the energy spectrum, and these are reflected in various optical experiments. For example, an understanding of bound states with a phonon participation enables us to look afresh at the question of valley–orbit splitting of exciton levels, which has been of recent interest (Ascarelli 1969, 1971, Dean *et al* 1969, Shaklee and Nahory 1970). In impurity centres this splitting is due to the mixing of electronic states from a number of equivalent valleys. It is clear that this mixing is not possible for the case of an exciton, because the exciton state must have a definite momentum. If, however, we consider the spectrum of the complex 'exciton plus phonon', a state with zero total momentum can be constructed from exciton states in different valleys by compensating each exciton momentum with the opposite phonon momentum. If this complex is in a bound state, the problem is analogous to an impurity centre, and valley–orbit splitting should occur. On the other hand, there are no grounds for expecting a splitting if the complex is not in a bound state.

Bound states with a phonon participation can also affect a number of other phenomena, although the number of examples which can be quoted at present is not large. Munn and Siebrand (1970a) constructed a theory of electrical conductivity in narrow-band systems, taking bound states into account, and concluded that this

mechanism is the determining factor in a number of organic crystals. On the same basis, Munn and Siebrand (1970b) put forward a theory of exciton diffusion. It was shown by Zeldovych and Ovchinnikov (1971) that phonon anharmonicity can lead to a progressive condensation of phonons, with the formation of highly excited molecules.

References

AGRANOVICH V M *et al* 1970a *Fiz. Tverd. Tela* **12** 562–70
—— 1970b *Zh. Eksp. Teor. Fiz.* **59** 246–53
—— 1971 *Fiz. Tverd. Tela* **13** 1032–43
AHLBURN B T and RAMDAS A K 1968 *Phys. Rev.* **167** 717–29
ASCARELLI G 1969 *Phys. Rev.* **179** 797–815
—— 1971 *Phys. Rev.* B **3** 1498–9
BACHRACH R Z and BROWN F C 1968 *Phys. Rev. Lett.* **21** 685–8
—— 1970 *Phys. Rev.* B **1** 818–31
BAKANAS R and LEVINSON Y 1969 *Lithuanian Physics Collected Papers* **9** 143–7 in Russian
BALDINI G, BOSACCHI A and BOSACCHI B 1969 *Phys. Rev. Lett.* **23** 846–8
BALDINI G and BOSACCHI B 1969 *Phys. Rev. Lett.* **22** 190–2
—— 1970 *Proc. 10th Europ. Cong. Molecular Spectroscopy, Liège* 1969, *Mém. Soc. R. Sci. Liège* pp305–24
BASS F G and LEVINSON Y B 1965 *Zh. Eksp. Teor. Fiz.* **49** 914–24
BETHE H 1931 *Z. Phys.* **71** 205–26
BOGOLYUBOV N N 1950 *Ukr. Mat. Zh.* **2** 3–24
BOYD R G and CALLAWAY J 1965 *Phys. Rev.* **138** A1621–9
BRANDT R C and BROWN F C 1969 *Phys. Rev.* **181** 1241–50
BRANDT R C, LARSEN D M and COHN D R 1970 *Proc. 10th Int. Conf. Physics of Semiconductors, Cambridge, Mass.* (Oak Ridge, Tenn.: United States Atomic Energy Commission) pp162–6
BROUDE V L, RASHBA É I and SHEKA E F 1966 *Zh. Eksp. Teor. Fiz. Pis'ma Red.* **3** 429–34
—— 1967 *Phys. Stat. Solidi* **19** 395–406
BROUDE V L and TOMASHCHIK A K 1964 *Ukr. Fiz. Zh.* **9** 39–45
BRYKSIN V V and FIRSOV YU A 1970a *Zh. Eksp. Teor. Fiz.* **58** 1025–39
—— 1970b *Fiz. Tverd. Tela* **12** 1030–7
COHEN M H and RUVALDS J 1969 *Phys. Rev. Lett.* **23** 1378–81
COHN D R, LARSEN D M and LAX B 1970 *Solid State Commun.* **8** 1707–9
—— 1972 *Phys. Rev.* B **6** 1367–75
CRAIG D P and WALMSLEY S H 1961 *Molec. Phys.* **4** 113–24
DATE M and MOTOKAWA M 1966 *Phys. Rev. Lett.* **16** 1111–4
—— 1968 *J. Phys. Soc. Japan* **24** 41–50
DAVIES R W and ZEIGER H J 1970 *Proc. 10th Int. Conf. Physics of Semiconductors, Cambridge, Mass.* (Oak Ridge, Tenn.: United States Atomic Energy Commission) pp 256–61
DAVYDOV A S 1951 *Theory of Light Absorption in Molecular Crystals* (Kiev: *Izv. Akad. Nauk Ukr. SSR*) in Russian [English Translation 1962, *Theory of Molecular Excitons* (New York: McGraw-Hill)]
—— 1964 *Usp. Fiz. Nauk* **82** 393–448
DAVYDOV A S and SERIKOV A A 1970 *Phys. Stat. Solidi* **42** 603–15
—— 1971 *Phys. Stat. Solidi* **44** 127–38
DEAN P J, MANCHON D D Jr and HOPFIELD J J 1970 *Phys. Rev. Lett.* **25** 1027–30
DEAN P J, YAFET Y and HAYNES J R 1969 *Phys. Rev.* **184** 837–43; see also 1970 *Phys. Rev.* B **1** 4193–4 (erratum)
DICKEY D H, JOHNSON E J and LARSEN D M 1967 *Phys. Rev. Lett.* **18** 599–602
DICKEY D H and LARSEN D M 1968 *Phys. Rev. Lett.* **20** 65–9
DILLINGER J *et al* 1968 *Phys. Stat. Solidi* **29** 707–14
DUNN D D 1968 *Phys. Rev.* **166** 822–7
DWORIN L 1965 *Phys. Rev.* **140** A1689–704
ELLIOTT R J 1957 *Phys. Rev.* **108** 1384–9

ELLIOTT R J and LOUDON R 1960 *J. Phys. Chem. Solids* **15** 196–207
ELLIOTT R J *et al* 1968 *Phys. Rev. Lett.* **21** 147–50
ENCK R C, SALEN A S and FAN H Y 1969 *Phys. Rev.* **182** 790–4
FANO U 1961 *Phys. Rev.* **124** 1866–78
FEDOSEEV V F 1970 *Preprint* FAI-5 *Institute of Physics and Astronomy Tartu* (Tallinn: Estonian SSR Academy of Sciences)
FIRSOV YU A, GUREVICH V L, PARFENIEV R V and SHALYT S S 1964 *Phys. Rev. Lett.* **12** 660–2
FLEURY P A 1968 *Phys. Rev. Lett.* **21** 151–3
FREEMAN S and HOPFIELD J J 1968 *Phys. Rev. Lett.* **21** 910–13
FRENKEL J 1931 *Phys. Rev.* **37** 17–44, 1276–94
GOR'KOV L P and DZYALOSHINSKY I E *Zh. Eksp. Teor. Fiz.* **53** 717–22
GUREVICH V L and FIRSOV YU A 1961 *Zh. Eksp. Teor. Fiz.* **40** 198–213
GUSH H P, HARE W F, ALLIN E J and WELSH H L 1957 *Phys. Rev.* **106** 1101–2
—— 1960 *Can. J. Phys.* **38** 176–93
HANUS J 1963 *Phys. Rev. Lett.* **11** 336–8
HARPER P G 1967 *Proc. Phys. Soc.* **92** 793–9
—— 1969 *Phys. Rev.* **178** 1229–35
HARPER P G, HODBY J W and STRADLING R A 1973 *Rep. Prog. Phys.* **36** 1–101
HARPER P G *et al* 1970 *Proc. 10th Int. Conf. Physics of Semiconductors, Cambridge, Mass.* (Oak Ridge, Tenn.: United States Atomic Energy Commission) pp166–71
HASEGAWA H and HOWARD R E 1961 *J. Phys. Chem. Solids* **21** 179–98
HECK R J and WOODRUFF T O 1971 *Phys. Rev.* B **3** 2056–9
HENRY C H and HOPFIELD J J 1972 *Phys. Rev.* B **6** 2233–8
HERMANSON J C 1970 *Phys. Rev.* B **2** 5043–51
HOLSTEIN T 1964 *Ann. Phys.* **29** 410–535
HROSTOWSKI H J and KAISER R H 1958 *J. Phys. Chem. Solids* **4** 148–53
HUANG K 1951 *Proc. R. Soc.* A **208** 352–65
IVANOV M A 1966 *Fiz. Tverd. Tela* **8** 3299–309
JOHNSON E J and DICKEY D H 1970 *Phys. Rev.* B **1** 2676–92
JOHNSON E J and LARSEN D M 1966 *Phys. Rev. Lett.* **16** 655–9
JORTNER J and RICE S A 1966 *J. Chem. Phys.* **44** 3364–74
KANZAKI H *et al* 1967 *J. Phys. Soc. Japan* **24** 652
—— 1968 *J. Phys. Soc. Japan* **24** 1184
KAPLAN B Y and LEVINSON Y B 1972a *Fiz. Tverd. Tela* 1412–25
KAPLAN B Y and LEVINSON Y B 1972b *Fiz. Tverd. Tela* 1663–70
KAPLAN R 1966 *J. Phys. Soc. Japan* **21** suppl 249–53
KAPLAN R, NGAI K L and HENVIS B W 1972 *Proc. 11th Int. Conf. Physics of Semiconductors, Warsaw* (Warsaw: *PWN—Polish Scientific Publishers*) vol 2 pp1208–13
KAPLAN R and WALLIS R F 1968 *Phys. Rev. Lett.* **20** 1499–502
KLYUKANOV A A and POKATILOV E P 1971 *Zh. Eksp. Teor. Fiz.* **60** 1878–89
KNOX R S 1963 *Theory of Excitons, Solid State Physics* ed F Seitz and D Turnbull (New York: Academic Press) suppl 5
KOGAN SH M and SURIS R A 1966 *Zh. Eksp. Teor. Fiz.* **50** 1279–84
KOHN W 1957 *Solid State Physics* ed F Seitz and D Turnbull (New York: Academic Press) **5** pp257–320
KOROVIN L I 1969 *Fiz. Tverd. Tela* **11** 508–10
—— 1970 *Zh. Eksp. Teor. Fiz.* **58** 1995–2004
KOROVIN L I and PAVLOV S T 1967a *Zh. Eksp. Teor. Fiz.* **53** 1708–16
—— 1967b *Zh. Eksp. Teor. Fiz. Pis'ma Red.* **6** 970–2
—— 1968 *Zh. Eksp. Teor. Fiz.* **55** 349–56
KOZHUSHNER M A 1971 *Zh. Eksp. Teor. Fiz.* **60** 220–9
KURITA S and KOBAYASHI K 1969 *J. Phys. Soc. Japan* **26** 1557
—— 1970 *J. Phys. Soc. Japan* **28** 1096–7
—— 1971 *J. Phys. Soc. Japan* **30** 1645–53
LAMPERT G 1958 *Phys. Rev. Lett.* **1** 450–3
LANDAU L D and PEKAR S I 1948 *Zh. Eksp. Teor. Fiz.* **18** 419–23
LARSEN D M 1964 *Phys. Rev.* A**135** 419–26
LARSEN D M and JOHNSON E J 1966 *J. Phys. Soc. Japan* **21** (suppl) 443–7

LEE T D, LOW F E and PINES D 1953 *Phys. Rev.* **90** 297–302
LEVINSON Y B 1970 *Zh. Eksp. Teor. Fiz. Pis'ma Red.* **12** 496–9
—— 1972 *Zh. Eksp. Teor. Fiz. Pis'ma Red.* **15** 574–7
LEVINSON Y B and MATULIS A YU 1970 *Zh. Eksp. Teor. Fiz. Pis'ma Red.* **11** 360–2
LEVINSON Y B, MATULIS A YU and SCHERBAKOV L M 1971a *Zh. Eksp. Teor. Fiz.* **60** 859–66
—— 1971b *Zh. Eksp. Teor. Fiz.* **60** 1097–108
—— 1971c *Zh. Eksp. Teor. Fiz.* **61** 843–58
LEVINSON Y B and RASHBA É I 1972 *Zh. Eksp. Teor. Fiz.* **62** 1502–12
LIANG W Y and YOFFE A D 1968 *Phys. Rev. Lett.* **20** 59–62
LITTON C W, REYNOLDS D C, COLLINS T C and PARK Y C 1970 *Phys. Rev. Lett.* **25** 1619–21
MCCOMBE B D, BISHOP S G and KAPLAN R 1967 *Phys. Rev. Lett.* **18** 748–50
—— 1968 *Proc. 9th Int. Conf. Physics of Semiconductors, Moscow* (Leningrad: Nauka) vol 1 pp301–6
MCCOMBE B D and KAPLAN R 1968 *Phys. Rev. Lett.* **21** 756–9
MCCOMBE B D and WAGNER R J 1971 *Phys. Rev.* B **4** 1285–8
MCCOMBE B D, WAGNER R J and PRINZ G A 1969 *Solid State Commun.* **7** 1381–5
MCRAY E G 1961 *Austral. J. Chem.* **14** 354–71
—— 1963 *Austral. J. Chem.* **16** 295–314, 315–33
MAJUMDAR C K 1970 *Phys. Rev.* B **1** 287–96
MANCHON D D Jr and DEAN P J 1970 *Proc. 10th Int. Conf. Physics of Semiconductors, Cambridge, Mass.* (Oak Ridge, Tenn.: United States Atomic Energy Commission) pp760–6
MATULIS A Y 1972 *Fiz. Tverd. Tela* **14** 2987–91
MEARS A L, STRADLING R A and INALL E K 1968 *J. Phys. C: Solid State Phys.* **1** 821–6
MEL'NIKOV V I and RASHBA É I 1969 *Zh. Eksp. Teor. Fiz. Pis'ma Red.* **10** 95–98, 359 (erratum)
MEL'NIKOV V I, RASHBA E I and EDEL'SHTEIN V M 1971 *Zh. Eksp. Teor. Fiz.* **13** 269–72
MELTZER R S, CHEN M Y, MCCLURE D S and LOWE-PARISEAU M 1968 *Phys. Rev. Lett.* **21** 913–6
MELTZER R S, LOWE M and MCCLURE D C 1969 *Phys. Rev.* **180** 561–78
MOSKALENKO S A 1958 *Opt. i Spektr.* **5** 147–55
MOTT N F 1938 *Trans. Faraday Soc.* **34** 500–
MUNN R W and SIEBRAND W 1970a *J. Chem. Phys.* **52** 6391–406
—— 1970b *J. Chem. Phys.* **52** 47–63
NAKAYAMA M 1969 *J. Phys. Soc. Japan* **27** 636–45
NGAI K L 1971 *Phys. Rev.* B **3** 1303–15
NGAI K L and JOHNSON E J 1972 *Phys. Rev. Lett.* **29** 1607–10
NIEMAN G C and ROBINSON G W 1963 *J. Chem. Phys.* **39** 1298–307
OGUCHI T 1971 *J. Phys. Soc. Japan* **31** 394–402
ONO I, MIKADO S and OGUCHI T 1971 *J. Phys. Soc. Japan* **30** 358–66
ONTON A, FISHER P and RAMDAS A K 1967a *Phys. Rev.* **163** 686–703
—— 1967b *Phys. Rev. Lett.* **19** 781–3
ORBACH R 1958 *Phys. Rev.* **112** 309–16
PALIK E D and FURDYNA J K 1970 *Rep. Prog. Phys.* **33** 1193–322
PATZER K 1969 *Phys. Stat. Solidi* **32** 11–22
PAVLOV S T and FIRSOV Yu A 1967 *Fiz. Tverd. Tela.* **9** 1780–93
PEKAR S I 1946 *Zh. Eksp. Teor. Fiz.* **16** 341–7
—— 1951 *Investigations in the Electron Theory of Crystals* (Moscow: Gostekhizdat) in Russian
PHILPOTT M R 1967 *J. Chem. Phys.* **47** 2534–44, 4437–45
—— 1969 *J. Chem. Phys.* **51** 2616–24
—— 1970a *J. Chem. Phys.* **53** 136–45
—— 1970b *J. Chem. Phys.* **52** 5842–50
PITAEVSKII L P 1959 *Zh. Eksp. Teor. Fiz.* **36** 1168–78
PRIKHOT'KO A F 1948 *Izv. Akad. Nauk SSSR, Ser. Fiz.* **12** 499–503
PRIKHOT'KO A F, SOSKIN M S and TOMASHCHIK A K 1964 *Opt. i Spektr.* **16** 615–8
PURI S M and GEBALLE T H 1963 *Bull. Am. Phys. Soc.* **8** 309
RABIN'KINA N V, RASHBA É I and SHEKA E F 1970 *Fiz. Tverd. Tela* **2** 3569–78
RASHBA É I 1957 *Opt. i Spektr.* **2** 568–77
—— 1964 *Usp. Fiz. Nauk SSSR* 557–78
—— 1966 *Zh. Eksp. Teor. Fiz.* **50** 1064–80

RASHBA É I 1968 *Zh. Eksp. Teor. Fiz.* **54** 542–58
—— 1970 *Fiz. Tverd. Tela* **12** 1801–4
—— 1972a *Zh. Eksp. Teor. Fiz. Pis'ma Red.* **15** 777–80
—— 1972b *Physics of Impurity Centres in Crystals* (Tallinn: Estonian SSR Academy of Sciences) pp415–28
RASHBA É I and EDEL'SHTEIN V M 1971 *Zh. Eksp. Teor. Fiz.* **61** 2592–3008
RASHBA É I and GURGENISHVILI G E 1962 *Fiz. Tverd. Tela* **4** 1029–31
REYNOLDS D S, LITTON C W and COLLINS T C 1971 *Phys. Rev.* B **4** 1868–72
RODRIGUEZ S and SCHULTZ T D 1969 *Phys. Rev.* **178** 1252–63
RON A and HORNIG D E 1963 *J. Chem. Phys.* **39** 1129–30
RUVALDS J, ECONOMOU E N and NGAI K L 1971 *Phys. Rev. Lett.* **27** 417–20
RUVALDS J and ZAWADOWSKI A 1970 *Phys. Rev.* B **2** 1172–5
SAK J 1970a *Phys. Rev. Lett.* **25** 1654–7
—— 1970b *Proc. 10th Int. Conf. Physics of Semiconductors, Cambridge, Mass.* (Oak Ridge, Tenn.: United States Atomic Energy Commission) pp525–9
SHAKLEE K L and NAHORY R E 1970 *Phys. Rev. Lett.* **24** 942–5
SHEKA E F 1971 *Usp. Fiz. Nauk* **104** 593–643
—— 1972 *Physics of Impurity Centres in Crystals* (Tallinn: Estonian SSR Academy of Sciences) pp429–42
SILBERGLITT R and HARRIS A B 1968 *Phys. Rev.* **174** 640–58
SOSKIN M S 1962 *Ukr. Fiz. Zh.* **7** 635–42
SUMMERS C J, DENNIS R B, SMITH S D and LITTON C W 1968a *Proc. 9th Int. Conf. Physics of Semiconductors, Moscow* (Leningrad: Nauka) vol 2 pp1029–35
SUMMERS C J, HARPER P G and SMITH S D 1967 *Solid State Comm.* **5** 615–20
SUMMERS C J *et al* 1968b *Phys. Rev.* **170** 755–62
SUNA A 1964 *Phys. Rev.* A**135** 111–23
TJABLIKOV S V 1951 *Zh. Eksp. Teor. Fiz.* **21** 377–88
TOLPYGO K B 1950 *Zh. Eksp. Teor. Fiz.* **20** 497–509
TORRENCE J B, Jr and TINKHAM M 1968 *J. Appl. Phys.* **39** 822–3
—— 1969a *Phys. Rev.* **187** 587–94
—— 1969b *Phys. Rev.* **187** 595–606
TOYOZAWA Y 1971 *Proc. 3rd Int. Conf. Photoconductivity* (Oxford: Pergamon Press) pp151–5
TOYOZAWA Y and HERMANSON J 1968 *Phys. Rev. Lett.* **21** 1637–41
TRLIFAJ M 1963 *Czech. J. Phys.* **13** 631–43
VAN KRANENDONK J 1959 *Physica* **25** 1080–94
—— 1960 *Can. J. Phys.* **38** 240–61
VELLA-COLEIRO P G 1969 *Phys. Rev. Lett.* **23** 697–700
WALDMAN J *et al* 1969 *Phys. Rev. Lett.* **23** 1033–7
WALLIS R F, MARADUDIN A A, IPATOVA I P and KAPLAN R 1970 *Solid State Commun.* **8** 1167–71
WALKER W C, ROESSLER D M and LOH E 1968 *Phys. Rev. Lett.* **20** 847–8
WANNIER G H 1937 *Phys. Rev.* **52** 191–7
WHITED R C and WALKER W C 1969 *Phys. Rev. Lett.* **22** 1428–30
WHITFIELD G and PUFF R 1965 *Phys. Rev.* A**139** 338–42
WORTIS M 1963 *Phys. Rev.* **132** 85–97
ZELDOVYCH YA B and OVCHINNIKOV A A 1971 *Zh. Eksp. Teor. Fiz. Pis'ma Red.* **13** 636–9